

## **Response to reviewer comments**

### ***Reviewer #1:***

- Tables 3.3.1, 3.3.2 and 3.3.3 have something to do with the payload mass budget, but it is not clear what information these tables are trying to convey. A clearly identified mass budget (component mass, uncertainty in component mass, mass value identified as "measured", "calculated", or "estimated", plus total mass and uncertainty) should be provided.

***Action taken:*** New table with mass budget was created in the Table 4.5.1.1 in the Section 4.5.1

- Power circuit diagram including connections to the HASP EDAC connector pins, voltage conversion, and voltage distribution. The major parts of the power circuit should be identified with make and model.

***Action taken:*** The power circuit diagram was added and can be found in the Figure 4.3.2.1

- Section 3.2.3 "Usage of HASP Serial" implies that the team thinks they will be able to communicate with their Raspberry Pi in real-time over the HASP serial port during the flight. The team need to read the HASP Student Payload Interface Manual (available on the HASP website) to understand what is and is not possible for flight telemetry. In particular, there is no real-time connection to payloads during flight. Rather the payload needs to downlink its own data frame. These frames are collected and made available to the teams roughly every 5 to 10 minutes. Similarly commands can be occasionally uplinked to the payload.

***Action taken:*** Information about the usage of HASP Serial was added in the sections **6.2 Uplink using HASP Serial** and **6.3 Downlink via HASP Serial**

- If a payload team wishes to exceed a resource (e.g. data or dimensions) then the application must include a special section requesting a waiver. This is fully specified in the HASP 2018 Call for Payloads. No special waiver was requested, therefore it appears that this team will not elevate or rotate their telescope outside the given dimensions of the payload envelope. If this is not the case, then the team must apply for a waiver and the request must include ALL the information specified in the CFP. The team must apply for a waiver if it wishes to move the telescope beyond the standard payload envelope. The waiver request must include ALL the information as specified in the HASP 2018 CFP. REVISED APPLICATION ADDRESSING ALL THE ISSUED RAISED BY THE REVIEWERS IS REQUIRED.

***Actions taken:*** With an updated design a waiver is now requested in the **Section 7. Special Requests**. It includes sub-sections **7.1 Height request**, **7.2 Width request** and **7.3 GPD Time and Position Data request**.

**Reviewer #4:**

- Difficult to identify procedures for integration and operation. A separate section for these would have been very helpful

**Actions taken:** New Sections **5. Experiment Integration to HASP** and **6. Operation during Flight** were added.

- Difficult to identify level of professional mentoring.

**Actions taken:** Section **1.5.2 External support** was added with information about details of Academic Lead and Mentor.

- Unable to find estimate of personnel present at integration and flight, as in the reviewer guidelines.

**Actions taken:** Information about expected personnel present at integration and flight can be found in the **Section 1.5.3 Team members**.

- Some sort of chart showing interaction between team members listed in section 1.4.2 would have been helpful.

**Actions taken:** New team organization chart was created and can be found in the **Section 1.5.4**



# HASP Revised Student Payload Application for 2018

Payload Title: Sheffield University Nova Balloon Lifted Telescope		
Institution: The University of Sheffield		
Payload Class: LARGE		Submit Date: 16.02.2018
<p><b>Project Abstract:</b></p> <p>Sun surveillance from the ground is often difficult as the thick atmosphere of the Earth blocks and distorts much of the incoming light. Learning about the Sun is critical in modern society, when solar flares have the potential to cripple telecommunication and global navigation systems. In the UK alone, €22mn was invested in the Space Situational Awareness program emphasising the need to better understand and predict solar events. Project SunbYte (Sheffield University Nova Balloon Lifted Telescope) aims to revolutionise the industry of solar observations by using a high-altitude balloon to lift a telescope to an altitude of 25-35km, where SunbYte has the potential to capture images of much better quality.</p> <p>As the existing ground and space telescopes are large, complex and expensive, the number of scientists who have access to such resources are quite limited. Even though experimental studies using high-altitude balloon telescopes have been previously conducted, these are, in terms of cost, inaccessible to many mainstream research institutions across the world.</p> <p>Combining the latest practices in manufacturing, astrophysics science and engineering, the team aims to deliver a low cost high quality method of imaging the Sun. The experiment was launched on BEXUS 25 from ESRANGE, Sweden in Oct 2017 as part of the REXUS/BEXUS programme. This document will discuss the new design for launch on HASP based on the lessons learnt.</p>		
Team Name: SunbYte		Team or Project Website <a href="http://sunbyte.group.shef.ac.uk">http://sunbyte.group.shef.ac.uk</a>
Student Leader Contact Information:		Faculty Advisor Contact Information:
Name:	Iakov Bobrov	Dr. Viktor Fedun
Department:	Department of Aerospace Engineering	Department of Automatic Control and Systems Engineering
Mailing Address:	Department of Automatic Control and Systems Engineering University of Sheffield	Department of Automatic Control and Systems Engineering University of Sheffield
City, State, Zip code:	S1 3JD, Sheffield	S1 3JD, Sheffield
e-mail:	ibobrov1@sheffield.ac.uk	v.fedun@sheffield.ac.uk
Office Telephone:	+447557381923	+44 114 2225197
Mobile Telephone:	+44 7554902627	+44 114 2225197

# Contents

<b>Contents</b>	<b>2</b>
<b>1. Introduction</b>	<b>4</b>
1.1 Scientific/Technical Background	4
1.2 Mission Statement	4
1.3 Experiment Objectives	4
1.4 Experiment Concept	4
1.5 Team Details	6
1.5.1 Contact point	6
1.5.2 External support	6
1.5.3 Team members	6
1.5.4 Team organization	8
<b>2. Experiment requirements and constraints</b>	<b>9</b>
2.1 Functional Requirements	9
2.2 Performance Requirements	9
2.3 Design Requirements	9
2.4 Operational Requirements	9
<b>3. Project Planning</b>	<b>10</b>
3.1 Schedule	10
3.1.1 Overall project Gantt Chart	10
3.1.2 Project planning by sub-team	11
3.2 Risk	13
<b>4. Experiment description</b>	<b>14</b>
4.1 Optics	14
4.1.1 Optics Introduction	14
4.1.2 Optical Calculation	14
4.1.3 Telescope Selection	15
4.1.4 Filter selection	15
4.1.5 Optical system Design	17
4.2 Mechanical Design	18
4.2.1 Gimbal	18
4.2.2 Gimbal Frame	19
4.2.3 Telescope Clamps	20
4.2.4 Shaft Cross-section	21
4.2.5 Pitch Motor	21
4.2.6 Yaw Motor Housing	21
4.2.7 Motor shaft adapter	22
4.2.8 Electronics Box	23





4.3 Electronics	24
4.3.1 Electronics Overview	24
4.3.2 Inside the Electronics Box	25
4.3.3 1 Interface to HASP	26
4.3.4 External devices	26
4.3.5 E-box Internal Circuit Design	26
4.3.6 E-box Manufacturing	28
4.3.7 Forbidden Region	29
4.4 Software Design	31
4.4.1 Sun tracking system	31
4.4.2 First stage Sun tracking	31
4.4.3 Second stage Sun tracking	32
4.4.4 Monitoring and diagnostics	34
4.4.5 Redundancy of hardware and software	34
4.4.6 Main tracking and control system	35
4.4.7 Data storage system	35
4.5 System Budget	36
4.5.1 Mass Budget	36
4.5.2 Power Budget	38
<b>5. Experiment Integration to HASP</b>	<b>39</b>
5.1 Mechanical	39
5.2 Electronics	39
<b>6. Operation during Flight</b>	<b>40</b>
6.1 Analog and discrete channels design	40
6.2 Uplink using HASP Serial	40
6.3 Downlink via HASP Serial	40
6.4 Cyclic Redundancy Check (CRC) Checksum	43
6.5 Ground segment design	44
<b>7. Special Requests</b>	<b>45</b>
7.1 Vertical Extension	45
Sun Calculations	46
7.1.1. Vertical encroachment at 7cm extension request	49
7.1.2 Vertical encroachment at 13 cm extension request	51
7.3 GPD Time and Position Data request	53
<b>8. Post-Flight Activities</b>	<b>54</b>
Abbreviations and References	55
Abbreviations	55
References	56

# Introduction

## 1.1 Scientific/Technical Background

The Sun is the most important source of energy for the Earth and it is essential that we keep it under surveillance in order to understand how any changes will affect our planet.

In 1895, a solar coronal mass ejection hit the Earth's magnetosphere and caused Auroras to appear as far South as the Caribbean. In 1989, a geomagnetic storm took out much of Quebec's electricity grid plunging the country into chaos. If such an event were to occur nowadays, where delicate electronic devices affect important aspects of our lives such as security, the outcome would be even more devastating. In 2012, there was a solar storm of equal magnitude as the one that occurred in 1895 but luckily missed the Earth. Given the impact of these threatening events former U.S. President Barack Obama issued an executive order calling for preparations against solar flares in October 2016 [1]. Solar storms are one of the most significant outer space threats to normal life - hence the need for development of low cost access to monitoring of the Sun is imperative.

## 1.2 Mission Statement

Current Earth-based solar telescopes are very expensive in part due to the large and costly equipment required for compensation of astronomical "seeing" (Refraction and scattering distortions caused by Earth's atmosphere). This reduces the quality of images taken. Whilst space-based telescopes can avoid astronomical seeing and astronomical extinction (absorption of electromagnetic radiation in the ultraviolet, X-ray and gamma wavelengths), these require expensive rocket launchers and are practically impossible to modify or modernise once launched into orbit.

Traditionally, the best solution has been to locate observatories as high as possible to minimise the thickness of atmosphere. Lucky imaging is also used to capture moments when the turbulent atmosphere has no overall effect. Combining these conventional ideas, project SunbYte aims to use high altitude balloons to hoist a telescope to the edges of the Earth's atmosphere at 36 km altitude. High frame rate with allow "lucky imaging" and further increase the probability of acquiring scientifically worthwhile images.

## 1.3 Experiment Objectives

1. Primary objective: Track and image the Sun.
2. Secondary objectives: Acquire focused solar images to demonstrate scientific potential.
3. Tertiary objectives: Promote and increase space engineering studies in "aerospace engineering" courses across the country.

## 1.4 Experiment Concept

Based on the objectives, a full list of derived function, performance, design and operational requirements can be found in this report. To assess the validity of the design against these requirements, a test plan was established and can be found in Section 1.1 of the appendix.

In order to locate and track the Sun we have 2 tracking cameras attached to the telescope tube:

- a) **Wide-field tracker (360 camera):** using a conical mirror to provide 360 degree images that will enable the machine to determine the direction to slew the telescope to aim at the sun.
- b) **Precise tracker (precision camera):** using a high quality camera with narrower field of view to precisely track the sun in real-time.

Both of these cameras are connected to a Raspberry Pi (RPi), this will detect the bright disc of the sun in the images using Python code developed with OpenCV. A neutral solar filter at the front of the cameras (99.99% absorption) will ensure that only the disc of the sun is visible in images. Once the position of the Sun within the image is located, instructions are sent from the RPi to a Arduino



motor controller to reposition the telescope so that the center of the Sun is at the center of the telescope.

A science data acquisition camera will be attached to the prime focus of the telescope tube, this will be connected to a different RPi via USB and expected to capture images of 1920x1080 up to ~15 FPS (limited by the speed of the RPi). The images will be saved to an SD card for post-flight analysis. The system will also run a focusing routine to check and adjust the telescope focus as it expands and cools due to temperature/pressure changes. This will be carried out by shifting the focus, taking a sample picture and comparing the image to determine which image is in better focus.

Lastly, during flight, a selection of highly cropped and reduced images from each camera will be intermittently transmitted to the ground station to manually verify target and focus of the telescope.

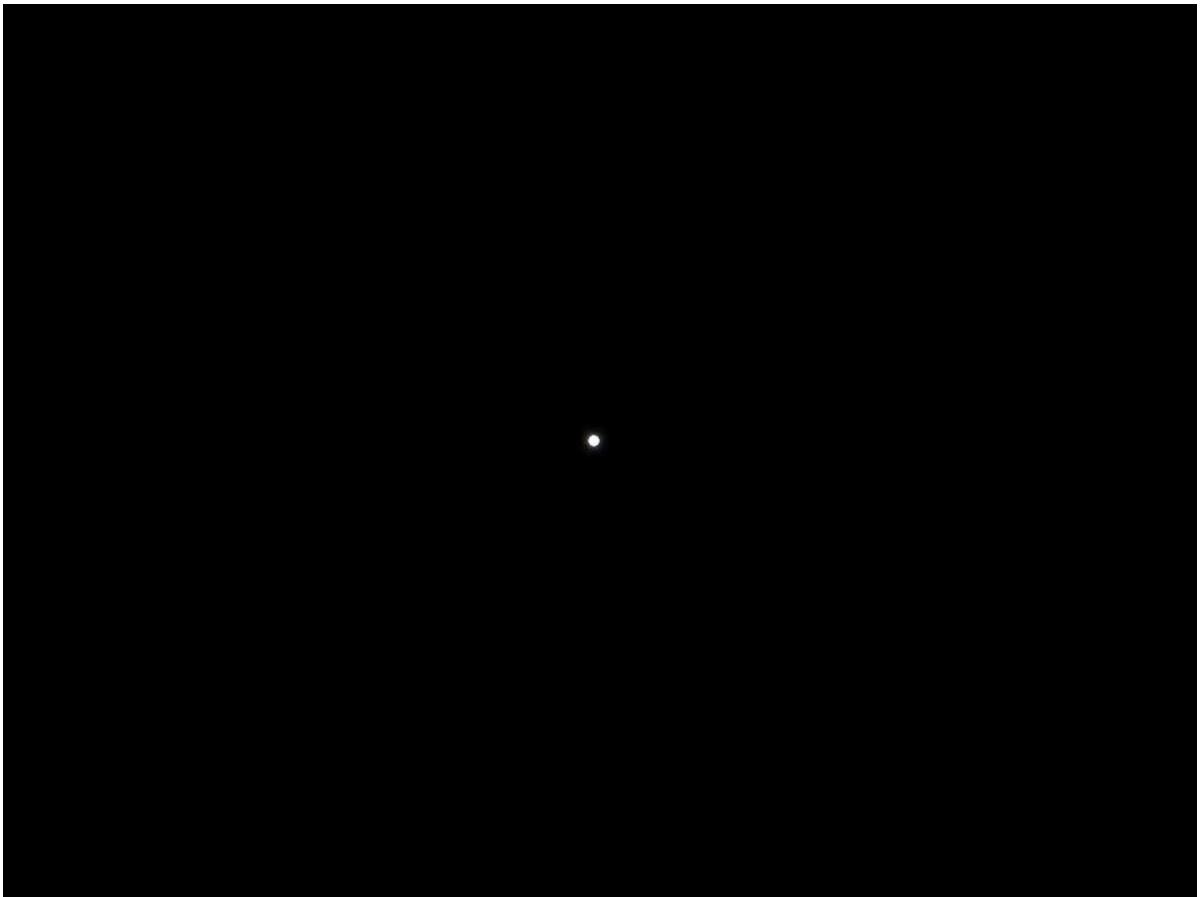


**Figure 1.4.1** – Images of the sun as taken by a RPi Camera Module v2.1 with Baader Planetarium AstroSolar Solar Filter film. The disc of the sun is clear and easy to track.



## 1.5 Team Details

### 1.5.1 Contact point

**Name:** Iakov Bobrov (team leader)  
**Address:** Department of Automatic Control and Systems Engineering  
 University of Sheffield  
 S1 3JD, UK  
**Tel:** +447554902627  
**E-mail:** ibobrov1@sheffield.ac.uk  
**Team E-mail:** SunbYte@sheffield.ac.uk



### 1.5.2 External support

Table 1.5.2.1 – External support



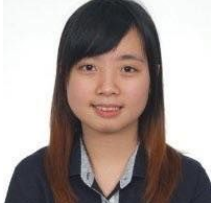


	<p><b>Name:</b> Dr. Viktor Fedun, Department of Automatic Control and Systems Engineering, PhD, The University of Sheffield (UK)</p> <p><b>Role:</b> Academic Lead</p> <p><b>Responsibilities:</b> Scientific and organisational support for funding and outreach purposes. Engages internal stakeholders and other departments.</p>
	<p><b>Name:</b> Yun-Hang Cho, Department of Civil Engineering, 2nd year PhD, The University of Sheffield (UK)</p> <p><b>Role:</b> Mentor</p> <p><b>Responsibilities:</b> Systems Engineering support and mentorship. Yun was previous team leader of SunbYte and lead the team to launch with the European Space Agency as part of REXUS/BEXUS program.</p>

### 1.5.3 Team members

Table 1.5.3.1 – Team members

	<p><b>Name:</b> Iakov Bobrov, 2nd year Aerospace BEng, University of Sheffield</p> <p><b>Role:</b> Team Leader</p> <p><b>Responsibilities:</b> Overall project management and coordination of all sub-teams. Previously a member of the mechanical team.</p>
	<p><b>Name:</b> Alex Hamilton, 2nd year Physics PhD, University of Hull</p> <p><b>Role:</b> Science and Optics Sub-team Leader</p> <p><b>Responsibilities:</b> Manage Science Sub-team and systems engineering between Science and software. Responsible for designing optical system and calculations regarding resolution.</p>



	<p><b>Name:</b> Joycelyn Fontanilla, 2nd year Chemical Engineering MEng, University of Sheffield</p> <p><b>Role:</b> Mechanical team leader</p> <p><b>Responsibilities:</b> Manage Mechanical sub-team and support technical design and implementation and outreach.</p>
	<p><b>Name:</b> Alexander Menzies, 3rd year Mechanical BEng, University of Sheffield</p> <p><b>Role:</b> Mechanical engineer</p> <p><b>Responsibilities:</b> CAD modelling assembly and Thermal Analysis</p>
	<p><b>Name:</b> Gianni Sin Yi Heung, 1st year Telecommunications MSc, University of Hong Kong</p> <p><b>Role:</b> Electrical team leader.</p> <p><b>Responsibilities:</b> Electronics, image focusing, telemetry and ground station interface.</p>
	<p><b>Name:</b> George Robinson, 2nd year Aerospace MEng, University of Sheffield</p> <p><b>Role:</b> Mechanical engineer</p> <p><b>Responsibilities:</b> CAD modelling and outreach</p>
	<p><b>Name:</b> Brandon John O'Connell. 3rd year Aerospace MEng, University of Sheffield</p> <p><b>Role:</b> Mechanical engineer</p> <p><b>Responsibilities:</b> CAD modelling and Finite Element Analysis</p>

**It is anticipated that between 4 and 6 students will participate in integration at CSBF and 8 students will participate in flight operations at Fort Sumner.**

#### 1.5.4 Team organization

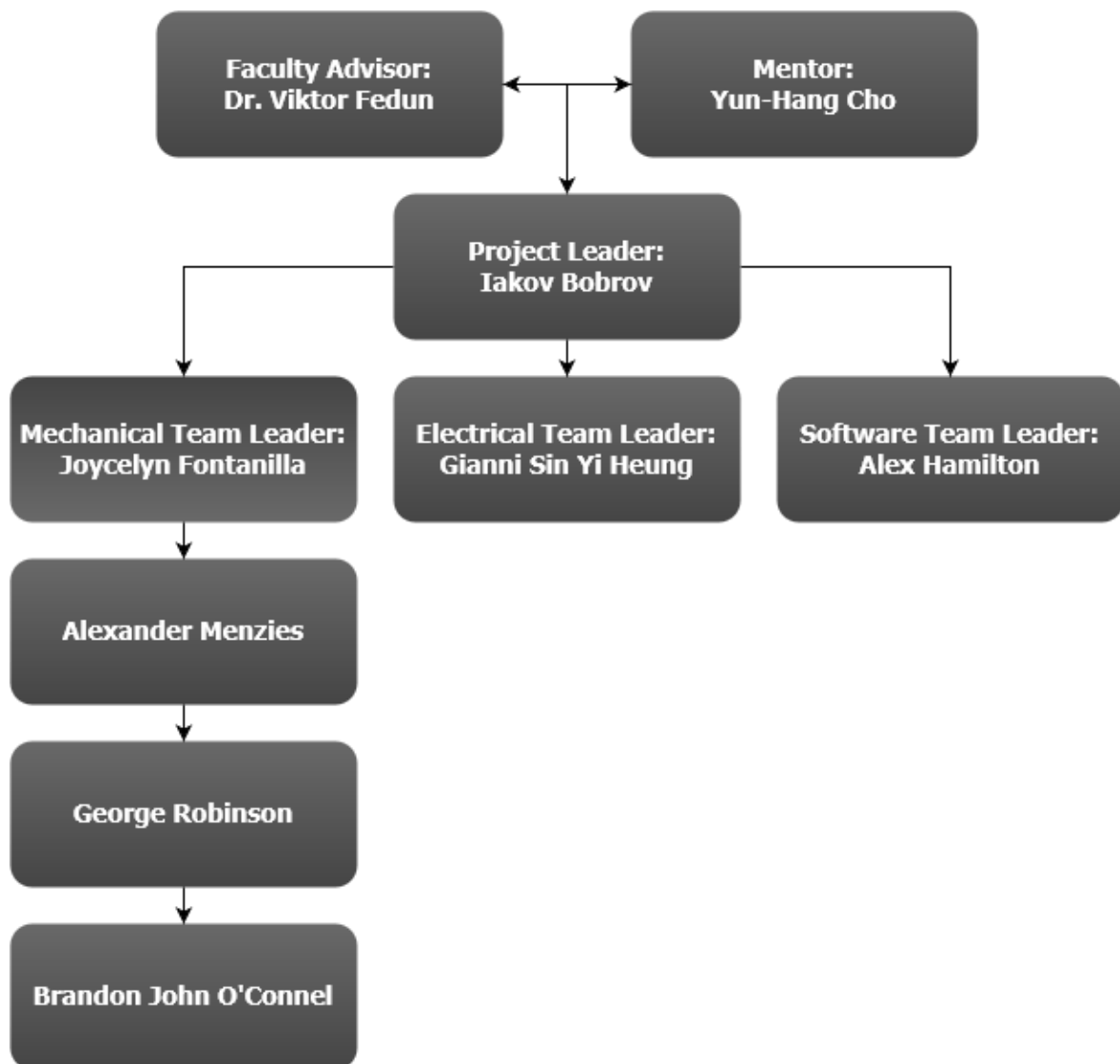


Figure 1.5.4.1 - Team organization chart

Team organization chart is shown in Fig 1.5.4.1. Project guidance is provided by Faculty Advisor and Mentor. Project leader is responsible for distributing task to leaders of each sub-team and overall management of the project. Project leader is responsible for ensuring each sub team meets their deadlines and objective. Each team leader allocates tasks and technical support to the members. End of each month, the project leader and sub-team leaders are producing a monthly report to present the progress of the project. This ensures all objective are met on time.



## **2. Experiment requirements and constraints**

### **2.1 Functional Requirements**

- F1. The camera shall successfully track the Sun.
- F2. The experiment shall image the Sun in the spectral line at 393 nm (K-Ca) or 656.28nm (H-alpha).

### **2.2 Performance Requirements**

- P1. The gimbal system shall direct the telescope towards the Sun with an accuracy of at least 1 arc minute.
- P2. The telescopes diffraction limited resolution shall be within a value of 1.5 arcsecs.
- P3. The Sun shall be imaged at a maximum rate of 40 fps.
- P4. The experiment shall produce an output image with a resolution of 0.6 arcsec at the vacuum wavelength of H-alpha line core - 656.28nm.
- P5. The maximum current drawn shall not exceed 2.5A.
- P6. The supporting structure shall withstand a maximum compressive load of 200N.
- P7. The tracking camera shall have a video resolution of no less than 640 by 480 pixels and 30 fps

### **2.3 Design Requirements**

- D1. The experiment shall operate in the temperature profile of the HASP vehicle flight and launch.
- D2. The experiment shall operate in the vibration profile of the HASP vehicle flight and launch.
- D3. The experiment shall operate in the pressure profile of the HASP vehicle flight and launch.
- D4. The experiment shall not disturb or harm the launch vehicle.
- D5. The experiment shall not broadcast at a frequency prohibited in New Mexico.
- D6. The diameter of the primary mirror shall not exceed 85 mm.
- D7. The length of the telescope shall not exceed 380 mm.
- D8. The mass of the experiment shall not exceed 20 kg.
- D9. The maximum tolerance of any gearing has to be within 0.2 arc minute.
- D10. The Sun sensor shall detect intensities of up to 100,000 lux.
- D11. The supporting structure shall not twist by more than 0.1 degrees.
- D12. The supporting beam shall not buckle under a safety factor of 2.
- D13. The experiment shall be able to run for up to 20 hours.
- D14. The datalogger shall able to receive signal and store it.
- D15. The main computer shall able to communicate with the ground station
- D16. The external focuser shall able to adjust focus up to 8mm.

### **2.4 Operational Requirements**

- O1. The experiment shall accept control of the focusing motor for manual focus if a command is sent.
- O2. The experiment shall enter the searching pattern if the location of the Sun is not found according to the astronomical algorithm.
- O3. The experiment shall transmit images to the ground when requested.
- O4. The experiment shall cease to rotate on landing.
- O5. The experiment shall be able to read data from a GPS device.

### 3. Project Planning

The project is managed on a day-to-day basis by the sub-team leaders. As principal participant, the team leader is responsible for overall project management and direction. The project will be supervised by the Academic Lead with mentoring support to conduct internal project reviews. This will highlight the progress made, and allow for planning and discussion for further advancement of the project.

The team leader is responsible for the successful running and delivery of the following tasks:

1. Meeting the contractual obligations of the project (financial, administrative, and scientific).
2. Monitoring the progress of the project and ensuring deliverables are met.
3. Organising, chairing and reporting of project meetings.
4. Ensuring good, timely communications between the members of the team and stakeholders.

At the operational level, each task has a responsible student lead (supported by an Academic Advisor when necessary). His/her main responsibility also includes understanding of other the other work carried out by their sub-team and how it fits within the project deliverables.

#### 3.1 Schedule

##### 3.1.1 Overall project Gantt Chart

The project can be divided into 7 main phases; these are shown in the table below alongside with non-productive periods, such as exams and holidays.

The table below explains some of the key activities taking place during each stage.

Phase	Name	Description
0	Concept	Develop concept and feasibility analysis of mission
A	Preliminary Design	Develop requirements and first design
B	Detailed Design	Build test prototypes to validate and develop design
C	Manufacturing	Manufacture, test and assembly of flight model
D	Integration	Integrate payload into launch vehicle
E	Launch	Launch activities, monitor status, downlink data, uplink commands
F	Post Processing	Analyse data and compare against industry standards

**Figure 3.1.1.1 – Legend for Gantt Chart**

Using the work breakdown structure, the Gantt chart below shows a detailed breakdown of the tasks undertaken by each sub-team during the current phase (detailed design) and the periods of when the activities began and will finish.





	2017			2018											
	Oct	Nov	Dec	Jan	Feb	Mar	Apr	May	Jun	Jul	Aug	Sep	Oct	Nov	Dec
s	Launch			Exam				Exam	Holiday						
e O	Concept														
e A		Preliminary													
e B				Detailed Designs											
e C						Manufacturing, AIT									
										Payload integration with HASP, July 23 – July 2					
e D															
e E												Launch, September 2			
e F													Post processing		
					Revised application or response to reviewer due - Feb 26		Preliminary Payload Specification & Integration Plan (PSIP) due - April 27		Final Payload Specification & Integration Plan (PSIP) due - June 22	Final Flight Operation Plan (FLOP) due - July 19; Flight Ready Payload due - July 23					Final Flight / Science Report due - Dec 7

Figure 3.1.1.2 – Gantt Chart

### 3.1.2 Project planning by sub-team

Figure 3.1.2.1 shows the project plan for the mechanical team. No work is to take place during the exam periods. Spare days have been planned to account for possible delays.

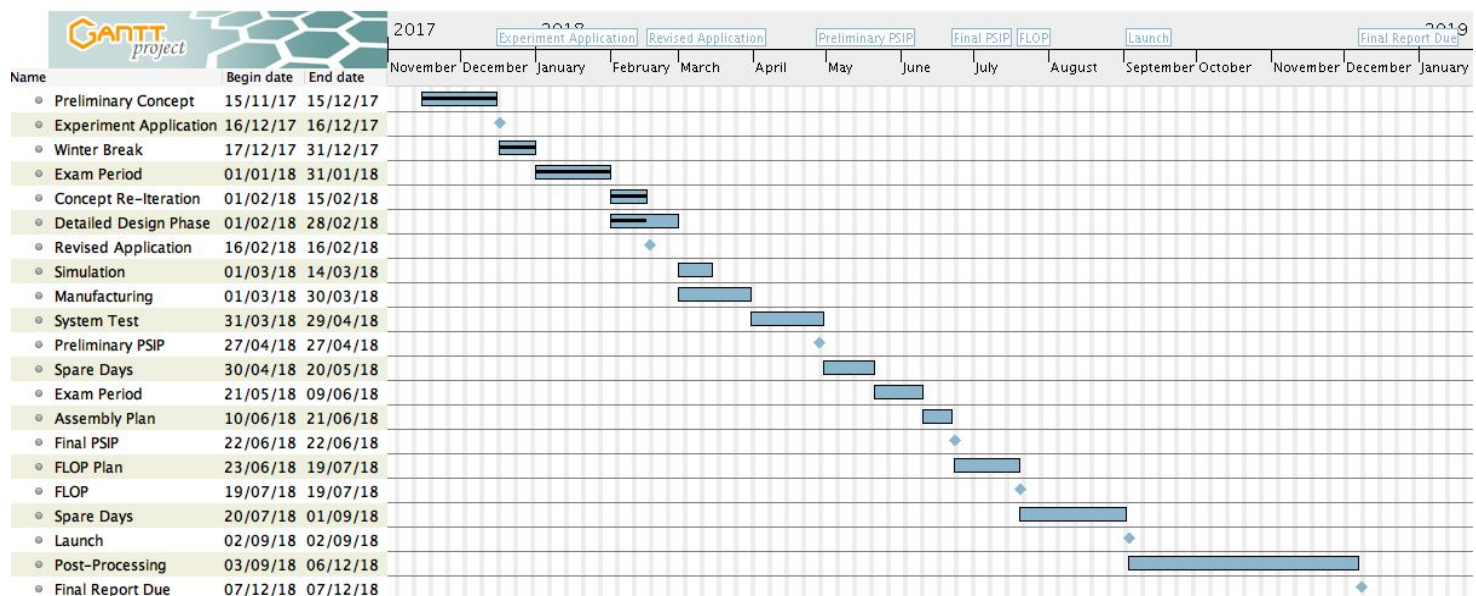


Figure 3.1.2.1 – Mechanical Team Gantt Chart

The Work Breakdown Structure is shown in Table 3.1.2.1, and details the allocation of sub-tasks and their estimated duration.

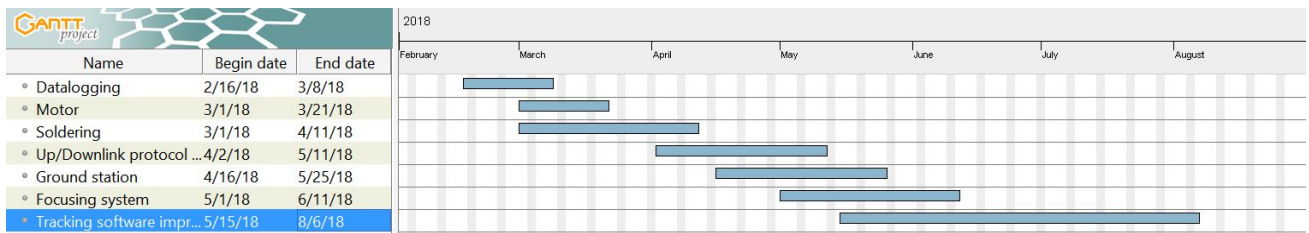


Figure 3.1.2.2– Electrical and Software Team Gantt Chart

Table 3.1.2.1 – Mechanical Team Work Breakdown Structure

Task	Details	Duration (Days)	Lead
<b>Preliminary Concept</b>		31	Joycelyn
Design Concept	Generation of preliminary design concept	20	Joycelyn
CAD Modelling	CAD Modelling in SOLIDWORKS of preliminary concept	11	Alexander
<b>Concept Re-Iteration</b>		15	Joycelyn
Design Concept	Feedback used to generate revised concept	7	Joycelyn
CAD Modelling	CAD Modelling in SOLIDWORKS of revised concept	8	Alexander
<b>Detailed Design</b>		28	Alexander
Engineering Drawings	Production of technical drawings in SOLIDWORKS for manufacturing	7	Brandon & George
Manufacturing Plan	Assigning manufacturing tasks, send requests to workshops for complex parts	14	Alexander
Purchasing	Ordering material (to be done in parallel to other tasks)	7	Joycelyn
<b>Simulation</b>		14	Brandon
Structural FEA	Analysis using ANSYS software	14	Brandon
Thermal FEA	Analysis using ANSYS software	14	Brandon
<b>Manufacturing</b>		30	Joycelyn
Manufacturing	Manufacturing of mechanical components, collection from workshops	25	Joycelyn
Assembly	Integration with electronics hardware	5	George
<b>System Test</b>		30	Iakov
<b>Assembly Plan</b>		12	George
<b>Spare Days</b>		21 (Pre-FLOP) + 44 (Post- FLOP)	Joycelyn

Table 3.1.2.2 – Electrical/Software Team Work Breakdown Structure

Task	Details	Duration (Days)	Lead
<b>Electronic Sub Team</b>		61	Gianni
Focusing system	Developing an arduino code for focusing system	61	Gianni
Motor	Developing a stoppable telescope protection system	15	Gianni
Soldering	Soldering all parts together	10	Iakov
Data logging	Building the sensors to monitor the system performance	15	Gianni
Updown/ Download cable	Up/Downlink protocol development	45	Gianni
<b>Software Sub Team</b>		75	Alex
Tracking	Software improvement	75	Alex
Ground Station	Design a ground station that collects all real time data and displays it	61	Gianni/Alex



### **3.2 Risk**

A list of safety, project and technical risks can be found in the Appendix on page 40. Actions to reduce these risks are stated where necessary.

## 4. Experiment description

This section can be split into five sections:

1. Optics
2. Mechanical structure
3. Electronics
4. Software
5. System Budget

### 4.1 Optics

#### 4.1.1 Optics Introduction

The Sun subtends an angle of approximately 1,865 arc seconds (0.52 degrees) to an observer on the Earth. The diameter of the Sun is  $1.392 \times 10^9$  m (864,949 miles).

Since the telescope will be limited to making observations of the Sun only, it will be acceptable to use an optical system with a narrow field of view.

#### 4.1.2 Optical Calculation

Telescope resolution is also limited by atmospheric distortion and diffraction. At ground level, atmospheric distortion limits telescope resolution depending on altitude/location. Most Earth telescopes are limited by atmospheric distortion but within the HASP operating environment, atmospheric distortion is minimised because there is low pressure. The diffraction limit arises due to the size of the primary reflecting optic. This may be calculated as: (1 radian = 206,265 arcsec.)

The angular resolution is determined by:

$$\begin{aligned}\text{Angular resolution} &= 1.22 \times \frac{\text{wavelength}}{\text{optic diameter}} \\ &= 1.22 \times \frac{656.28\text{nm}}{90\text{mm}} = 0.032 \text{ arcsec}\end{aligned}$$

Likewise angle of view is limited by:

$$\begin{aligned}\text{FoV} &= \arctan\left(\frac{\text{sensor size}}{\text{focal length}}\right) \\ &= \arctan\left(\frac{6\text{mm}}{1250\text{mm}}\right) = 990 \text{ arcsec}\end{aligned}$$

Sensor resolution is limited by:

$$\begin{aligned}\text{Sensor resolution} &= \arctan\left(\frac{\text{pixel spacing size}}{\text{focal length}}\right) \\ &= \arctan\left(\frac{6\text{mm}/1280}{1250\text{mm}}\right) = 0.7727 \text{ arcsec}\end{aligned}$$

#### 1. Environmental considerations

- Temperature variations: It is expected that the telescope will suffer an extreme range of temperatures. Due consideration will be given to thermal expansion (contraction) which may impact the primary and secondary mirror alignment as well as the positioning of the imaging sensor at the focal point of the telescope.
- Condensation of water vapour: Consideration will also be given to the possibility that water vapour may condense on the optics at altitude due to low temperatures.



## 2. Filter selection

Energy Rejection filter (ERF) to block the majority (99.99%) of light, especially in the UV and IR parts of the spectrum to protect optics and sensors. The Etalon filter is placed in the optical path just before the camera, this will block all but the 656.281 nm ( $\pm 0.6 \text{ \AA}$  HBW), giving a high contrast image in the H-alpha band.

### 4.1.3 Telescope Selection

Because of considerations outlined above, a cassegrain type telescope is used due to long focal length with a compact length and volume. The telescope selected is the Meade ETX 90. This uses a Maksutov Cassegrain reflector design.

This design differs from the classic Cassegrain design by having a corrective negative lens at the front of the telescope to correct for the off-axis aberrations. The design has a relatively narrow field of view making it suitable for solar observations.

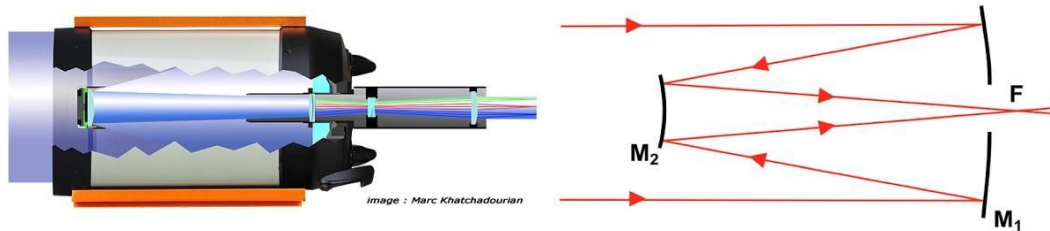


**Figure 4.1.3.1 – Telescope configuration**

A 90 mm primary optic offers a 1.54 arcsecond resolution for light 550 nm. (1 radian = 206,265 arcsec.)

### 4.1.4 Filter selection

In order to evaluate the performance of the focus control, a resolution of  $<2$  arcsec at the vacuum wavelength of H-alpha line core (656.28 nm) is required. The choice of the line is based on the following factors:

- The sensitivity of most CCD/CMOS cameras are close to its maximum at this wavelength;
- This wavelength is close to the peak of the Planck function, which approximately describes the solar radiation spectrum as a black body radiation with the effective temperature of 5700 K;
- H-alpha line core is formed mostly in the solar chromosphere with some lower corona influence, making it especially attractive for scientific applications;
- H-alpha line core etalons are commercially available as they are commonly used in amateur astronomy.
- The images produced will have a high range of contrast, with light and dark feature visible, which should be ideal for allowing the image to focus.

As an alternative, consideration has been given to the use of a CaK (394 nm  $\pm 80 \text{ \AA}$  HBW) dielectric lens filter. This has the following considerations:

- A similar section of the spectrum to H-alpha, so suitable for most optical setups and cameras.
- Has a wider suitable bandpass, making it more suitable for shorter focal length setups. We could also “double stack” two filters to narrow the bandpass.



- Is cheaper, lighter and requires no power supply to maintain the correct bandpass.
- The CaK emission is mostly in the Chromosphere, overlapping H-alpha but ending higher in the solar atmosphere, this will show features like granulation, sunspots and faculae.

Figure 4.1.4.1 shows a comparison between the images which can be obtained using Baader, H-alpha and CaK.

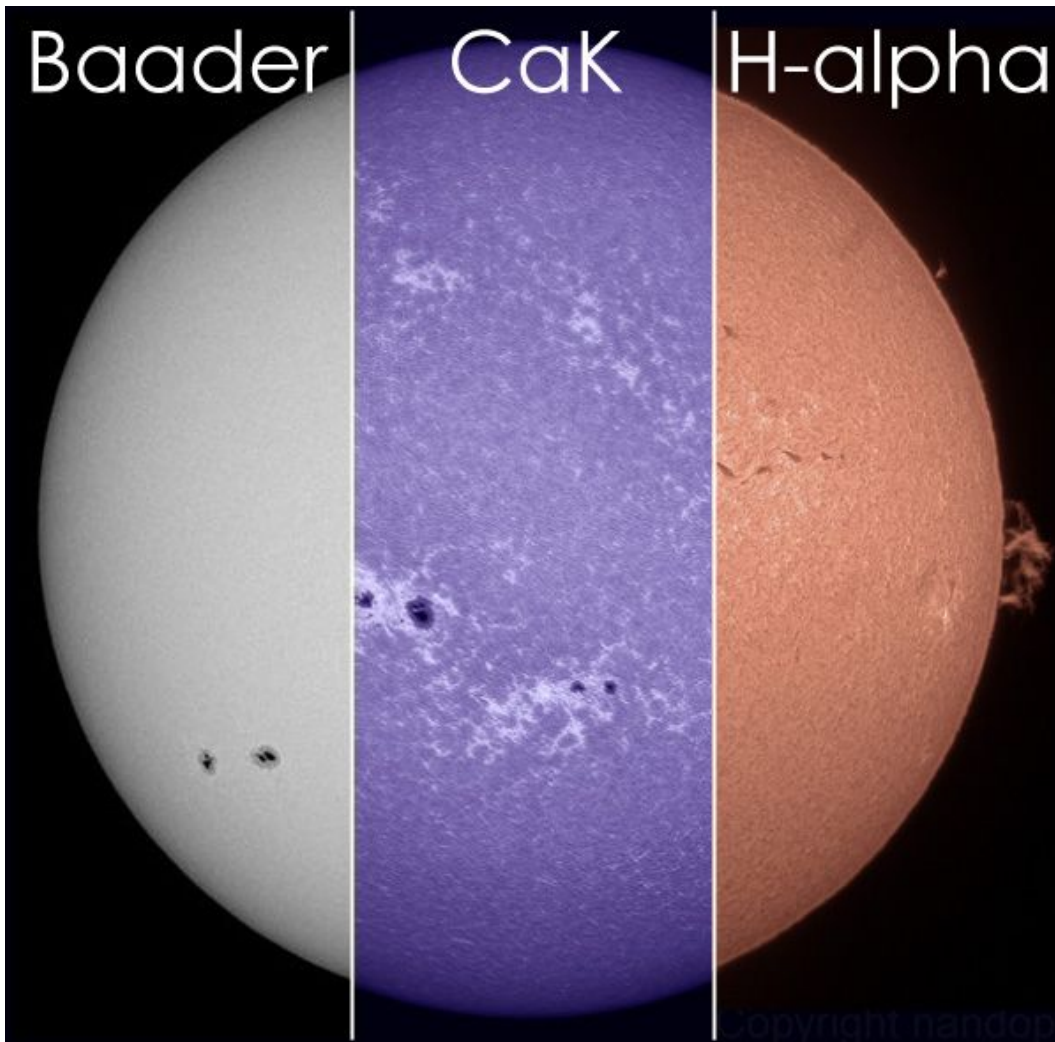


**Figure 4.2.1.1** – Image comparison of Baader white-light filter (left), K-Ca and H-alpha etalon filter. As can be seen, the white light shows little detail beyond sunspots, while the CaK and H-alpha filters show a good variety of details. [4]

1 arcsec resolution is achieved by a telescope with a primary mirror of 80 mm diameter, which its diffraction-limited resolution is 0.825 arcsec at the required wavelength. It is preferential to use bursts of short exposures for solar imaging to reduce impact of imperfections in the stabilisation system. This will reduce the blur caused by the residual gondola movement, and application of standard solar imaging processing software (SunPy and IDL SolarSoft) to the obtained data will eliminate shifts and align images, further improving the effective resolution. Taking into account the broad frequency spectrum of gondola motions, short exposures of 0.05 seconds are needed to maintain sufficient image quality. However, short exposures lead to less light arriving at sensor. Therefore, a highly sensitive CCD such as the ZWO ASI120mm (mono) are used.



#### 4.1.5 Optical system Design

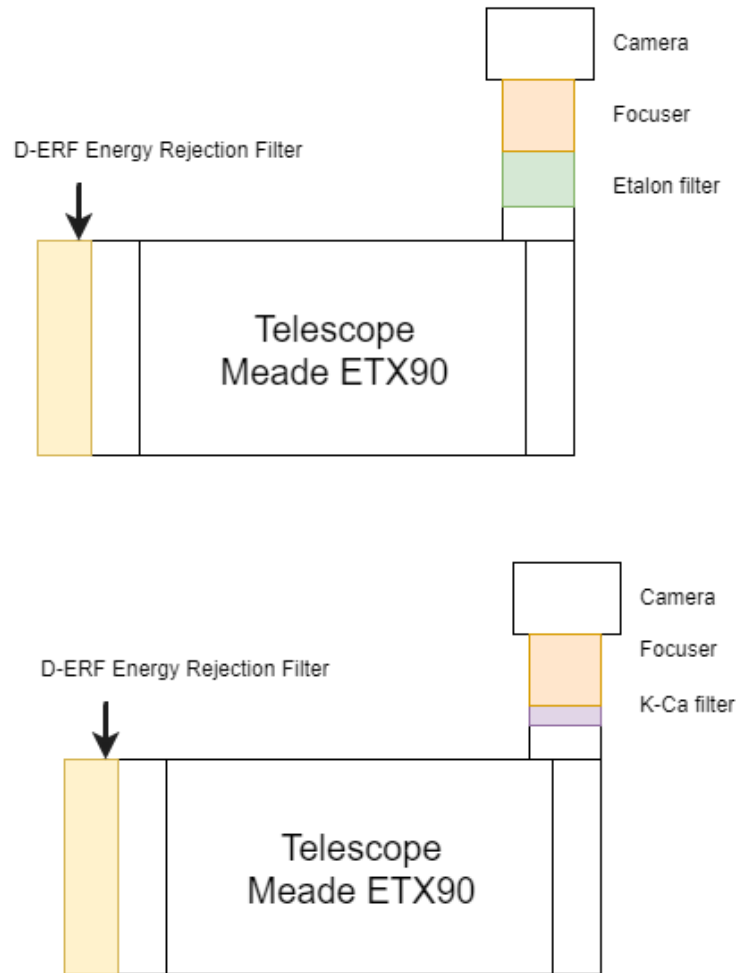


**Figure 4.1.5.1 – Schematic of optical system**

Figure 4.1.5.1 shows the optical design concepts, the upper diagram is the primary design of the system. Energy rejection filter is installed at the front end, it reduces the total flux into the telescope and thus protects the mirrors from heating up. The telescope is optically placed in the middle, etalon and focuser are attached on top of the viewfinder. The internal focuser moves the primary mirror, this is not used in flight because it requires good lubrication to get smooth movement, which cannot be guaranteed given the extreme variation of environment the telescope will be subjected to. Therefore an external helical focuser will be used. The scientific camera is placed at the end of the optical path to capture images.

One concern is the survival of the relatively expensive etalon filter, at high altitudes the extremely low temperature and pressure could cause damage and make it hard to maintain the correct temperature for the etalon to accurately fix on the correct bandpass, as an alternative, if vacuum tests show an issue a much simpler K-Calcium (K-Ca) lens filter can be used instead, This does not require a constant temperature to operate correctly hence eliminating the need for a power supply while also being lighter and more durable.

The allocation of the secondary design are shown in the bottom of Figure 4.1.5.1 Etalon filter is replaced by K-Ca filter.

## 4.2 Mechanical Design

### 4.2.1 Gimbal

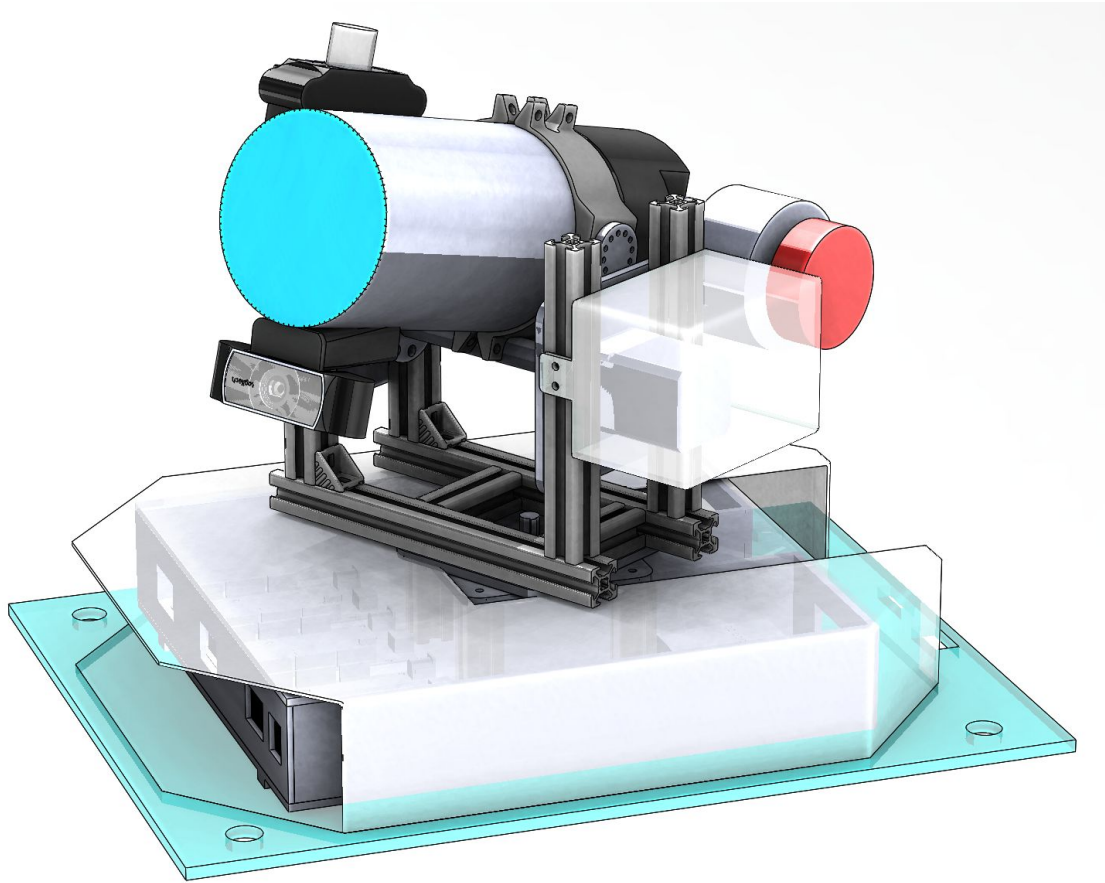


**Figure 4.2.1.1** – Gimbal design

A telescope shaft is mounted with flanges to circumferential telescope clamps. The shaft flanges attach directly to the motor output preventing angular error. The motor flange output is geared and has bearings able to support estimated peak loads. The electronics housing is constructed of transparent acrylic with a sliding draw for easy access upon which the PCBs are mounted. Yaw and pitch rotation are powered by two identical motors, and their drivers are mounted beneath the roof of the electronics housing.





## 4.2.2 Gimbal Frame

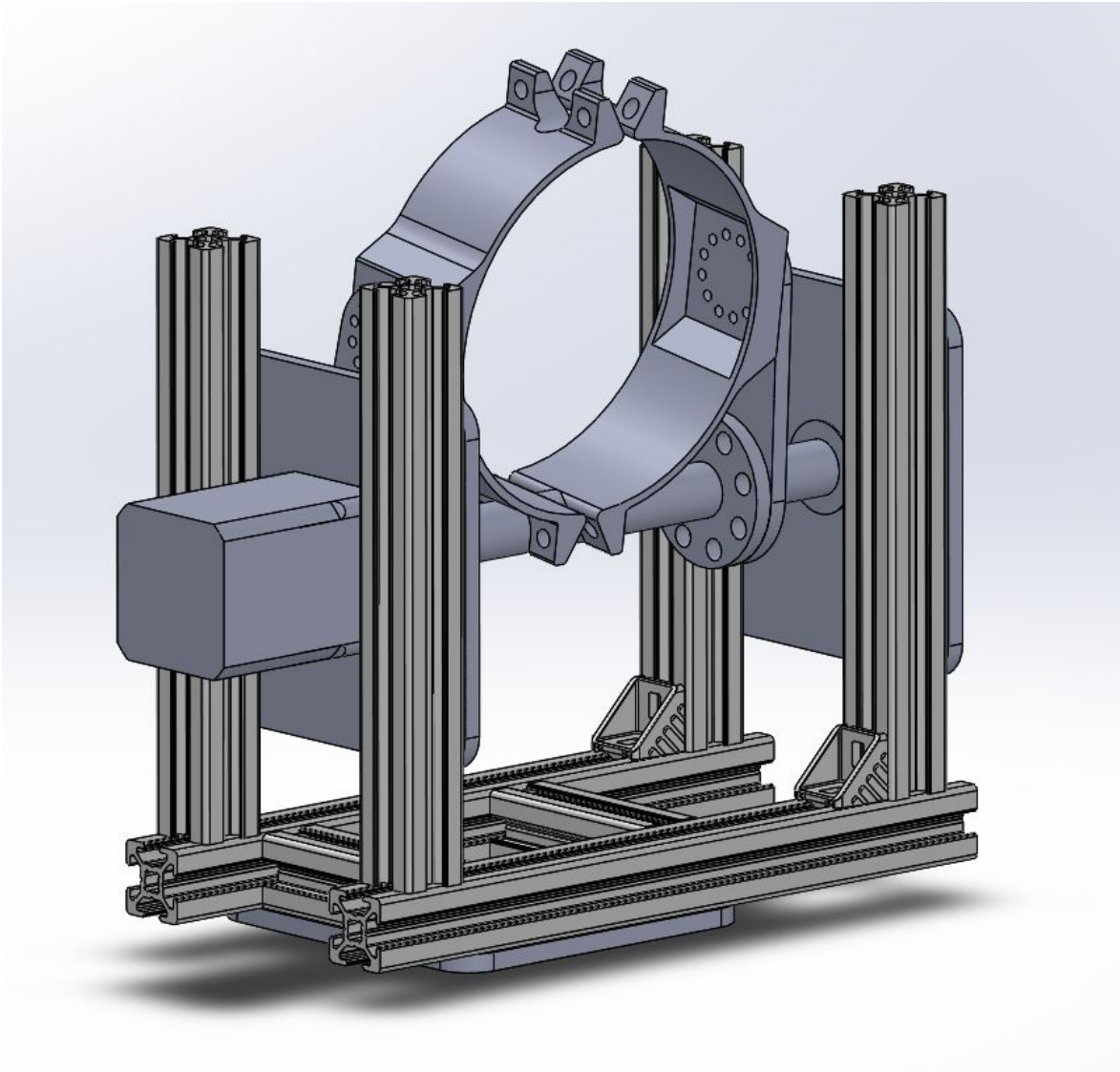


**Figure 4.2.2.1** – Gimbal frame

The gimbal frame is constructed from Bosch extrudes, this is to allow adjustability of the precise dimensions during calibration. This will also improve the speed with which the structure can be assembled and disassembled for transport or during testing.

### 4.2.3 Telescope Clamps

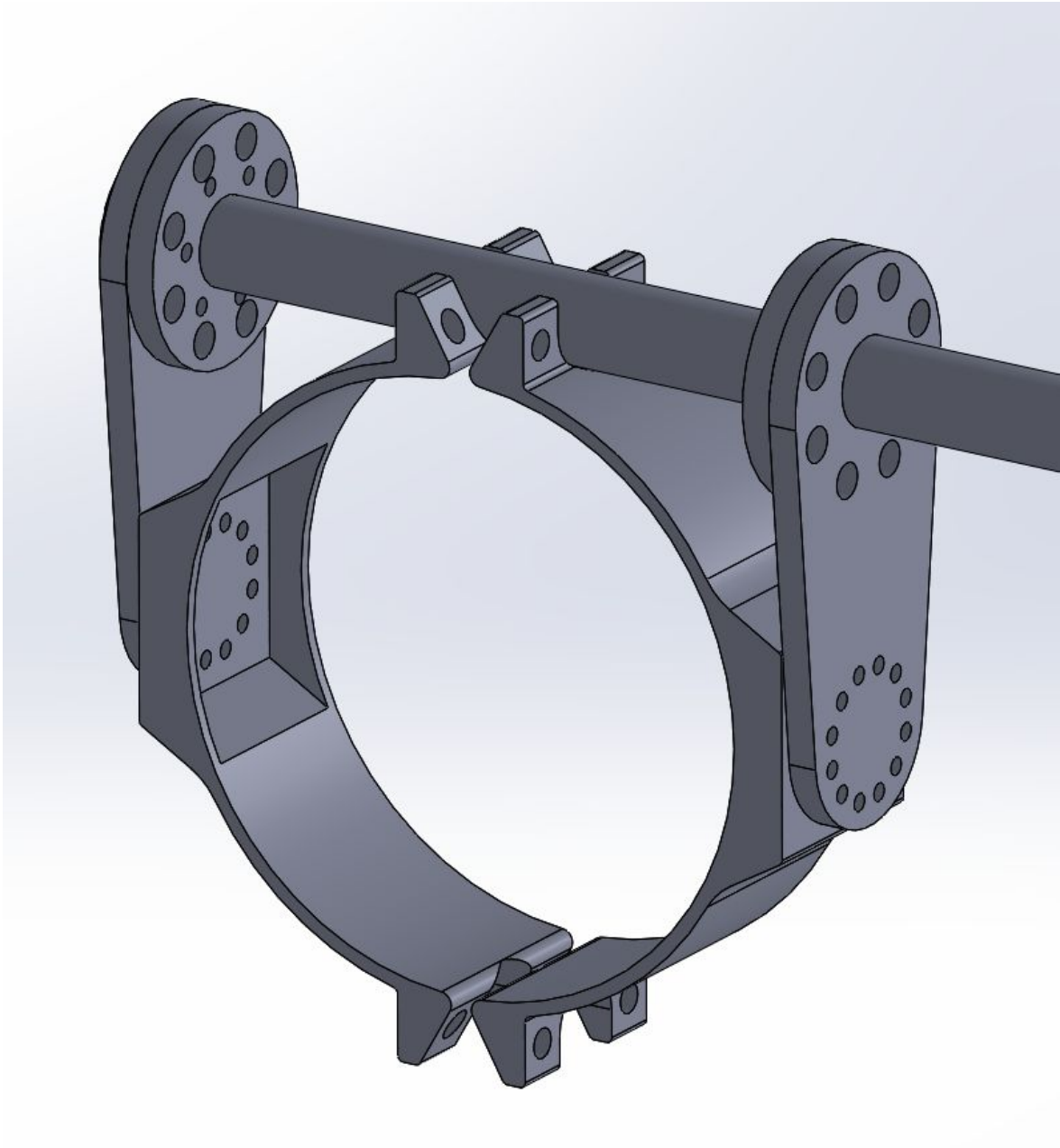


**Figure 4.2.3.1** – Telescope clamps  
Used to clamp the telescope to the motor shaft for pitch movement.



#### 4.2.4 Shaft Cross-section

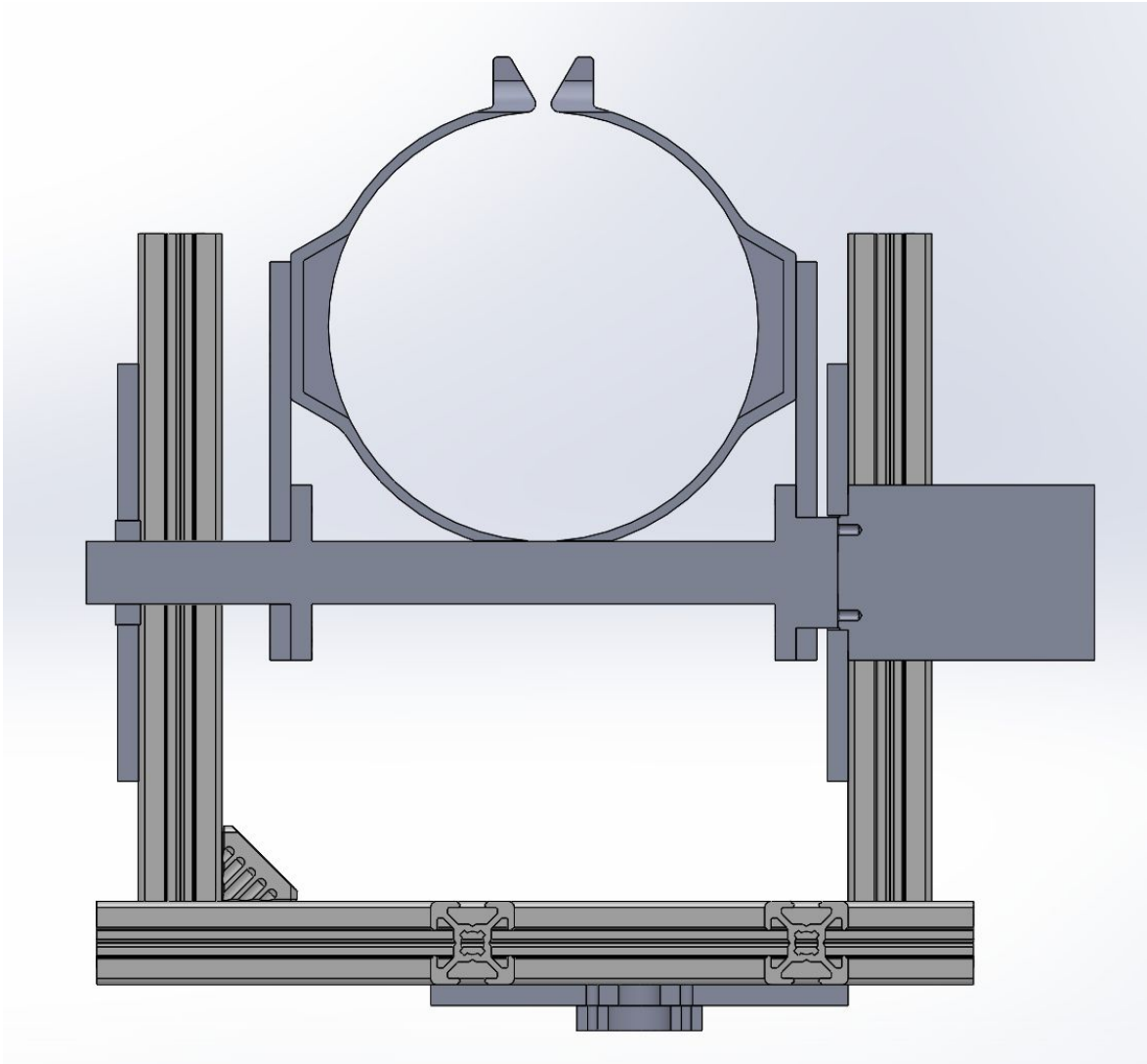


**Figure 4.2.4.1** – Shaft Cross-section design

On the left plate there is a bearing with the compression fit shaft in its interior. On the right plate the motor is mounted onto a plate, and mounted to the motor output flange is the shaft. The interface between telescope clamps and shaft consist of two 5 mm adapters to be made from Aluminium metal.

#### 4.2.5 Pitch Motor

The motor driving the pitch movement of the telescope is to be mounted on one of the side support plates. It shall be enclosed within foam insulation and aluminized mylar foil which will be wrapped around the foam to protect possible overheating of the enclosure via solar radiation. There shall be a hole for cables to escape from the bottom face of the insulation. The motor specifications and dimensions can be found within the Appendix.

#### 4.2.6 Yaw Motor Housing

The motor driving the yaw of the telescope shall be mounted onto a square plate, which in turn is mounted onto four Bosch-extrude legs. This mounting is achieved by tapping the ends of the Bosch legs and screwing the plate onto the legs as shown in Figure 4.2.6.1.

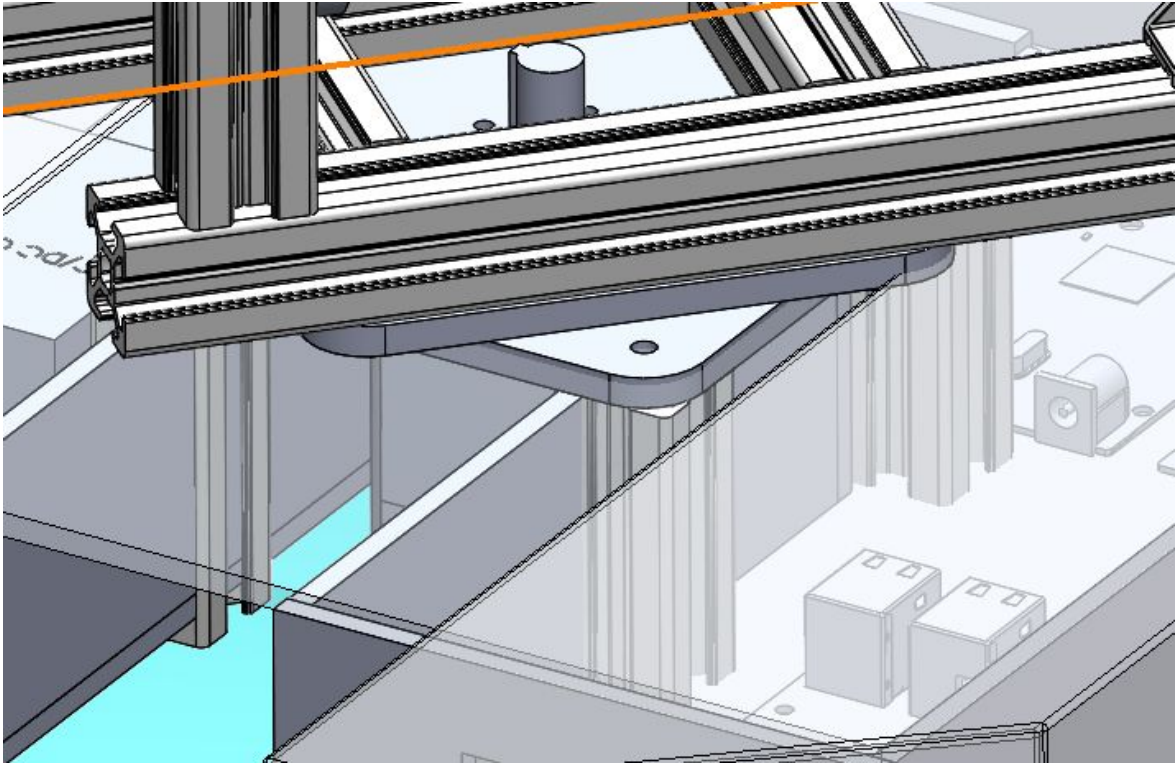


**Figure 4.2.6.1 - Yaw motor structure**

The housing shall be made of laser-cut acrylic of 3mm thickness screwed to the sides of the Bosch legs. Its purpose is to enclose a layer of insulating foam around the motor.

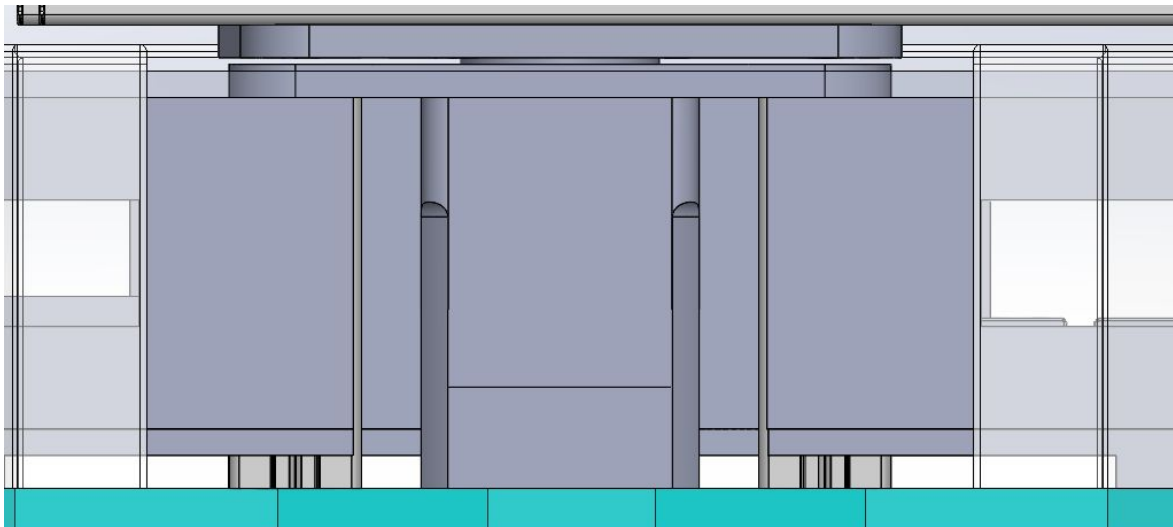


**Figure 4.2.6.2. – Yaw motor housing on assembly**

#### **4.2.7 Motor shaft adapter**

The motor adaptor linking the output flange to the gimbal will be made a simple machined aluminium piece.



#### **4.2.8 Electronics Box**

To facilitate easy testing, assembly and access, the electronics are mounted on a sliding drawer which can be pulled out from underneath the gimbal. This is locked during flight to prevent sliding. The electronics box will be covered by a box, made of transparent, laser-cut acrylic sheeting and glued together. A layer of 3cm insulating PE foam will be fixed inside this covering to protect the electronics from the cold temperatures. There shall be holes on the wall of the covering for cables to exit. The entry of cold air will be prevented by covering any gaps with Kapton tape.

## 4.3 Electronics

### 4.3.1 Electronics Overview

The main goal of the electronic components is to provide a platform for the software that allows an effective tracking of the Sun and correct adjustment of the telescope. During the entire duration of this project the electronic components selected have changed continuously, this has been possible due to a total lack of custom electronic designs. We rely entirely on off-the-shelf components already integrated in an easy to use platform.

The elements have been summarized below.

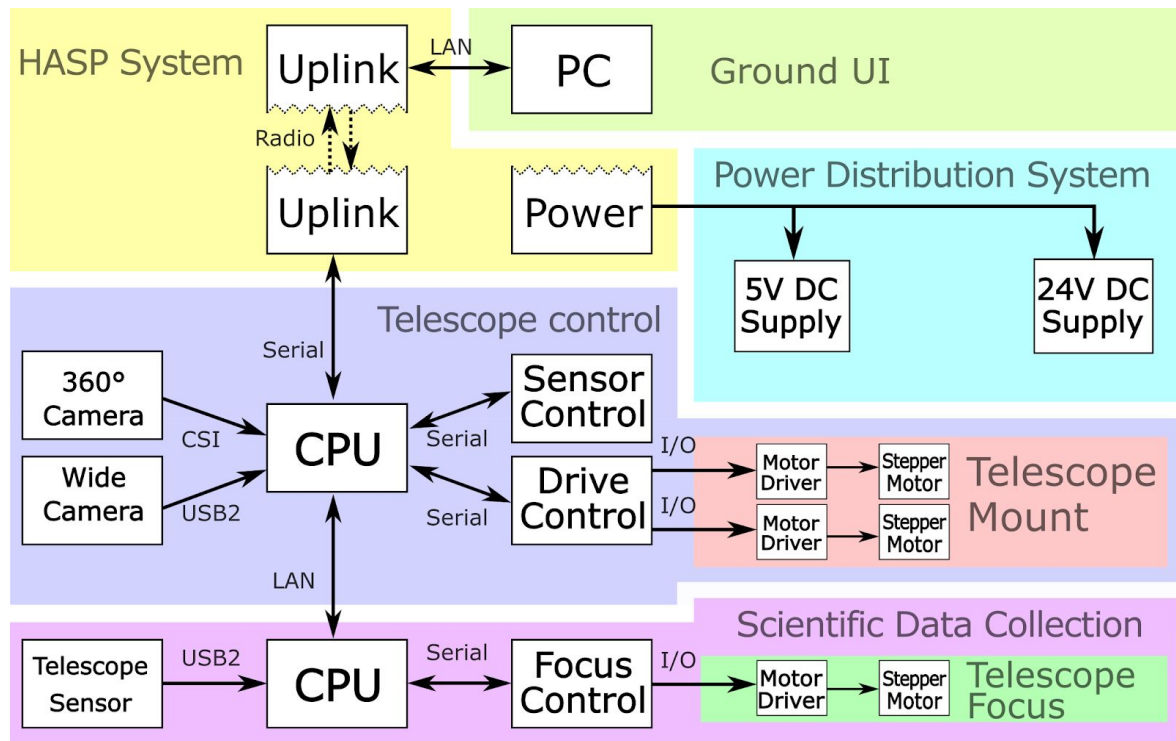


Figure 4.3.1.1– Overall electrical architecture interface.

In its current state, the entire system is composed of a RPi in charge of overall control of the experiment and Sun tracking through a 360 degree camera (360 camera) and a precise camera (Precise camera), three Arduino-based EtherMegas for motor control and monitoring sensors, a second RPi (Sci-RPi) for data acquisition with our CCD camera, 2 high resolution stepper motors, 1 focusing system, 3 DC/DC converters, 2 CVK series drivers for controlling the motors and several sensors for monitoring current sensors, temperature and acceleration.

- **Arduino Mega** The Arduino is the base for motor control. Additionally, it will provide some extra ports for sensors. During testing each bipolar stepper motor has required at least 4 of the 14 available digital I/O ports. Since the motors will be substituted in the future by 5 phase motors, the final employed Arduino microcontroller platform will most likely be Arduino MEGA opposed to the Arduino UNO used during most testing up to date. The reason for this change is the far superior amount of available digital and analogue connections.
- **Raspberry PI v3** is the brain of proposed Sun tracking and position estimation algorithms. It provides communication with the ground station as well as manages all interfaces between electronic devices.



- Webcam Logitech C920 Linux allows for the use of many webcams. Logitech C920 provides 1080P@30 Hz with hardware MPEG H.264 compression over USB2.0.
- **Stepper Motors** Due to incredibly demanding accuracy, ultimately these motors will be substituted by 5-phase stepper motors with as little as 0.36 degrees per step. In addition, a method of operation known as micro-stepping will be carried out through the CVK series drivers to reduce the need of a very precise gearbox / harmonic drive. All elements involved have already been acquired and the method described is an industry-proven solution.
- **DC/DC buck Converters** Due to the fact that, regarding power testing is currently carried out by use of several DC power supplies, the final DC/DC converters have not been selected. However the needed conditions are at this point almost certain with 3 converters. Two of them will deliver 12 and 5V supply to electronic devices located inside the gondola while the other one will deliver a 12V supply both to the stepper motors and motor as well as the sCMOS camera.
- **Adafruit 10 DoF** This element is particularly useful to provide basic telemetry as well as to provide the necessary information for one of the Sun locating solutions based on position of the gondola with respect to the magnetic pole of The Earth and the date/time during the HASP flight. It includes Gyroscope, Magnetometer, Barometer and Thermometer.

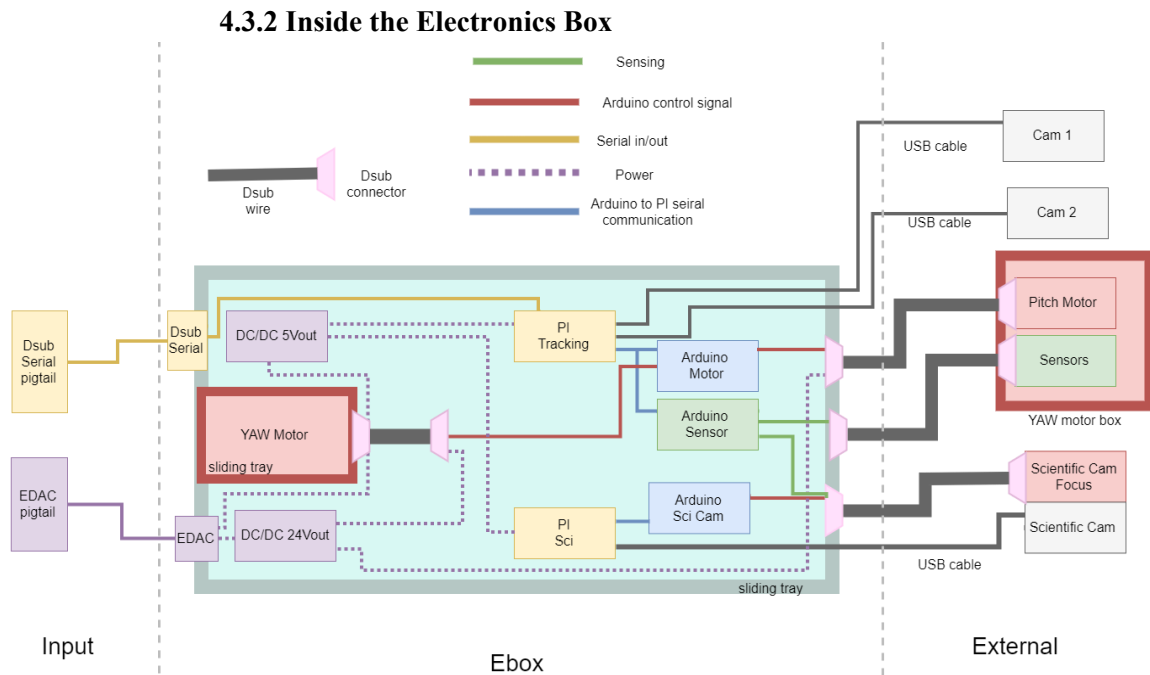


**Figure 4.3.2.1** – The wiring diagram of the e-box

The wiring diagram is shown in Figure 4.3.2.1. There are two parts of the E-box. They are marked in red and blue. The blue box is a sliding box which the electronics can be slide in and out without removing the telescope. The Yaw motor is unremovable, the red box is fixed. All other electronics are accessed via the sliding tray. A locking system to secure the position of the tray during flight.

The circuit is divided into 3 parts: Interface to HASP, E-box Internal and external devices. The wires were labeled in four colors. Power is labeled in purple which connects the power for motor and RPis. The blue cables are Arduino-Pi connection, it provided a linkage between the main computer to output command to the motor via arduino as well as received data from sensor. Dsub 15 cable marked in black, when the box is sliding, the distance between the yaw motor box and



arduino is increased so a longer cable is used to extend the port in order to protect the wire. Each part is explained in details below.

#### 4.3.3 1 Interface to HASP

Interface to HASP is from Serial and EDAC pigtails plugged into the E-box.

#### 4.3.4 External devices

Left hand side the box is the main monitoring system which include 3 cameras, 1 set of sensors and 2 motors.

#### 4.3.5 E-box Internal Circuit Design

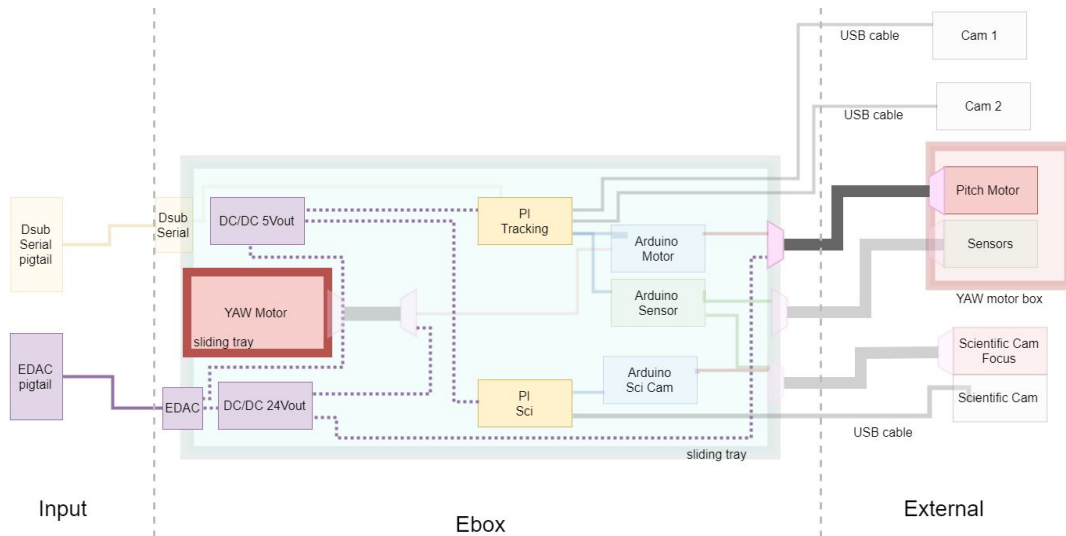


**Figure 4.3.5.1**– The wiring diagram of the e-box power supply

Power supply are marked in purple demonstrated in Figure 4.3.5.1. There are 2 DC/DC converters, it steps down the provided 30v supply to 24v to the motor and 5v to the RPi. The power is supplied to the tracking-RPi and Sci-PRi. Therefore only pin A,BW,T are in used of the EDAC connector. As the converters are placed apart there are wires tracing the YAW motor box to source the Tracking Pi.

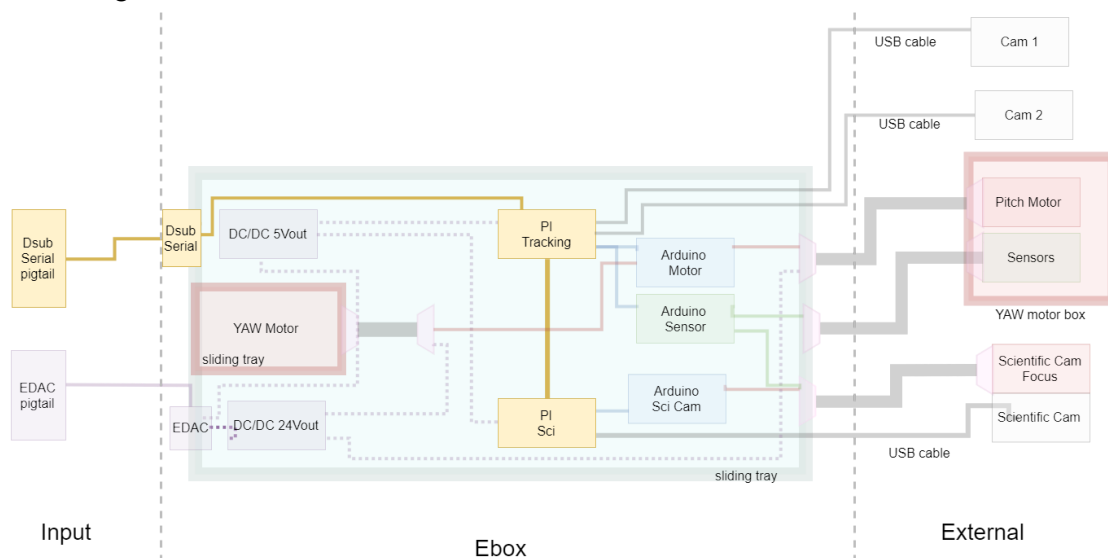


**Figure 4.3.5.2** – The wiring diagram of the e-box serial connection





The main control system with serial connection is marked in yellow in Figure 4.3.5.2. Two RPi's used are indicated in yellow, it is the Main OnBoard Computer (Main OBC) which delivers control signal and receives data collected from sensors and returns it to ground. They are connected via a direct network connection, using a crossover cable, this allows the Sci-Pi to be accessed via the tracking- RPi terminal. As a result, it will allow remote access to reconfigure and even reboot a computer during the flight. The Sci-RPi receives data from scientific camera and stores it.

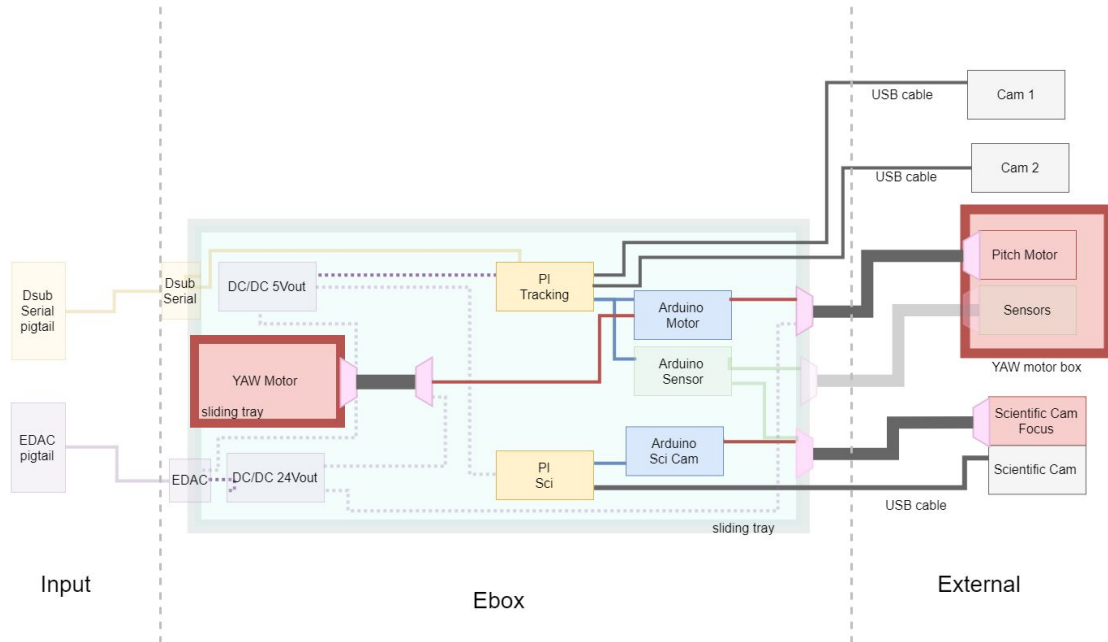


**Figure 4.3.5.3** – The wiring diagram of the e-box motor control

Figure 4.3.5.3 shows the camera system and the motor control system. Three blue boxes are Arduinos. The upper one delivers command to motor driver and protects the motor from the forbidden region. The lower one provides signal to the focusing motor.

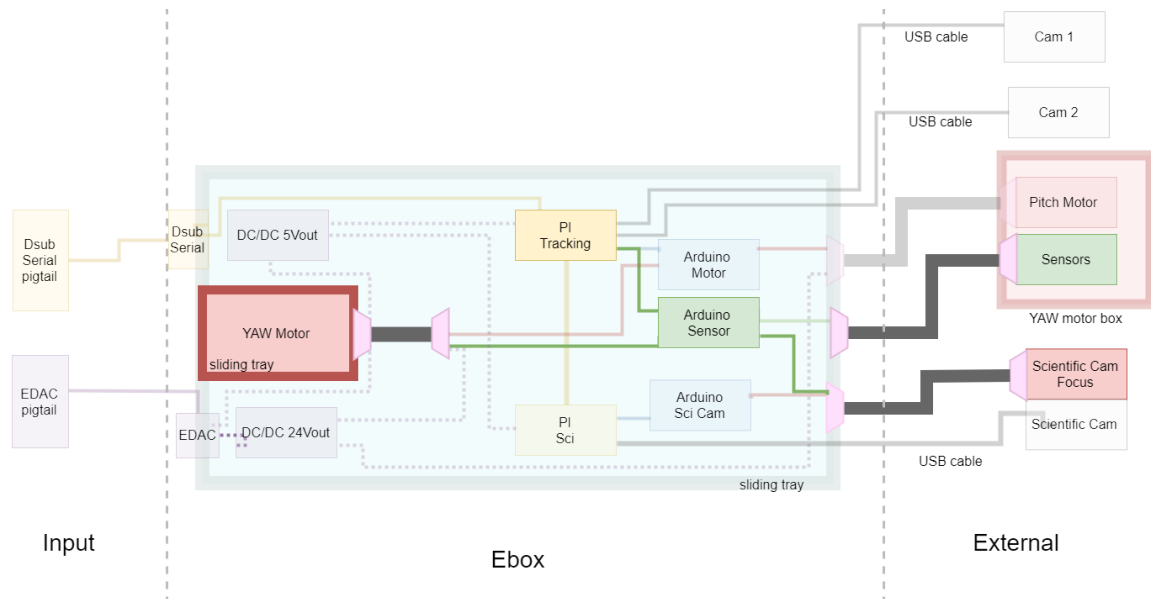


**Figure 4.3.5.4** – The wiring diagram of the E-box data logging path

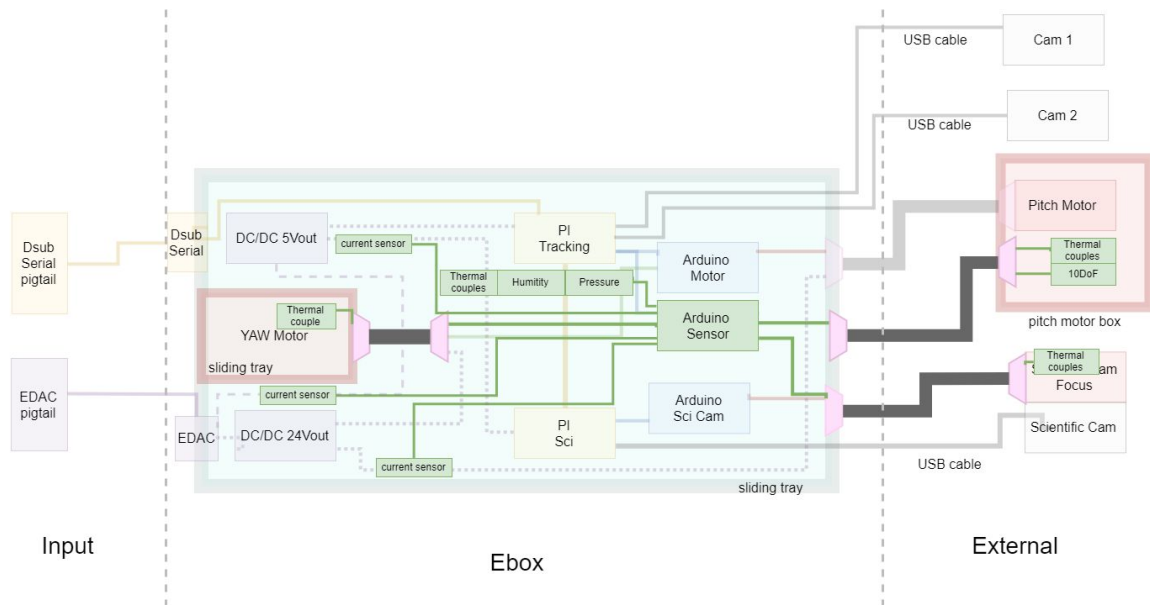


**Figure 4.3.5.5** – The wiring diagram of the e-box data logging details

The data logging path is shown in Figure 4.3.5.4 Arduino uses as a data logger, which collects scientific data such as pressure, humidity and temperature. It is connected to the sensors in the pitch motor box. As well as the sensor which placed in the E-box. Figure 4.3.5.5 Shown the circuit design of the sensor. Most of the sensor are connected to the Arduino via SCL, SDA and power supply. Mostly there are only 4 wire are connecting the sensors.

#### 4.3.6 E-box Manufacturing

The electronic wiring configuration has tested and manufactured, it is shown in picture 1, where the position of the power converter are need to interchange with the RPi. Further manufacturing can be done when the Yaw motor housing and E-box is finished by the Mechanical sub team.

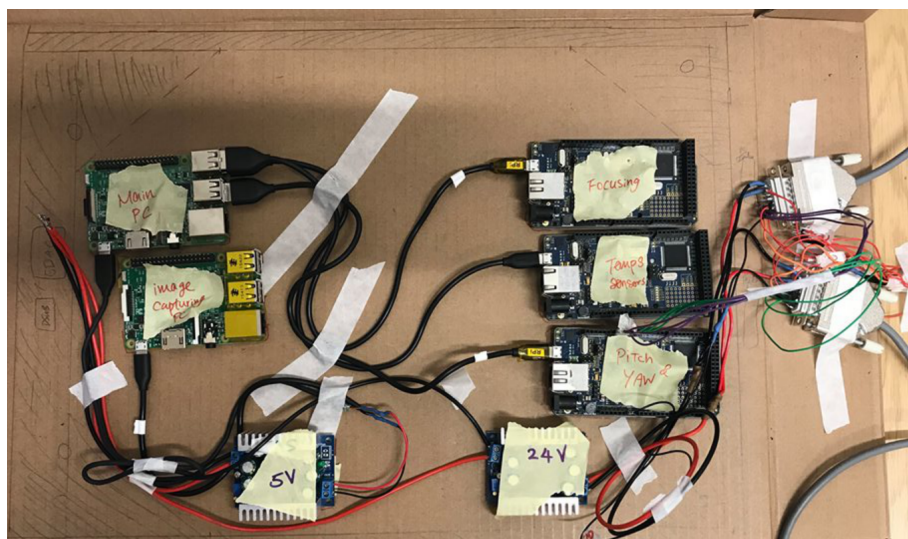


**Figure 4.3.6.1**– Wiring configuration for E-box



#### 4.3.7 Forbidden Region

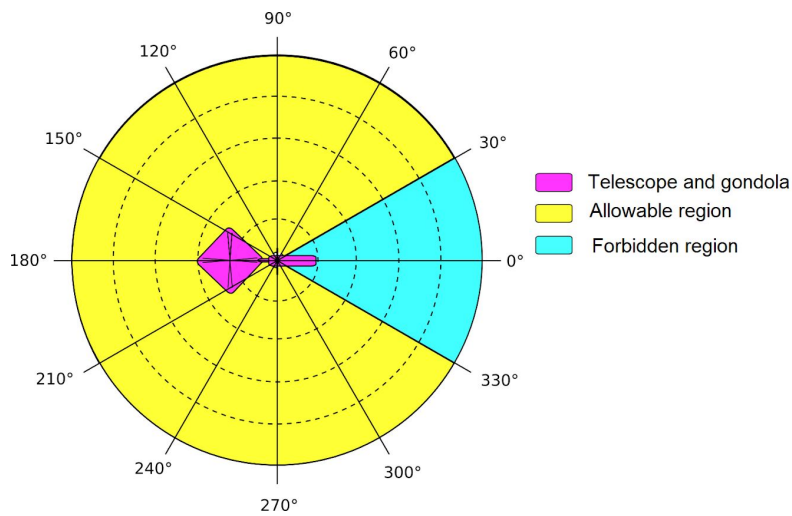


**Figure 4.3.7.1** – Forbidden region and allowable region

There are 6 cable connecting the E-box to the Pitch motor box. In order to protect the cable from stretching there is a forbidden region which the telescope are forbidden to drive in. It is illustrated in **Figure 4.3.7.1** The yellow region are allowable region when the cable is not intention. The region marked in blue is the forbidden region when the cable is potential to stretch and break. Protection is done by placing 2 mechanical switches to the end of the allowable region and stop the motor when it entering the forbidden zone.

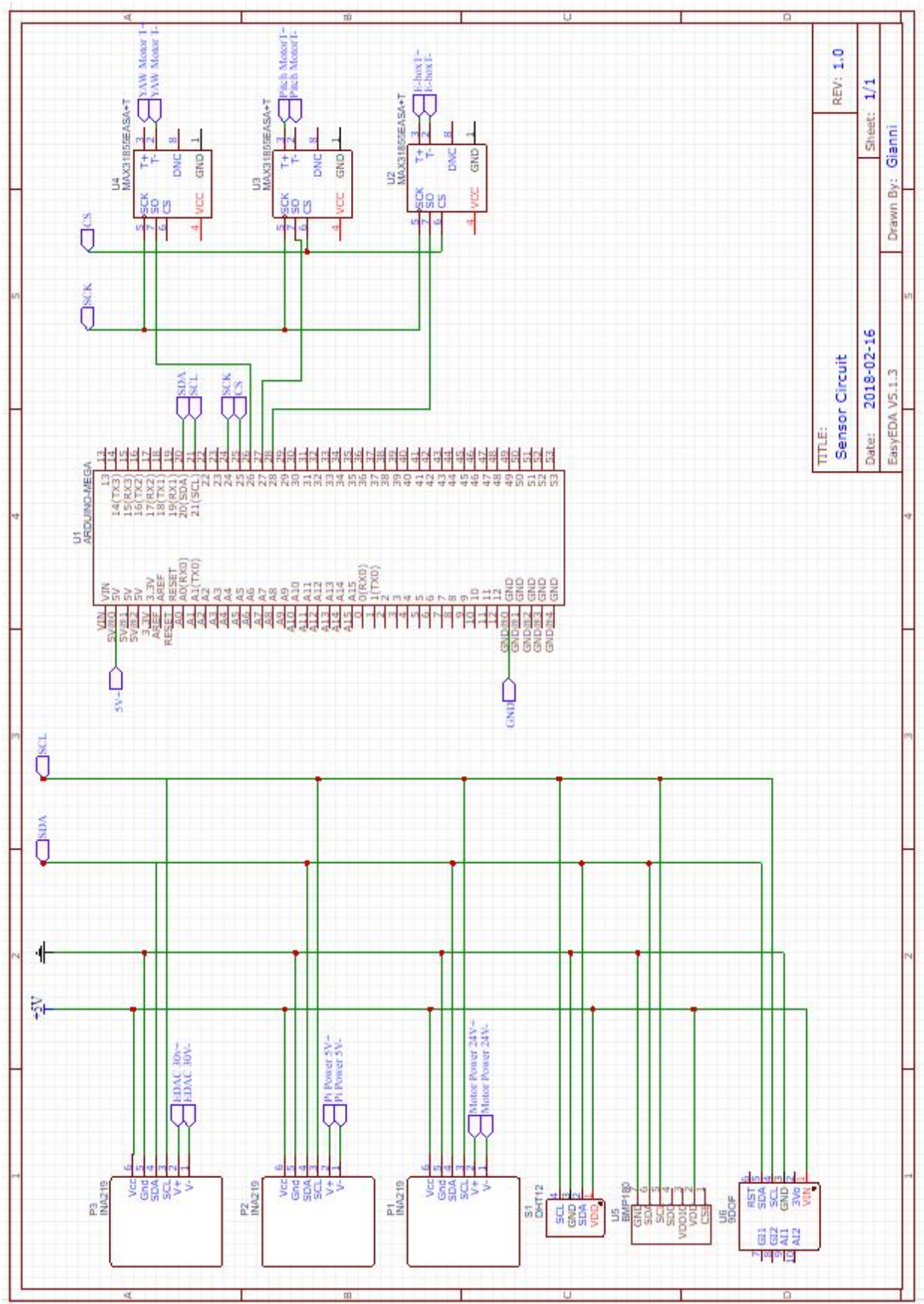


Figure 4.3.7.2– The circuit diagram of the e-box data logging details



## 4.4 Software Design

In this section, the software architecture as well as its supporting hardware are discussed. The hardware is only mentioned at an elevated level and only brought into view particularly if it has some limiting characteristics which needs to be circumvented. The software design concerns several directions:

1. Sun tracking system
2. Monitoring and diagnostics
3. Redundancy of hardware and software
4. The main tracking and control system
5. The data storage system

To successfully complete the experiment, a minimal setup consisting only of the Sun tracking and image processing needs to be present and able to function in fully autonomous manner. Given the challenging environmental conditions and the fact that physical access to the experimental setup during the flight is impossible, some redundancy as well as monitoring (through telemetry) should be implemented. This in turn requires the presence of the ground station systems which will allow manual (i.e. operator based) intervention using telemetry as well as in-flight data collection.

### 4.4.1 Sun tracking system

The tracking system is divided into two parts; the high-speed tracking and the fine adjustment tracking system. This functionality refers to both location and correction of the telescope position until the Sun's center coincide with the camera center. The tracking is split into two parts:

1. first stage tracking going on at high speed but lower accuracy using either full or half-step control for the stepper motors. The telescope initial position is not important, it is done by a 360 camera;
2. second stage which does a more accurate positioning as well as detection and involves using microstepping control but is slower in speed. The telescope initial position will assume that the Sun disc is already contained in the tracking camera field of view due to the first stage completion. The precise camera is used for this purpose.

The reason why there arises a need to perform tracking in two parts is because the visual tracking system is expensive in terms of computational resources as it requires using computer vision algorithms to process the video stream coming from the tracking camera. Furthermore, the current design of detection algorithm can only work once the Sun disc is entirely contained in the tracking camera field of view.

### 4.4.2 First stage Sun tracking

The first stage Sun tracking can be implemented using one of the following options:

1. using look-up tables with astronomical data and input from sensors, GPS or compass;
2. using photoresistors;
3. using a 360° camera.

The look-up table solution starts from the idea that the Sun location is accurately known at each time of the year in advance. This schematic and calculation is shown in Figure 4.4.1.1. As a proof of concept, using very simple hardware and a LabVIEW implementation, an experiment was conducted showing that the positioning error is within  $\pm 5$  degrees. This, was the method of choice for early development but it had issues with reliability, requiring the combination of multiple sensors to work together before it's functional, leading to reliability issues.



The photoresistors solution using multiple photoresistors surrounding the gondola with a band of photoresistors which can give an indication based on the light they receive about the Sun position. This solution are unlikely to be implement as it requires a lot of wires and sensors spread across the whole of the gimbal.

The 360 degrees camera option is more robust and more reliable. It is actuate because it rely on the image resolution taken from the camera. So a high resolution camera can tackle this problem easily. In addition, it is proven in the previous launch that it is practical. Therefore it is used.

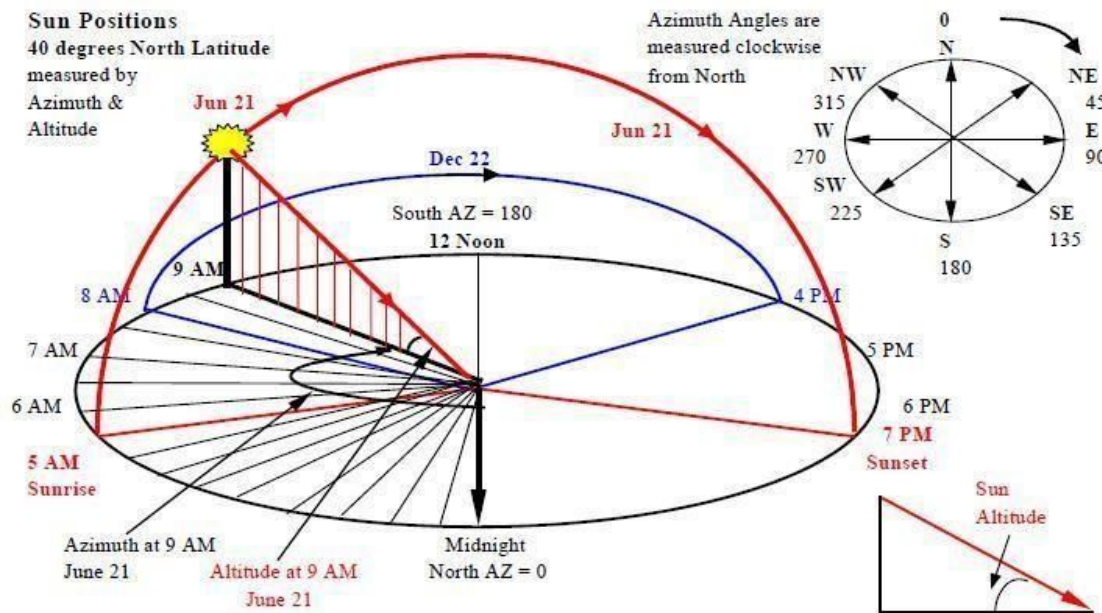


**Figure 4.4.2.1.** – Position of the Sun relative to a point on Earth at specific time in spherical coordinates.

#### 4.4.3 Second stage Sun tracking

The second stage implements a different Sun tracking algorithm and only kicks in when the first stage positioning has brought the Sun disc into the camera's field of view. At this stage, an actual detection of the Sun shape (and hence position) is going on based on OpenCV computer library operating on the video stream from the tracking camera.

In order to clearly distinguish between first and second stages we are going to refer to the first one as either the exploration phase or the actual Sun tracking phase while when it comes to the second one as detection or vision tracking stage. A third phase would be required (capture the images) to ensure the experiment success. The details concerning each phase and how they work together are detailed next:

1. **Exploration Phase** The video signal acquired from the camera is continuously investigated until bright regions above a certain area (i.e. pixels with luminosity of range 230-255) from the image are detected. This assumes that the brightest object in the image is the Sun. In fact, detecting bright regions is a condition to ensure the success of the exploration phase and continue with the detection phase. Once bright regions are detected, a vector is created that contains the Euclidean distance from the centre of the input image to the centre of the region of the brightest pixels. This idea is demonstrated below:

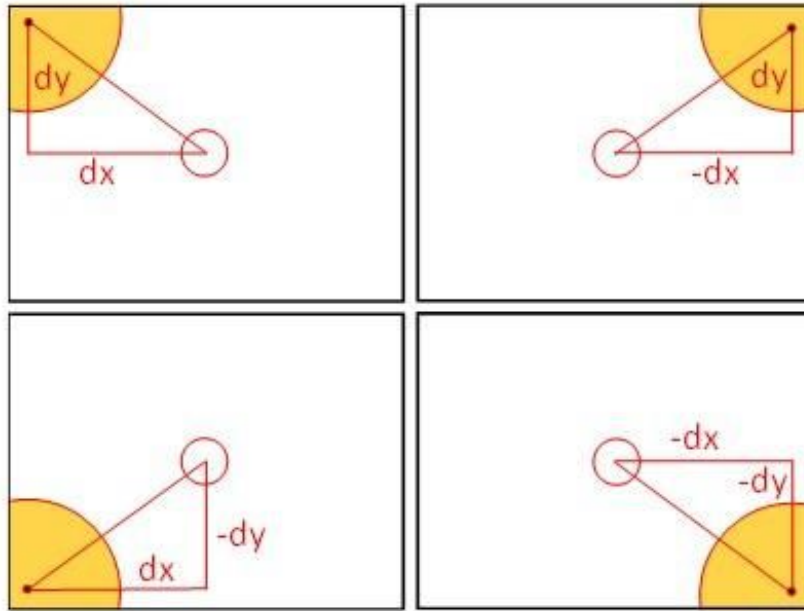


**Figure 4.4.3.1** – Cases where the bright regions are detected with various possibilities.

*Note this is NOT synonymous to tracking of the centroid of the Sun in phase 2, although the two methods have similar underlying methods, the purpose of this example is to align the telescope to the brightest section of the image*

2. **Detection Phase** Once in line, the Phase 2 will begin by running a shape detection algorithm that will check to see if the captured bright image is a circle. Once detected it will then obtain its centroid and align it to the centre of the image. Therefore, this is similar with stage 2 mentioned above
3. **Capturing Phase** The final phase will result in signalling the computer handling the more expensive camera to start taking shots of the Sun and hence store in the memory storage as the telescope was aligned in the proper direction. The entire process can be visualized below.

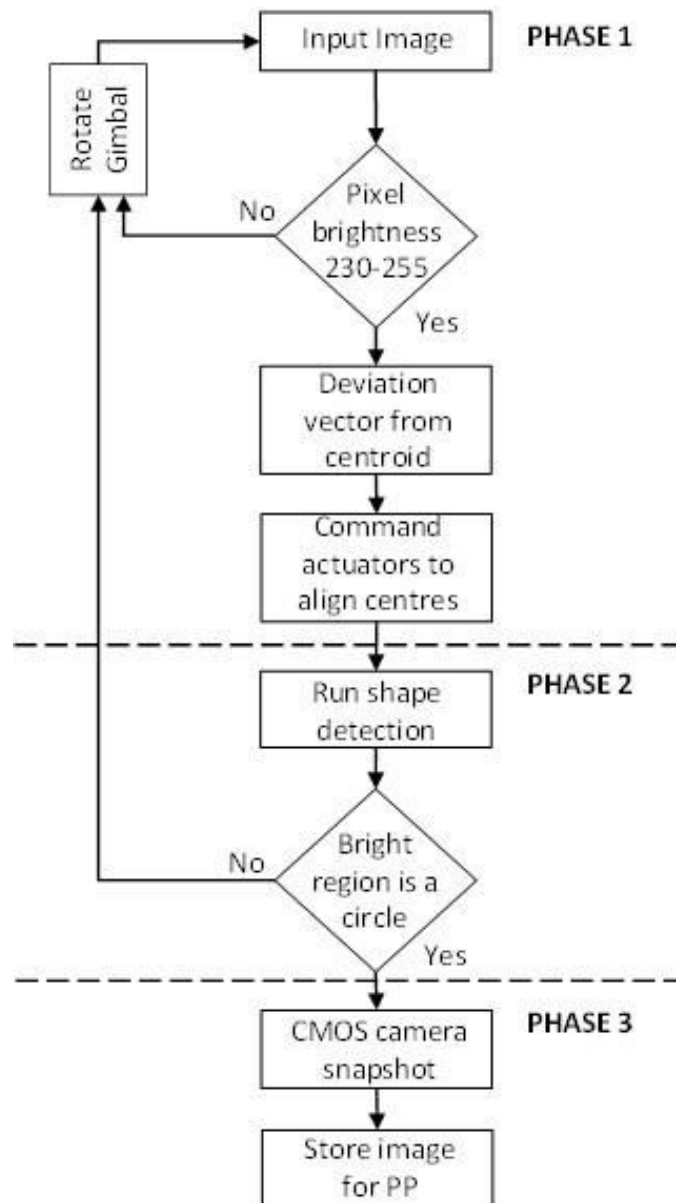


**Figure 4.4.3.2** – Proposed design for the algorithm flowchart.

#### **4.4.4 Monitoring and diagnostics**

The diagnostics are going to be performed if during the monitoring phase some sort of fault occurs. The diagnostic functionality can be split in two stages:

- during the prototype phase and pre-flight when extensive measurements are conducted (for example energy usage scenarios are tested to determine compliance with the available battery capacity)
- during the flight itself when only a very useful handful of diagnostics are collected

The possible actions available to the ground station operator are going to be taking control (manual mode) of the telescope positioning and focusing, restarting the on-board computers, etc.

#### **4.4.5 Redundancy of hardware and software**

Single focal point telescope accepts only one camera, due to constraints of telescope design, weight and power consumption, redundancy cannot be fully implemented for these two components. However, extra care is taken for auxiliary systems such as sensing and tracking. The sensing signal





are stored in the SD card of the sensing arduino and send a copy to the Raspberry Pi as well as the ground station. Therefore, there are 3 copies of the data.

The tracking system are implemented by using two camera. 360 camera and tracking camera. In case of fault condition of the cameras, there is a backup panning mode software that can be activated from the ground station and replacing the functionality of the on board tracking. The telescope are swapping from left to right and it can eventually taken some picture of the sun.

In addition, there are a manual vertical control and horizontal control listed in Uplink Command Format. This functionality will not activated except from a very unlikely event, when all the automatic software lost its functionality. The telescope will be manually positioned in a particular allocation in each hour which then taken image from that position, when the uplink is limited by once per hour.

#### **4.4.6 Main tracking and control system**

The team are developing a two-stage tracking system for pinpointing the location of the Sun in real-time for normal operation. It consists of correcting the position of the Sun as the geometric distance to the centre of the image acquired.

During most testing the hardware platform of choice has been a Raspberry Pi due to ease of implementation, however it is possible that this device can be substituted in the future by a more powerful CPU.

And the redundancy panning mode and manual mode as mentioned in redundancy section will be added as a additional backup functionality.

#### **4.4.7 Data storage system**

Images and data recorded by the telescope imager will be stored onto a SD micro card in the science acquisition Raspberry Pi. This will be downloaded after retrieval for analysis. All systems will be tested for low temperatures, outgassing and other space hazards such as atomic oxygen.

We want to obtain images of the Sun using the Balmer series H-alpha deep-red visible spectral line at wavelength 656.28 nm. Using a 125 mm diameter aperture and effective 1900 mm focal length, we will connect this onto a ZWO ASI120MM sensor with an H-alpha etalon/filter.

## 4.5 System Budget

### 4.5.1 Mass Budget

The mass budget is listed in details in table 4.5.1.1. The total mass budget is calculated by conducting researches online from the manufacturer data sheet and relevant engineering assumption. However the measured mass and uncertainty mass is unable to provide because majority of the component is under shipping. It will be updated as soon as all the components are arrived.

**Table 4.5.1.1**– Mass of various components in kg

Mass (Kg)		
Actuators	Data Sheet	Calculated
Raspberry Pi 3	0.4	-
Arduino Mega	0.4	-
Arduino Mega USB cable	0.05	-
Electrical motor (x2)	2 x 0.5	-
Focusing motor	0.17	-
Driver hardware including heat sinks (x2)	2 x 0.15	-
Harmonic drive HFUC-20-2UH	0.98	-
DC-DC converters (x2)	2 x 0.2	-
DB15 socket (x6)	6 x 0.1	-
DB 15 wire 0.5m (x3)	3 x 0.2	-
Connection wires (5% of the mass)	0.2	-
<b>Actuator Sub-Total:</b>	<b>5.1kg</b>	
Datalogger	Data sheet	Calculated
Arduino Mega	0.4	-
Arduino Mega USB cable	0.01	-
Thermocouple Amplifier - MAX31850K (x3)	3 x 0.01	-
Switches (x2)	2 x 0.02	-
INA219 High Side DC Current Sensor	0.01	-
DHT11 humidity sensor	0.03	-
10-DOF Accel/Mag/Gyro+Temp Breakout Board	0.03	-
BMP180 Barometric Pressure Sensor	0.02	-



Sensors connection cables (10% of the mass)	0.02	-
<b>Datalogger Sub-Total:</b>	<b>1.61kg</b>	
<b>Image Acquisition System</b>	<b>Data Sheet</b>	<b>Calculated</b>
Raspberry Pi 3	0.4	-
Arduino Mega	0.4	-
Arduino Mega USB cable	0.05	-
Scientific camera (ZWO ASI120MM-S)	0.1	-
Camera cable	0.05	-
Connection wires (10% of the mass)	-	0.1
<b>Acquisition Sub-Total:</b>	<b>1.1kg</b>	
<b>Optics</b>	<b>Data Sheet</b>	<b>Calculated</b>
Telescope tube (Meade ETX 90)	2.5	-
Additional optics (etalon, ERF, focuser)	0.9	-
Tracking camera (HD PRO WEBCAM C920)	0.4	-
Tracking camera cable (x2)	2 x 0.05	-
<b>Optics Sub-Total:</b>	<b>3.9kg</b>	
<b>Mechanical structure</b>	<b>Data Sheet</b>	<b>Calculated</b>
Gimbal structure and electronic box (excluding hardware)	-	5.1
Focusing gear system	-	0.15
Nuts and bolts (assumed 5% of gimbal, ebox and focusing gear system)	-	0.2
Insulation (Polyethelene foam)	-	0.25
<b>Mechanical structure Sub-total:</b>	<b>5.7kg</b>	
<b><u>Total</u></b>	<b><u>17.41 kg</u></b>	

#### 4.5.2 Power Budget

A power distribution unit is being studied during the construction of the latest version of this document. Our preliminary power consumption details are given in the table below. Average power consumption (Current consumption ): 36.73W (1.35A)

**Table 4.5.2.1– Power System Breakdown**

	Voltage(V)	Current (A)	Power (Watt)	Quantity	Total (W)
Raspberry Pi 3	5	0.25	1.25	2	3
Arduino Mega	5	0.1	1	3	3
Electrical motors and Driver	24	0.5	12	2	24
Tracking camera (HD PRO WEBCAM C920)	5	0.15	0.75	2	1.5
Focusing Motor	24V	0.2	12	1	12
Scientific camera (ZWO ASI120MM-S)	5	0.15	0.75	1	0.75
DC-DC converters (efficiency 95%)	24 or 5	N/A	0.35	2	0.7
Wiring (10% of the total Power consumption)	N/A	N/A	0.165	N/A	3.343
<b>Total</b>	<b>N/A</b>	<b>1.35A</b>	<b>N/A</b>	<b>N/A</b>	<b>36.73W</b>

Values provided in the power table are rated values. It is now known from experience that the real power consumption is below those values which points out to the possibility of relying in the power management strategy described in this document.

The telescope actuation and image processing system consists of several components with the electrical power consumption roughly equally distributed among them. The system assumes two entry point coming from the balloon's batteries — from there the electrical power is brought to the parameters required by various components using DC-DC converters as it follows:

1. 1 converter 30/5 V for Arduino, Raspberry Pi, cameras and sensors,
2. 1 converter 30/24 V for motors

The DC/DC converters number is kept down by connecting multiple components in parallel if they share the same voltage parameters, the wiring is as shown in E-box Internal Circuit Design.



## 5. Experiment Integration to HASP

### 5.1 Mechanical

#### Positioning with respect to the gondola

It is intended to mount the telescope on one of the large slots allocated on the gondola.

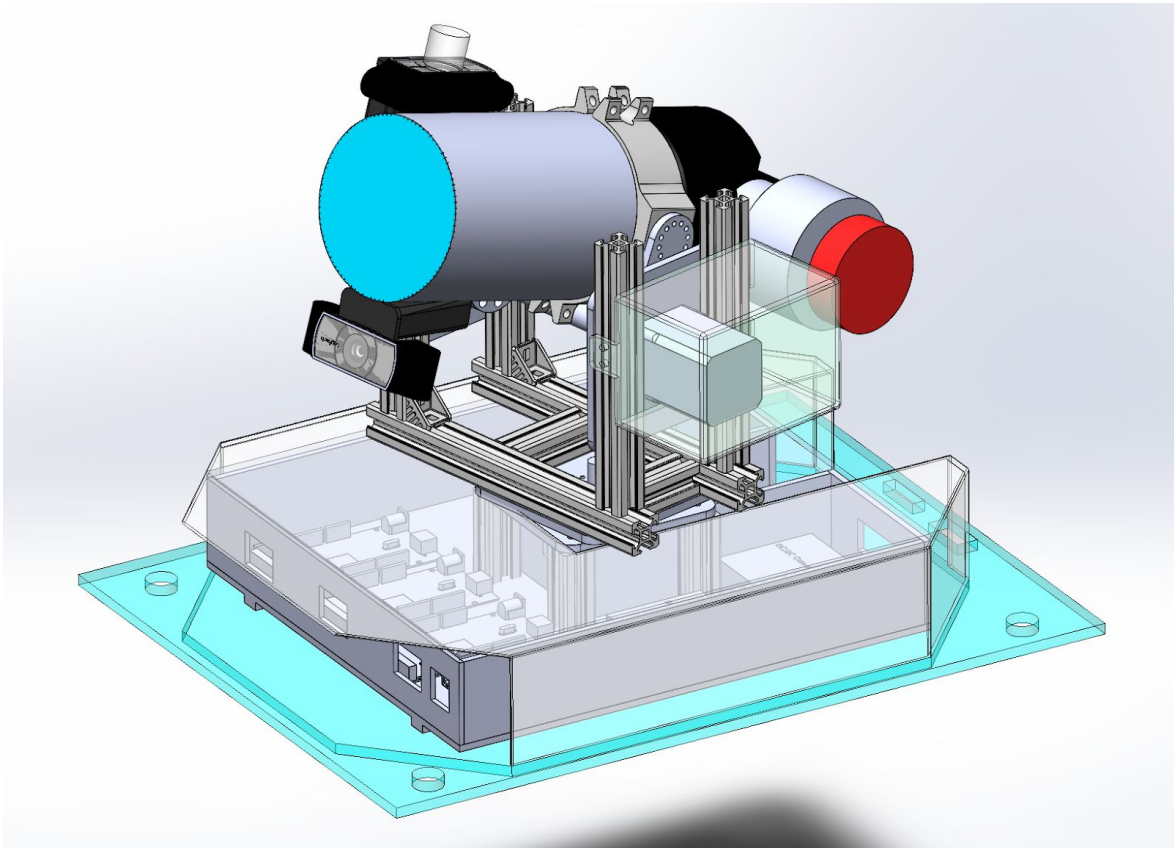


**Figure 5.1.1.** – Positioning with respect to the gondola

Bolts will be used to secure the structure onto the PVC board provided. The final size will be determined after additional structural calculations and testing. Dimensions can be found in Appendix.

### 5.2 Electronics

Pigtails from HASP for power and communication will be plugged into E-box. For more information, please see section 4.3 on Electronics design.

## **6. Operation during Flight**

### **6.1 Analog and discrete channels design**

The system is mostly autonomous so the analog and discrete channels are not in use.

### **6.2 Uplink using HASP Serial**

The system should be able to run autonomously once switched on, automatically finding and tracking the sun with the ability to focus on the fly. However to improve the reliability and enable troubleshooting during flight, the serial of the tracking Raspberry Pi will be accessible with a RS 232 terminal via the HASP serial interface [2].

The uplink command are used for manual adjustment of the system, it provide extra controllability in case of uncertain situation in flight. The first five bits are used for redundancy checksum, this provide a security for the command uplink, ensure the system are not answering other student payload comment in case of error. The command only executed when the return of checksum are matched. The command table below shows the possibility to turn on the Pan mode for both axis, it is a backup tracking method only used when automatic graphical tracking system is not functioning properly.

### **6.3 Downlink via HASP Serial**

Downlink is mainly used for downloading images from all the cameras, so we know how the camera is moving and if it is detecting the sun or other light sources. The data of other sensors also returned. Location, temp, humidity, attitude, pressure, the direction of the telescope and feedback of the motor are known. The data are stored in SD cards and every 10 mins it will send the most up to date version of file to the ground station. A small number of highly compressed and cropped images can also be downloaded to the Ground segment during flight, to give us an idea of the performance of tracking and focusing. The data format are shown below, data types are identified by a characters at the front. Requested GPS Time and Position Data helps to identify the movement of the gondola with respect to the telescope, it act as a reference information for the ground segment to determine if the telescope is tracking the sun in a correct operation mode.



**Table 6.2.1 – Uplink Command Format**

<b><u>Command</u></b>	<b><u>Byte</u></b>	<b><u>Notes</u></b>
CRC redundancy check sum	0x3E 0x00-0x00 0x00	First five bits reserved for CRC check
Ping	0x000x00	Ping the Raspberry Pi
Vertical Pan mode on (default off)	0x00 0x02	
Vertical Pan mode off	0x00 0x03	
Horizontal Pan mode on (default off)	0x00 0x04	
Horizontal Pan mode off	0x00 0x05	
Vertical control	0x00 0x06- 0x01 0x1E	Vertical position of gimble(0 to 70 deg) 0.25 deg steps
Horizontal control	0x01 0x1F- 0x02 0x7D	Horizontal position of gimble (+/-175 deg) 1 deg steps
Night Mode on (default off)	0x02 0x7E	
Night Mode off	0x02 0x7F	
Science Cam On	0x02 0x080	
Science Cam off	0x02 0x81	
Tracking camera Threshold removal	0x02 0x8 - 0x03 0x4A	Threshold to determine the black and white area
Tracking camera Gaussian blurred	0x03 0x04 - 0x03 0x54	9 value of Gaussian blur selections
Tracking camera erode filter	0x03 0x55 - 0x03 0x5F	9 value of erode filter
Tracking camera dilate filter	0x03 0x60 -0x03 0x6A	9 value of dilate filter
Tracking camera Filter selection	0x03 0x7C- 0x03 0x7B	Determine the filters (4x4 combinations)
Focus increment	0x03 0x7C - 0x03 0x87	Moving Focuser forward in ( 0.5mm per step)
Focus decrement	0x03 0x88 - 0x03 0x93	Moving Focuser forward in ( 0.5mm per step )
360 camera Threshold	0x03 0x94 - 0x04 0x5C	Threshold to determine the black and white area
360 camera Gaussian blurred region	0x04 0x5D - 0x04 0x66	9 value of Gaussian blur selections
360 camera erode filter	0x04 0x67 - 0x04 0x71	9 value of erode filter
360 camera dilate filter	0x04 0x72 - 0x04 0x7C	9 value of dilate filter
360 camera Filter selection	0x04 0x7D - 0x04 0x8D	Determine the filters (4x4 combinations)

**Table 6.3.1** – The communication protocol of downlink

Info	Byte	Format	Description
Housekeeping	2 Byte	SR	Start
	1 Byte	X	Record Type Indicator
	3 Byte	HH:MM:SS	Timestamp
	2 Byte	XX	Record Size
	1 Byte	X	8 bits of the record checksum
Time and Position Data	125 Byte	String	Requested GPS Time and Position Data
Power Data	5 Byte	A XXXX	Total power
	5 Byte	B XXXX	Main Pi power
	5 Byte	C XXXX	Sci Pi Power
Pitch Data	5 Byte	D XXXX	Pitch Motor Power
	5 Byte	E XXXX	Pitch Motor movement recorded
	5 Byte	F XXXX	Pitch Motor Temp
Yaw Data	5 Byte	G XXXX	Yaw Motor Power
	5 Byte	H XXXX	Yaw Motor movement recorded
	5 Byte	I XXXX	Yaw Motor Temp
Sensors details	5 Byte	G XXXX	Pressure
	5 Byte	K XXXX	Humidity
	36 Byte	R1XXXX - R6XXXX	Compass
Software parameter in use	5 Byte	S XXXX	Focuser position
	5 Byte	T XXXX	Tracking camera Threshold value
	5 Byte	U XXXX	Tracking camera Gaussian blurred region value
	5 Byte	V XXXX	Tracking camera erode filter value
	5 Byte	W XXXX	Tracking camera dilate filter value





	5 Byte	X XXXX	Tracking camera Filter selection value
	5 Byte	Y XXXX	360 camera Threshold value
	5Byte	Z XXXX	360 camera Gaussian blurred region value
	6 Byte	AA XXXX	360 camera erode filter value
	6 Byte	AB XXXX	360 camera dilate filter value
	6 Byte	AC XXXX	360 camera filter selection value
Picture	N Byte	String	Compressed Picture Taken
End	3 Byte	END	End of file

#### 6.4 Cyclic Redundancy Check (CRC) Checksum

CRC is selected because it is reliable and easy to use. CRC is a check scheme that used to detect accidental changes to raw data.

There are a predetermined number and it is stored in both receiver and transmitter. For a n-bit of transmission data, the first k bit is the useful message, the reminded (n-k) bit is the frame check sequence (FCS). The transmitter generate the FCS by divided by the predetermined pattern and it attached it to the end of the frame.

Receiver performed the identical division using the incoming frame and predetermined pattern. When the receiver calculated reminder is identical to the reciced FCK, the message is correct.

Example is shown in figure 6.4.1[3]

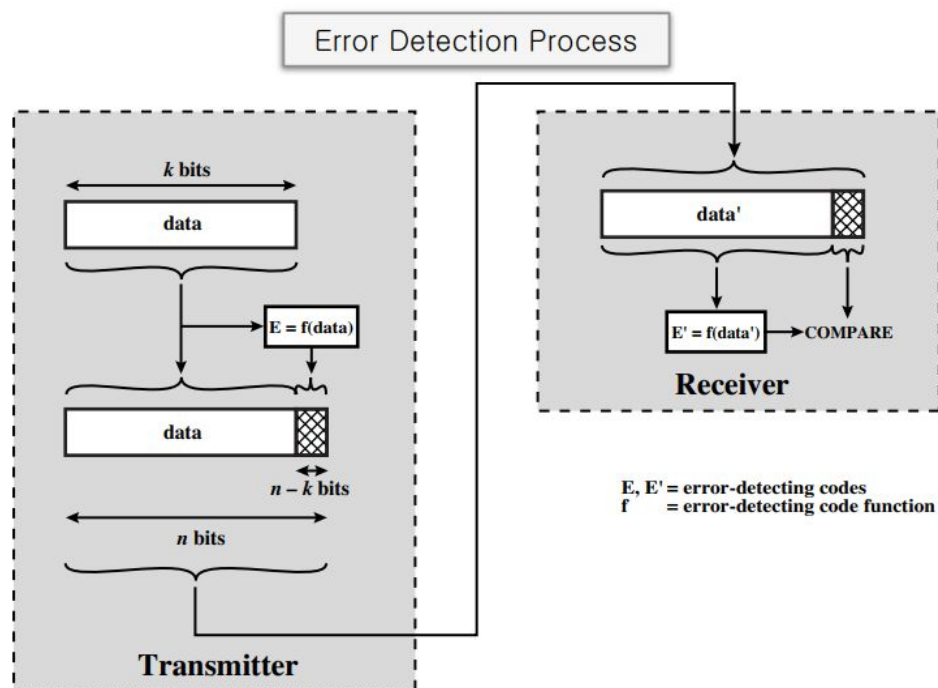


Figure 6.4.1 – Demonstration of CRC [3]

## 6.5 Ground segment design

It displays all the related parameters and the moving path of the telescope in the past hours. The condition of the system are record and displayed. It is useful for ground control to monitor the motor movement and compare it with the desire movement, so adjustment are made by importing data to the system via the serial connection. This will be programmed by Python.

The interface design is shown in Figure 6.5.1 , Temperature displays in the top left corner, and shown in blue line. Movement of gimble are shown in the up right corner, it is displayed using polar diagram so the movement path of the gimble can be read easily. The middle is the altitude and pressure. The voltage reading of system are listed at the bottom.

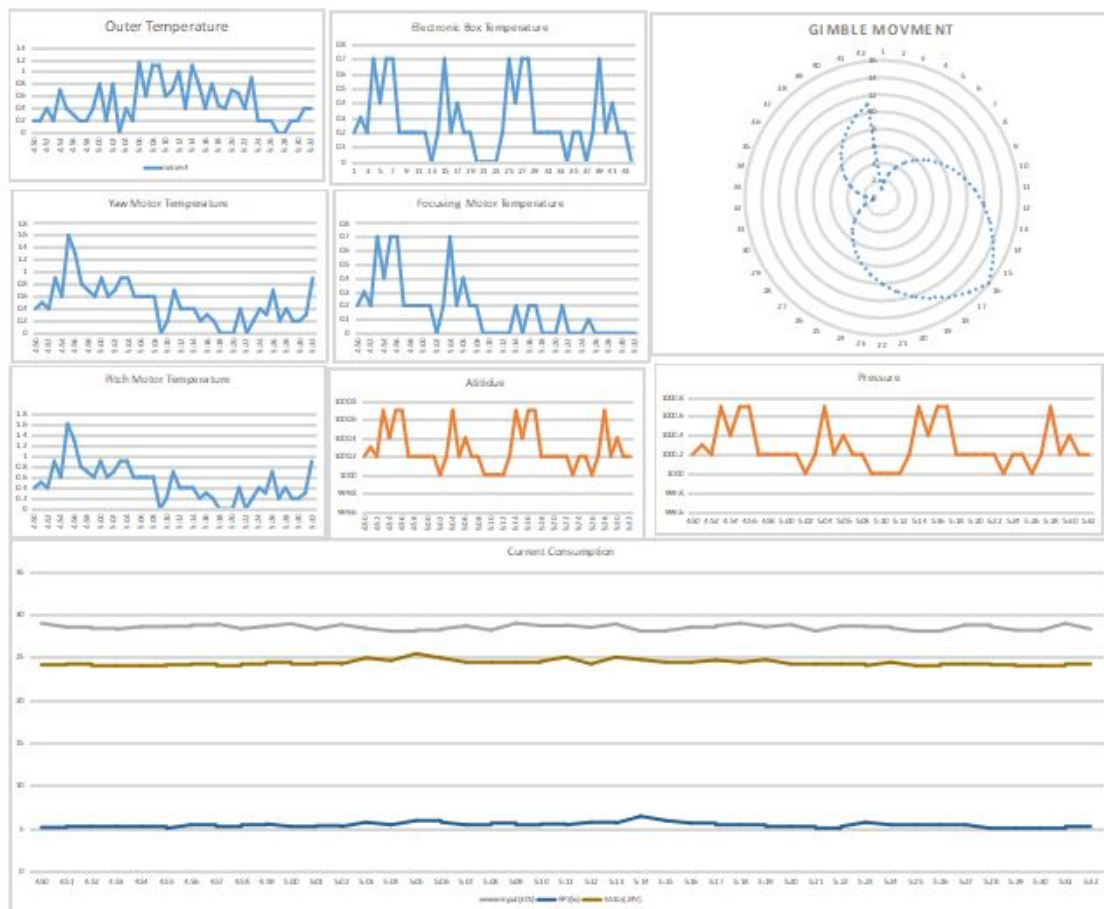


Figure 6.5.1 – The interface design



## 7. Special Requests

Due to the Sun tracking nature of the experiment, the structure is needs to dynamically rotate in the pitch and yaw axis by. It is expected to rotate up to 65 degrees, reflecting the maximum elevation of the sun in the sky. In summary, there are three requests:

1. Vertical extension (lower limit +7cm *or* ideally +13cm)
2. Horizontal extension (3cm from shorter side)
3. Access to GPS/time information (as stated in flight manual)

### 7.1 Vertical Extension

- **Lower limit request:** 7cm (total height is 37 cm)
- **Ideal request:** 13cm (total height is 43 cm)

**Reason:** Increase probability of achieving secondary objective to prove scientific value of telescope on a high altitude balloon platform.

#### Explanation:

- 7cm is the minimum height needed for the telescope to point at the Sun at an elevation of 65 degrees. If this is granted, the telescope can see the Sun over neighbouring experiments at around 62% of the daylight time.
- 13cm extension in height allows the telescope to point at the Sun at a lower elevation (because it can see over other experiments). If this is granted, the telescope can see the Sun at around 80% of daylight time.

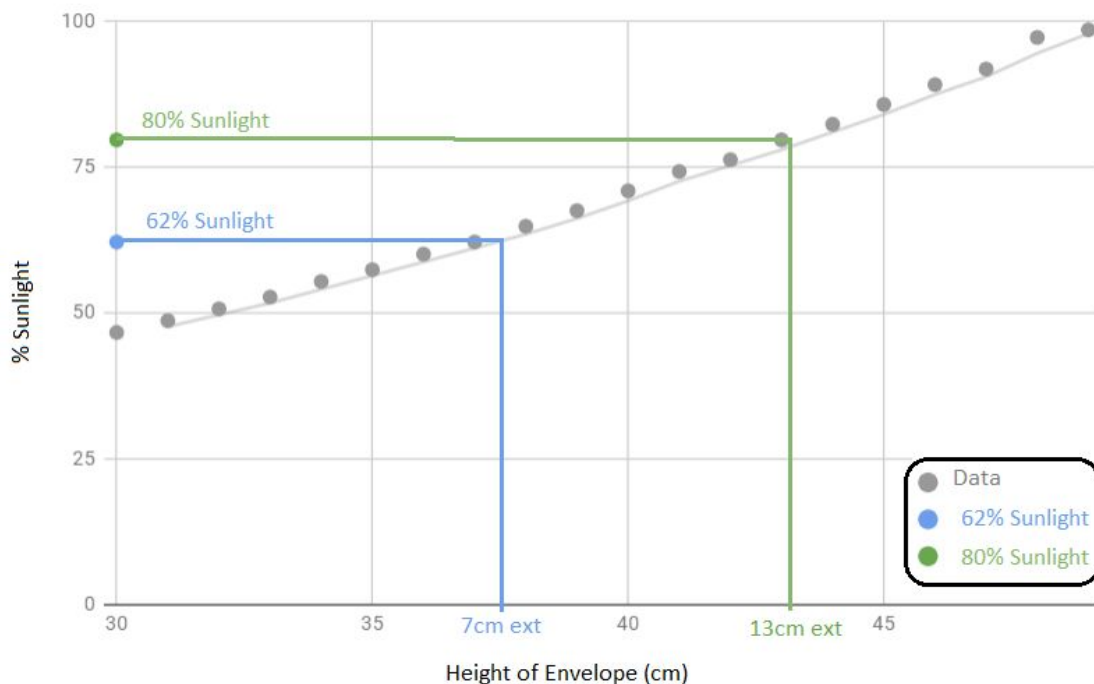


Figure 7.1.1 – Sunlight vs Height of envelope

#### NOT grant scenario:

- If 7cm minimum **NOT** granted:

Field of View will be limited to 41.6 degrees to 65 degrees when looking over experiments. It will be limited from 0 to 65 degrees when looking out over the gondola. This means the telescope can

only see the Sun over neighbouring 47% of daylight time. For more information please refer to full Sun Calculations below.

- **If 7cm granted but 13cm request NOT granted:**

Field of View will be limited to 30 degrees to 65 degrees when looking over experiments. It will be limited from 0 to 65 degrees when looking out over the gondola. This means the telescope can only see the Sun over neighbouring 47% of daylight time. For more information please refer to full Sun Calculations below.

## Sun Calculations

According to (Sunearthtools.com, 2018) position of the Sun in Fort Sumner, NM on 3rd of September 2018 starting from 7am is represented on a Figure 7.1.2

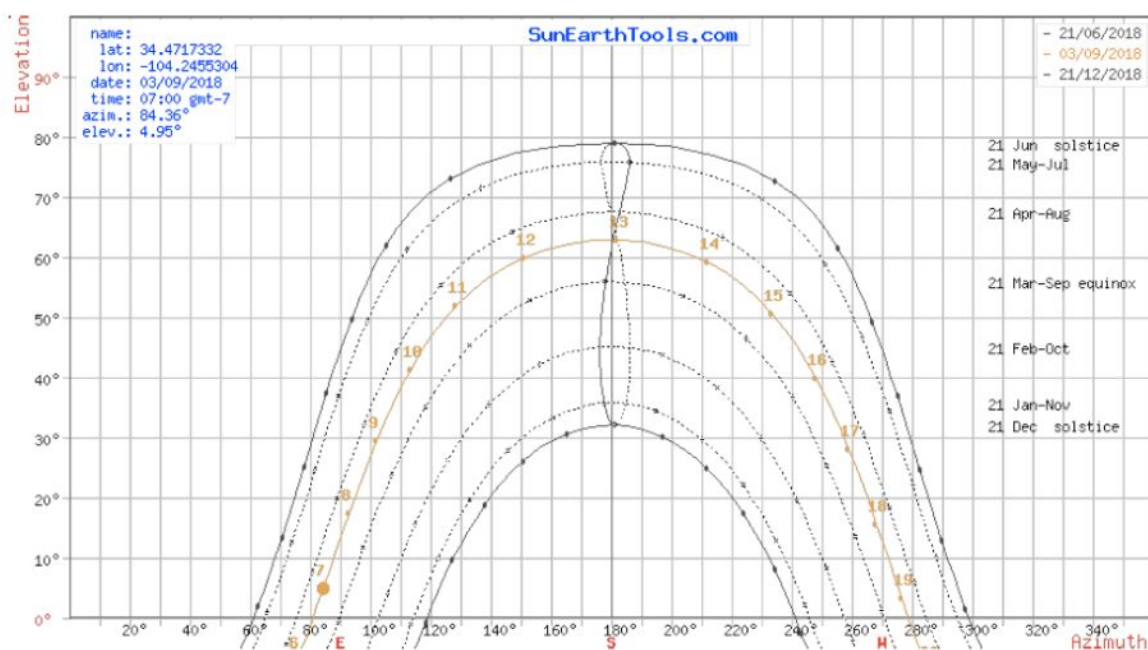


**Figure 7.1.2 – Position of the Sun**

This data is mapped into a lookup table which allows calculation of daylight duration to be conducted. Table 7.1.3 summaries this data. It assumes a 7am launch as Sunrise and Sunset are when the Sun is low in the sky. This is the time when the telescope maybe blocked by nearby experiments.



**Table 7.1.3** – The table represents the elevation of the Sun on the day of flight. Elevation in degrees.

	Time	Elevation
Sep 3rd	06:31	-0.833
	LAUNCH**	
DAYLIGHT	07:00	4.95
	08:00	17.3
	09:00	29.54
	10:00	41.31
	11:00	51.93
	12:00	59.95
	13:00	62.87
	14:00	59.15
	15:00	50.67
	16:00	39.84
	17:00	27.97
	18:00	15.68
	19:00	3.32
	19:20	-0.833
	20:00	
	21:00	
	22:00	
	23:00	
Sep 4th	00:00	
	END OF FLIGHT	

In Table 7.1.3, the values of the elevation of the Sun during the flight are recorded. \* The flight time was assumed to be 18 hours. \*\* the launch time was assumed to be 7am on the 3rd of September 2018 in Fort Sumner, NM. Using distance between our experiment and the neighbouring experiment (demonstrated in figure 7.1.3), the minimum angle of view from the telescope can be calculated using simple trigonometry.

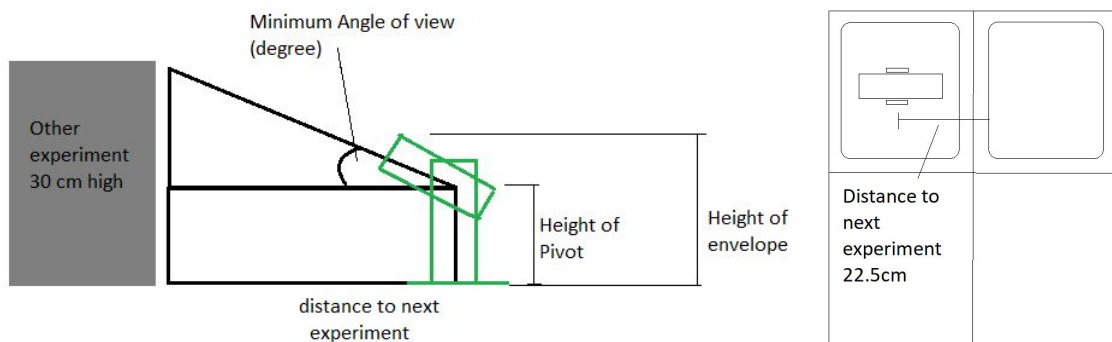


**Figure 7.1.3** - Angle of View schematic

Using the height of the pivot, the maximum height of the telescope system can be calculated by adding the height of the telescope above the pivot point (29.3cm).

Table 7.1.4 calculates the % of daylight time available for a given pivot height.

**Table 7.1.4 – Height of envelope vs % of Sunlight time observed**

Height of pivot point (cm)	Height of envelope (cm)	Angle of view (deg)	Hours of Sunlight	% of Sunlight time observed
10	30	41.6	5.75	47
11	31	40.2	6.00	49
12	32	38.7	6.25	51
13	33	37.1	6.50	53
14	34	35.4	6.83	55
15	35	33.7	7.08	57
16	36	31.9	7.41	60
17	37	30.0	7.67	62
18	38	28.1	8.00	65
19	39	26.1	8.33	68
20	40	24.0	8.75	71
21	41	21.8	9.16	74
22	42	19.6	9.41	76
23	43	17.3	9.83	80
24	44	14.9	10.16	82
25	45	12.5	10.58	86
26	46	10.1	11.00	89
27	47	7.6	11.33	92
28	48	5.1	12.00	97
29	49	2.5	12.16	99
30	50	0.0	12.16	100
31	51	-2.5	12.16	100
32	52	-5.1	12.16	100
	Ideal request			Minimum request



### 7.1.1. Vertical encroachment at 7cm extension request

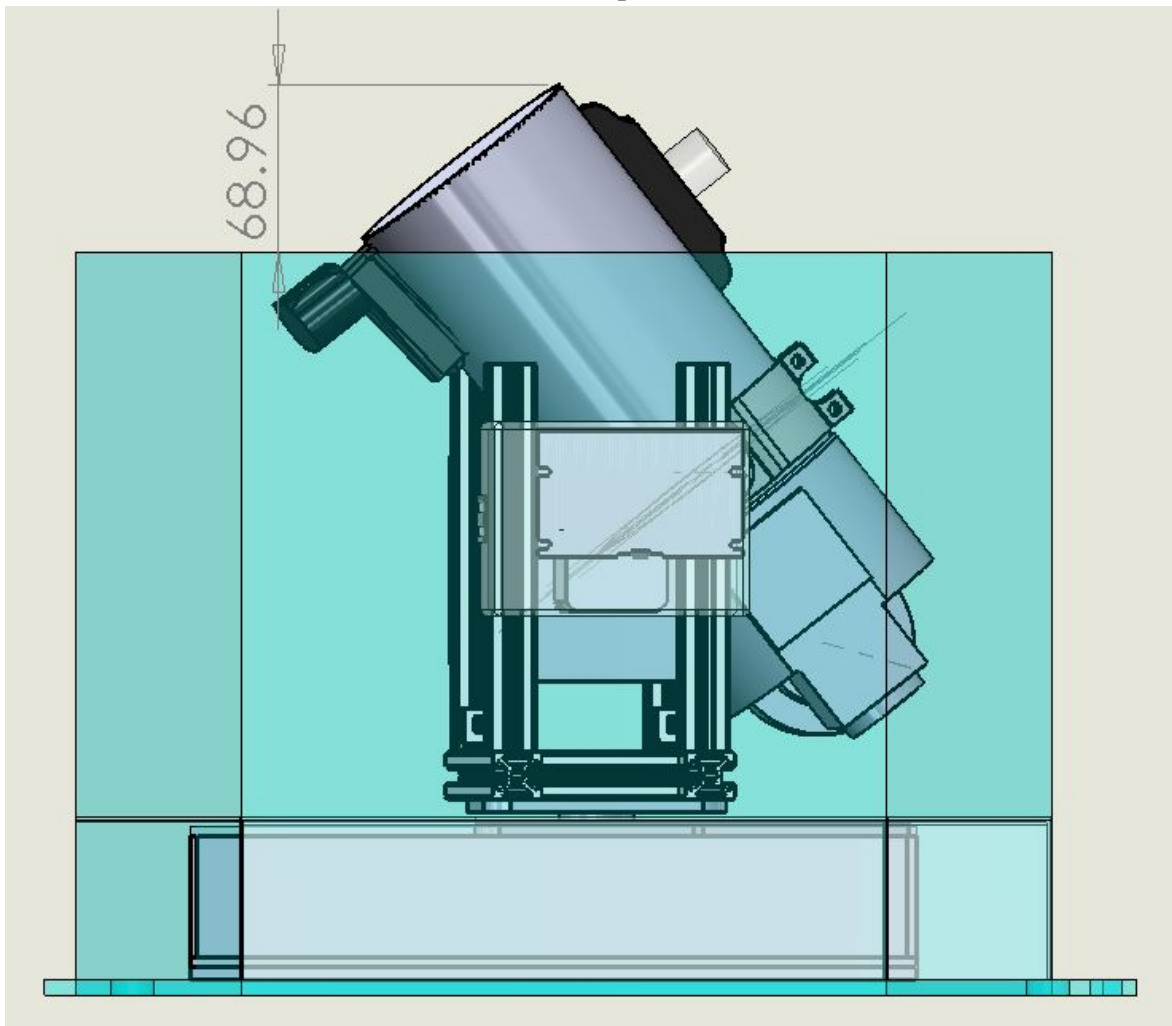


**Figure 7.1.1.1** – Maximum vertical encroachment (occurs at 52 degrees elevation)



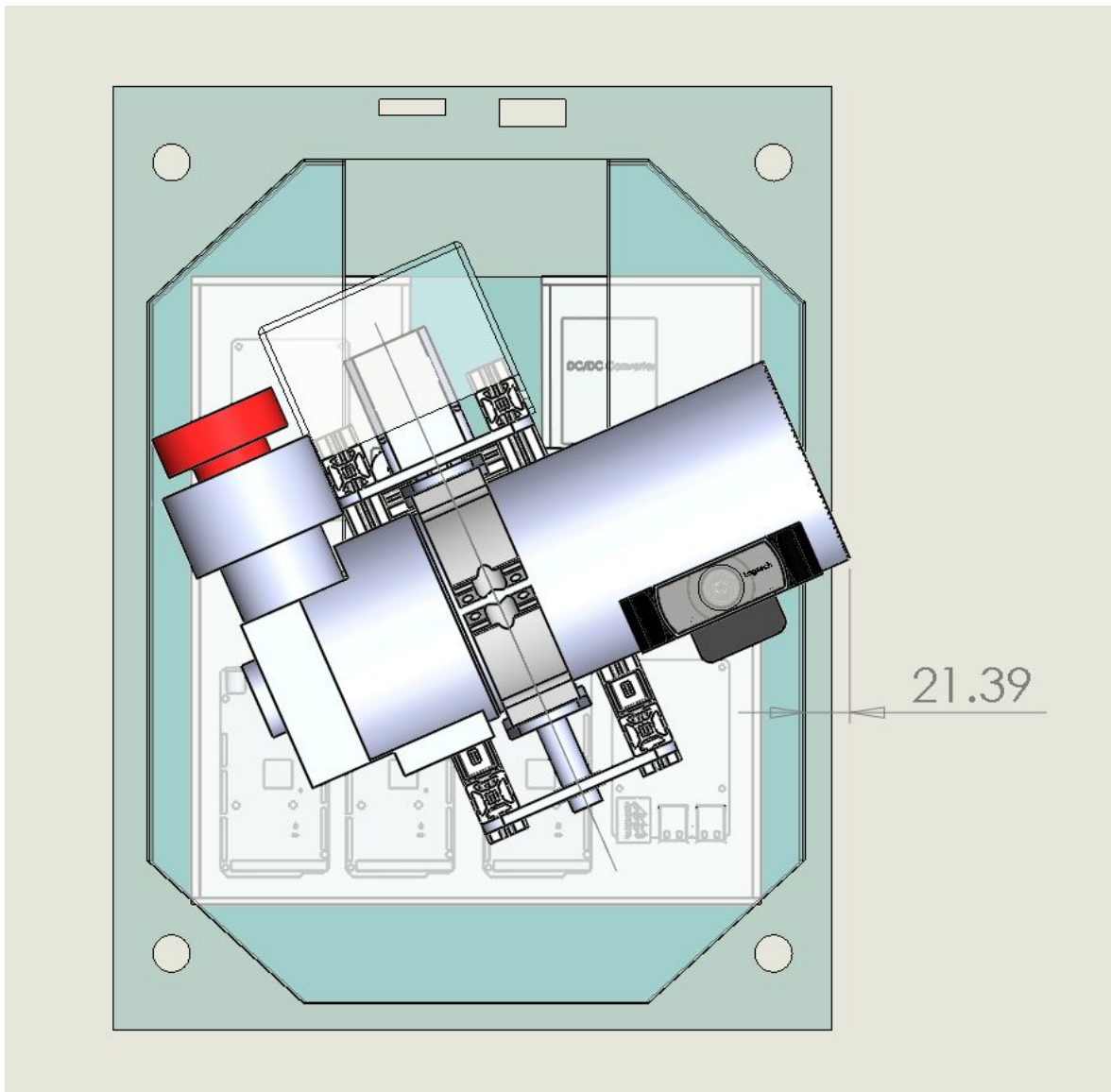


Figure 7.1.1.2 – Maximum horizontal extension of telescope tip (occurs at 0 degrees elevation)

Therefore, the maximum vertical encroachment equals to 68.96mm or 6.9cm and the maximum horizontal encroachment is less than 3cm.





### 7.1.2 Vertical encroachment at 13 cm extension request

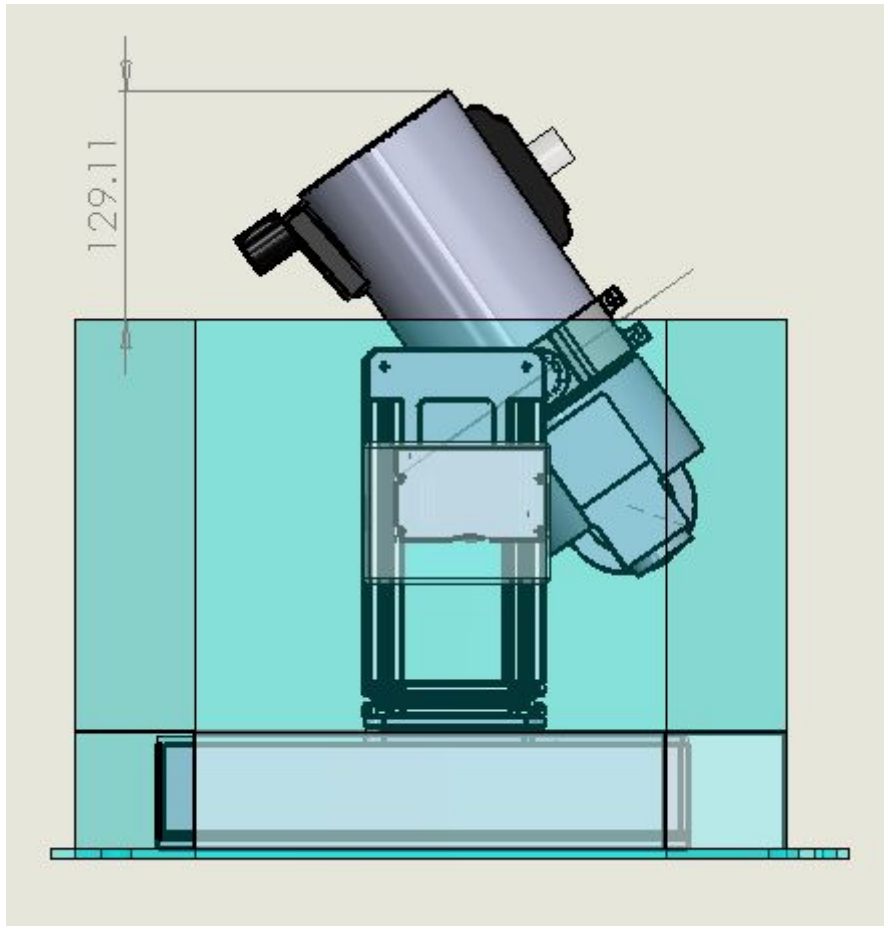


Figure 7.1.2.1 - Maximum vertical encroachment (occurs at 52 degrees elevation)

Therefore, in the 13cm ideal extension request, the maximum vertical encroachment equals to 129.11mm or 12.9 cm.

## 7.2 Width request

Horizontal extension:

- 3cm - (footprint: 36 cm x 38 cm)

Due to positioning of camera (using a 45 degree mirror), a small extension of 3cm is requested.

**If NOT granted**, the team will attempt to design a smaller optical chain OR limit the motion of the focuser (this will shorten the optical chain after the 45 degree mirror).

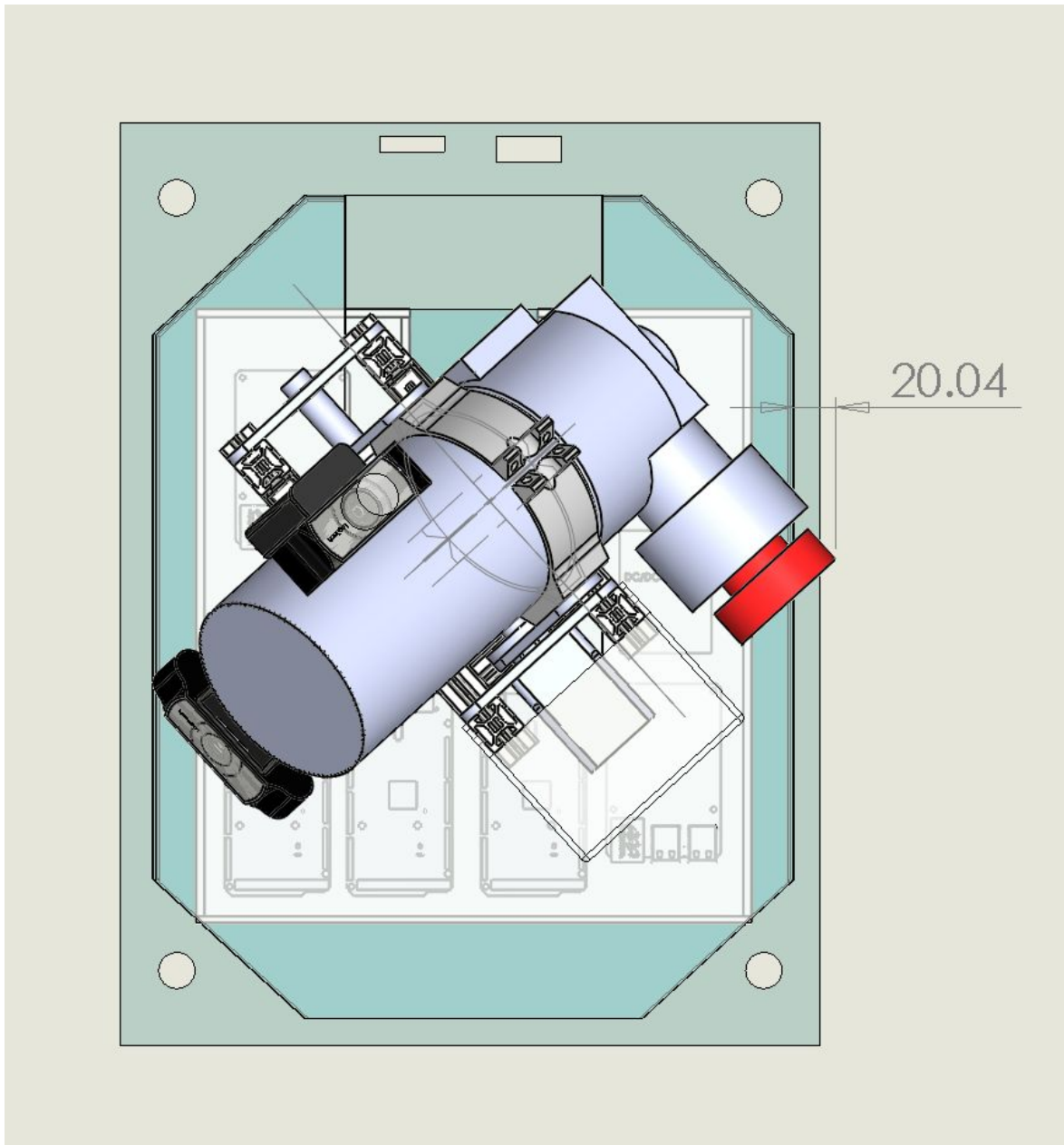


**Figure 7.2.1** – Maximum horizontal extension of camera tip (occurs at 30 degrees elevation)

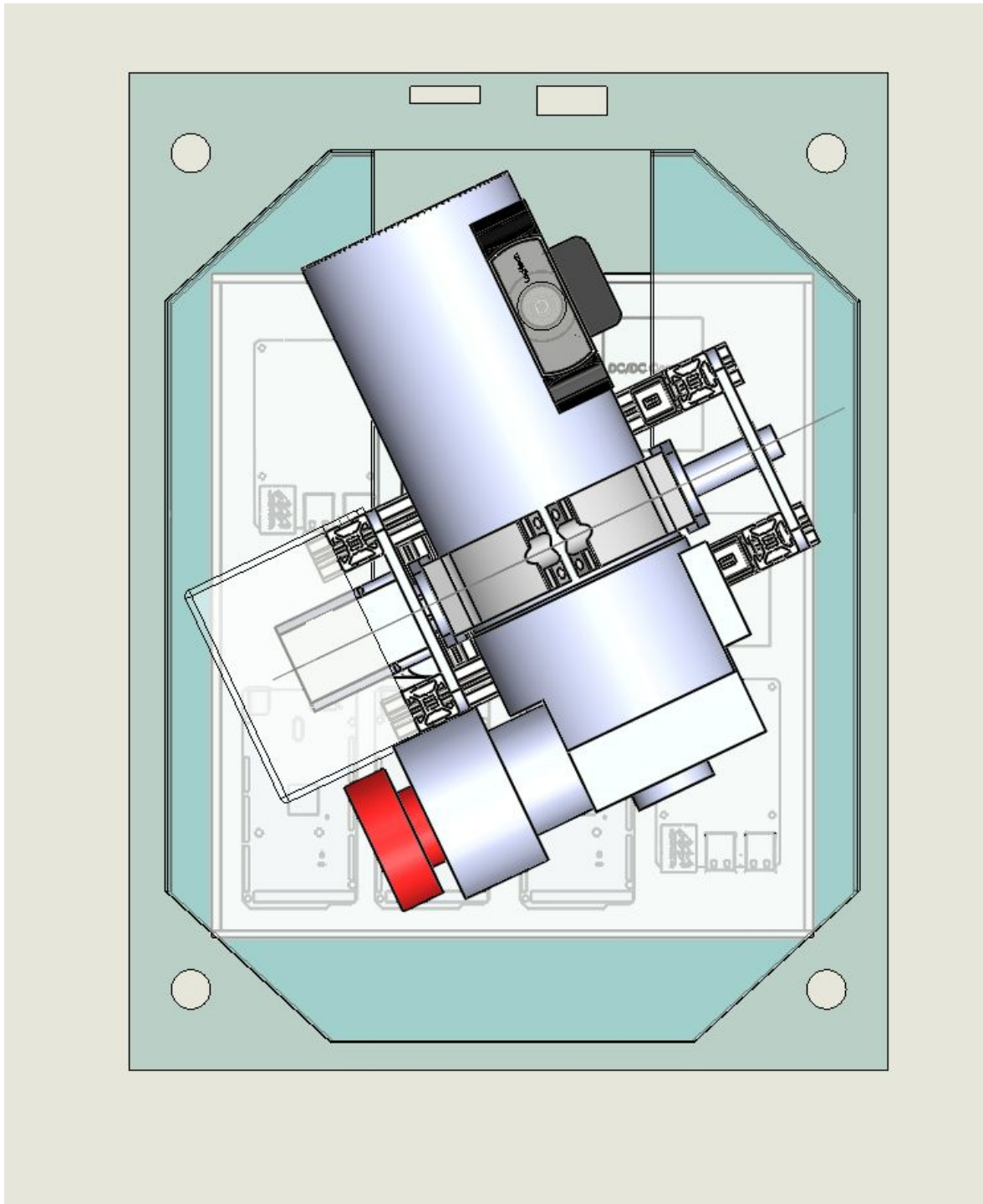


**Figure 7.2.1** – Horizontal encroachment over ends of the plate never extends beyond default experiment footprint

### 7.3 GPD Time and Position Data request

SunByte requests access to GPS, time and position data for use in analytically deriving sun angle. This additional layer of sun angle data will be compared with the internal 10DoF compass sensor data. With this data a decision can be made by the ground team to use manual rather than pan mode in guiding the telescope position. Additionally the data gathered will be time stamped accurately as the system includes no reliable electronic clock.

## 8. Post-Flight Activities

After the flight, the collected data will be downloaded for processing. However, since we aim to obtain scientific information from the time series of data, we intend to go beyond standard image processing, e.g., correcting intensity. For proper analysis of the plasma dynamics of the lower solar atmosphere we will have to remove the effects of e.g., solar rotation, spacecraft jitter and cosmic ray spikes, from the time series.

Although the first mission is planned for testing the proposed light-weight equipment, the obtained data will potentially have scientific value since the images will contain information on large-scale solar chromospheric activity, flows and oscillations measured with a very high time cadence. This information is much sought after in both the solar and stellar physics international communities. High-cadence full-disk, or Sun-as-a-star H-alpha observations will provide a connection between the integrated chromospheric intensity and the chromospheric activity, with potential applications to measurements of chromospheric activity of other stars. Furthermore, if a very high energy event takes place during the flight, e.g., a flare or coronal mass ejection, this will add even more scientific value to the obtained experimental data.

Additionally, we plan to compare data collected with data obtained by solar telescopes on the ground. For example superpositioning will enable us to determine the exact advantages of a balloon telescope system.

The high resolution solar images will also be used for outreach activities to promote Science and Engineering (see outreach section). From a more technical point of view, the proposed project will enable us to test the proposed stabilisation and observation system for using in the future missions. We anticipate that subsequent SunbYte telescopes shall become important and economically sustainable instruments of a high atmosphere- borne solar observatory. In the Figure 8.1 we have shown an example of images we expect to capture during SunbYte mission:

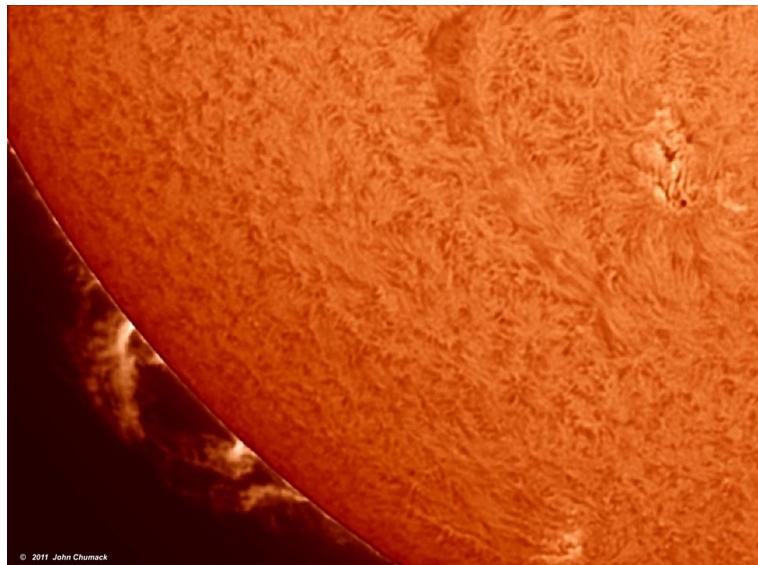


**Figure 8.1** – Image of the Sun with an H-alpha filter, courtesy of John Chumack



# Abbreviations and References

## Abbreviations

Add abbreviations to the list below, as appropriate and delete unused abbreviations.

AIT	Assembly, Integration and Test
asap	as soon as possible
CDR	Critical Design Review
COG	Centre of Gravity
CRP	Campaign Requirement Plan
DLR	Deutsches Zentrum für Luft- und Raumfahrt
EIT	Electrical Interface Test
ESA	European Space Agency
Espace	Espace Space Center
ESTEC	European Space Research and Technology Centre, ESA (NL)
ESW	Experiment Selection Workshop
FAR	Flight Acceptance Review
FST	Flight Simulation Test
FRP	Flight Requirement Plan
FRR	Flight Readiness Review
GSE	Ground Support Equipment
H/W	Hardware
ICD	Interface Control Document
I/F	Interface
IPR	Integration Progress Review
LO	Lift Off
LT	Local Time
LOS	Line of Sight

Mbps	Mega Bits per second
MFH	Mission Flight Handbook
PCB	Printed Circuit Board (electronic card)
PDR	Preliminary Design Review
PST	Payload System Test
RBF	Remove Before Flight
RPi	Raspberry Pi
SNSB	Swedish National Space Board
SODS	Start Of Data Storage
SOE	Start Of Experiment
S/W	Software
T	Time before and after launch noted with + or -
TBC	To be confirmed
TBD	To be determined
WBS	Work Breakdown Structure

## References

- [1] Obama, B., 2016 Executive Order: Coordinating efforts to prepare the nation space weather events, The White House.  
<https://obamawhitehouse.archives.gov/the-press-office/2016/10/13/executive-order-coordinating-ef-forts-prepare-nation-space-weather-events>
- [2] Guzik, G. T., 2017, HASP Student Payload Interface Manual  
[http://laspace.lsu.edu/hasp/documents/public/HASP\\_Interface\\_Manual\\_v21709.pdf](http://laspace.lsu.edu/hasp/documents/public/HASP_Interface_Manual_v21709.pdf)
- [3] En.wikipedia.org. (2018). Cyclic redundancy check. [online] Available at:  
[https://en.wikipedia.org/wiki/Cyclic\\_redundancy\\_check](https://en.wikipedia.org/wiki/Cyclic_redundancy_check)
- [4] Sunearthtools.com. (2018). *Calculation of sun's position in the sky for each location on the earth at any time of day.* [online] Available at:  
[https://www.sunearthtools.com/dp/tools/pos\\_sun.php](https://www.sunearthtools.com/dp/tools/pos_sun.php) [Accessed 16 Feb. 2018].

Useful guidance documents:

- European Cooperation for Space Standardization ECSS: Space Project Management, **Project Planning and Implementation**, ECSS- M-ST-10C Rev.1, 6 March 2009
- SSC Erange: **Erange Safety Manual**, REA00-E60 , 23 June 2010
- European Cooperation for Space Standardization ECSS: Space Engineering, **Technical Requirements Specification**, ECSS-E-ST-10- 06C, 6 March 2009
- European Cooperation for Space Standardization ECSS, Space Project Management, **Risk Management**, ECSS-M-ST-80C, 31 July 2008
- European Cooperation for Space Standardization ECSS: Space Engineering, **Verification**, ECSS-E-ST-10-02C, 6 March 2009
- Project Management Institute, **Practice Standard for Work Breakdown Structures - second Edition**, Project Management Institute, Pennsylvania, USA, 2006

# HASP Student Payload Application for 2018

## Revised Appendix

The University of Sheffield Sheffield University Nova Balloon Lifted Telescope

### Contents

<b>Verification</b>	<b>2</b>
Verification Plan	2
Test Plan	5
Test results	13
<b>Additional Technical Information</b>	<b>14</b>
Mechanical	14
General assembly drawings	14
Material Selection for the Gimbal and Support Structure	18
Reinforcing connections between various systems	21
Motors	21
Electrical	24
Image detection	24
Image focusing	25
Motion blur	26
Image processing	27
Testing	28
Sun position estimation by means of photoresistors:	34
Software	36
Sun Positioning System	36
Sun Visual Tracking System	37
Experimentation with Tennis Ball	37
Experimentation with Capture Dataset	37
Testing the 360 degrees camera with Raspberry Pi and OpenCV	38
<b>Data analysis and Results</b>	<b>39</b>
Data Analysis Plan	39
<b>Risk Analysis</b>	<b>40</b>
Safety Risks	40
Risk Register	40



# Verification

## Verification Plan

In order to verify the requirements stated in section 1 of the appendix, the following verification table has been created.

**Table 1.1.1.** – Verification table

ID	Requirement text	Verification	Test No.	Status
F1	The camera shall successfully track the Sun.	T	1, 2, 3	Achieved
F2	The experiment shall image the Sun in the spectral line of 656.28nm (H-alpha).	T,R	23	In Progress
P1	The gimbal system shall direct the telescope towards the Sun with an accuracy of at least 1 arcsecond	T,R	1, 2, 3, 23	In Progress
P2	The precision of the telescope shall be within a value of 1 arcsec.	T,R	4, 5, 23	In Progress
P3	The Sun shall be imaged at a maximum rate of 40 fps.	T, R	23, 26, 27	In Progress
P4	The experiment shall produce an output with a resolution of 1 arcsec at the vacuum wavelength of H-alpha line core - 656.28nm.	T, R	6, 7, 23, 26, 27	In Progress
P5	The maximum current drawn shall not exceed 3.5A.	T	8, 9	Achieved
P6	The supporting structure shall withstand a maximum compressive load of 200 N.	T, A	11	In Progress
P7	The tracking camera shall have a video resolution of no less than 640 by 480 pixels and 30 fps.	T, R	3, 26, 27	Achieved

ID	Requirement text	Verification	Test No.	Status
D1	The experiment shall operate in the temperature profile of the HASP vehicle flight and launch.	T, A, R	19, 22	In Progress
D2	The experiment shall operate in the vibration profile of the HASP vehicle flight and launch.	T, A	12	In Progress

D3	The experiment shall operate in the pressure profile of the HASP vehicle flight and launch.	T, A	24	Achieved
D4	The experiment shall not disturb or harm the launch vehicle.	I, R	-	Not completed
D5	The experiment shall not transmit on frequencies prohibited in Sweden.	R	-	N/A
D6	The diameter of the primary mirror shall not exceed 200 mm.	R	-	Achieved
D7	The length of the telescope shall not exceed 1000 mm.	R	-	Achieved
D8	The mass of the experiment shall not exceed 20 kg.	R	-	Achieved
D9	The maximum tolerance of any gearing has to be within 0.2 arcsec.	T, R	10, 13	In Progress
D10	The Sun tracking camera shall detect intensities of up to 100,000 lux.	T, R	3	Achieved
D11	The supporting structure shall not twist by more than 0.1 degrees.	T, A	11	In Progress
D12	The supporting beam shall not buckle under a safety factor of 2.	T, A	11	In Progress
D13	The experiment shall be able to run for up to 3 hours.	T,R	23, 24	In Progress
D14	The datalogger shall be able to receive signal and store it.	T,R	28	Not completed
D15	The main computer shall be able to communicate with the ground station	T,R	29	Not completed
D16	The focuser shall be able to focus and keep the contrasts	T	30	Not completed

<b>ID</b>	<b>Requirement text</b>	<b>Verification</b>	<b>Test No.</b>	<b>Status</b>
O1	The experiment shall accept control of the focusing motor for manual focus if a command is sent.	T	21, 23, 26, 27	In Progress
O2	The experiment shall enter the searching pattern if location of the Sun is not found according to the astronomical algorithm.	T	15, 17, 26, 27	Achieved
O3	The experiment shall transmit images to the ground when requested.	T	21, 22	In Progress
O4	The experiment shall cease to rotate on landing.	T	-	-
O5	The experiment shall be able to read data from a GPS device.	T	25	Achieved

## 1.1. Test Plan

Tests to be conducted in accordance to the verification table.

**Table 1.2.1.** – Test description

Test number	1
Test type	Software
Test facility	University of Sheffield
Tested item	Raspberry Pi tracking system
Test level/procedure and duration	This test was performed on a prototype of the Sun in the form a tennis ball. The idea was to gain confidence in the tracking abilities of the algorithm. The tennis ball was made to move in various positions and the distance from the centre of the screen and the center of the ball was recorded in two bits of data constituting the horizontal deflection cX and vertical deflection cY
Test campaign duration	1 hour
Test campaign date	8 March 2017
Test completed	Yes

**Table 1.2.2.** – Test description

Test number	2
Test type	Software
Test facility	University of Sheffield
Tested item	Raspberry Pi tracking
Test level/procedure and duration	This experiment was performed similar to P1 except it was repeated on a data set obtained from a camera with solar filter from one of the software team members (Alex Ian Hamilton).
Test campaign duration	6 hours
Test campaign date	15 March 2017
Test completed	Yes

**Table 1.2.3.** – Test description

Test number	3
Test type	Software
Test facility	University of Sheffield
Tested item	Raspberry Pi tracking
Test level/procedure and duration	The experiment was made to test the Sun visual tracking system in real time and was tested from the Raspberry Pi. The light source was taken to be a camera light from a cell phone. The purpose for this experiment was to test the performance of Raspberry Pi system).
Test campaign duration	3 hours
Test campaign date	17 March 2017
Test completed	Yes

**Table 1.2.4.** – Test description

Test number	4
Test type	Electrical
Test facility	University of Sheffield
Tested item	Arduino + Stepper motors
Test level/procedure and duration	The experiment was made to test control of at least two stepper motors with Arduino using as well the gimbal prototype for closest resemblance to final experiment. This would allow for two axis rotation of the telescope when tracking the Sun.
Test campaign duration	15 minutes
Test campaign date	17 March 2017
Test completed	Yes

**Table 1.2.5.** – Test description

Test number	5
Test type	Electrical
Test facility	University of Sheffield
Tested item	Arduino + Stepper motors
Test level/procedure and duration	Similar to test P4 but receiving the command values for rotation directly from the computer through serial communication. This test is crucial in order to set a connection between the hardware involved in Sun tracking and the Arduino which rules over the stepper motors.
Test campaign duration	15 minutes
Test campaign date	17 March 2017
Test completed	Yes

**Table 1.2.6.**

Test number	6
Test type	Software
Test facility	University of Sheffield
Tested item	PC Unit + Linux distribution + Andor SDK-based program + Andor camera
Test level/procedure and duration	Integrate and assess performance (fps, power consumption) of the data acquisition chain.
Test campaign duration	8 hours
Test campaign date	4 June 2017
Test completed	Yes

**Table 1.2.7. – Test description**

Test number	7
Test type	Software
Test facility	University of Sheffield
Tested item	Andor SDK
Test level/procedure and duration	Test and assess the Andor SDK for the features required by experiment by implementing various programs.
Test campaign duration	45 minutes
Test campaign date	28 April 2017
Test completed	Yes

**Table 1.2.8. – Test description**

Test number	8
Test type	Electrical
Test facility	University of Sheffield
Tested item	Raspberry Pi unit + Telescope camera (power consumption)
Test level/procedure and duration	Tested PC unit power consumption when operating Andor SCMOS camera under load using wattmeters.
Test campaign duration	45 minutes
Test campaign date	10 March 2018
Test completed	Yes

**Table 1.2.9. - Test description**

Test number	9
Test type	Electrical
Test facility	University of Sheffield
Tested item	DC/DC converters
Test level/procedure and duration	Test and assess performance and power losses of DC/DC converters under load operation (efficiency).
Test campaign duration	45 minutes
Test campaign date	14 May 2017
Test completed	Yes

**Table 1.2.10. – Test description**

Test number	10
Test type	Mechanical
Test facility	University of Sheffield
Tested item	Harmonic Drive
Test level/procedure and duration	Test harmonic drive.
Test campaign duration	1 day
Test campaign date	8 Aug 2017
Test completed	Yes

**Table 1.2.11. - Test description**

Test number	11
Test type	Mechanical
Test facility	University of Sheffield
Tested item	Gimbal Support Structure
Test level/procedure and duration	Load supporting structure 200N in compression for 3 hours.
Test campaign duration	3 hours
Test campaign date	15 August 2017
Test completed	Yes

**Table 1.2.12. - Test description**

Test number	12
Test type	Mechanical
Test facility	Sheffield
Tested item	Full Structure Assembly
Test level/procedure and duration	Vibrations test. Secure experiment in a van and drive on bumpy road.
Test campaign duration	3 hours
Test campaign date	12 September 2017
Test completed	No

**Table 1.2.13. – Test description**

Test number	13
Test type	Software
Test facility	University of Sheffield
Tested item	stepper motor control strategy
Test level/procedure and duration	The stepper motors will be tested with a microstepping driver for issues like accuracy, speed response, etc.
Test campaign duration	8 hours
Test campaign date	15 August 2017
Test completed	Yes

**Table 1.2.14. – Test description**

Test number	14
Test type	Electrical/Software
Test facility	University of Sheffield
Tested item	360 degrees camera + Raspberry-Pi + OpenCV
Test level/procedure and duration	Test feasibility of a 360 degree camera coupled with Raspberry-Pi for stage 1 Sun tracking method
Test campaign duration	3 hours
Test campaign date	24 Jan 2018
Test completed	No



**Table 1.2.15.**

Test number	15
Test type	Electrical/Software
Test facility	University of Sheffield
Tested item	Compass sensor + Arduino + Motor + LabVIEW
Test level/procedure and duration	Test feasibility of stage 1 Sun tracking method based on magnetic compass sensor and astronomical data.
Test campaign duration	8 hours
Test campaign date	06 Feb 2018
Test completed	No

**Table 1.2.16. – Test description**

Test number	16
Test type	Electrical/Software
Test facility	University of Sheffield
Tested item	Photoresistors + Arduino
Test level/procedure and duration	Test feasibility of a stage 1 Sun tracking method based on photoresistor array.
Test campaign duration	2 hours
Test campaign date	10 March 2018
Test completed	No

**Table 1.2.17. – Test description**

Test number	17
Test type	Electrical/Software
Test facility	University of Sheffield
Tested item	Sun tracking integration of stages 1 and 2
Test level/procedure and duration	Integrate the track algorithms. The main components involved in the test are the Raspberry pi and the EtherMega.
Test campaign duration	2 hours
Test campaign date	20 March 2018
Test completed	No

**Table 1.2.18. – Test description**

Test number	18
Test type	Electrical
Test facility	University of Sheffield
Tested item	DC/DC converter, driver, stepper motor and Arduino
Test level/procedure and duration	Level of noise measured with an oscilloscope in various points during working conditions.
Test campaign duration	45 minutes
Test campaign date	30 April 2017
Test completed	Yes

**Table 1.2.19** – Test description

Test number	19
Test type	Electrical/Thermal
Test facility	University of Sheffield
Tested item	Stepper motor
Test level/procedure and duration	Assess the ability of the stepper motor and sensors to withstand low temperature.
Test campaign duration	4 hours
Test campaign date	5 September 2017
Test completed	Yes

**Table 1.2.20.** – Test description

Test number	20
Test type	Software
Test facility	University of Sheffield
Tested item	Ether Mega operational test and integrated system response
Test level/procedure and duration	Test the main controller communication with other components and the system response (i.e. the speed with which the PC unit, camera, etc. come online after shutdown)
Test campaign duration	4 hours
Test campaign date	10 June 2017
Test completed	Yes

**Table 1.2.21.** – Test description

Test number	21
Test type	Software
Test facility	University of Sheffield
Tested item	Energy management (entire system)
Test level/procedure and duration	Test and tweak the energy consumption (test performed mainly at the main controller level)
Test campaign duration	4 hours
Test campaign date	12 June 2017
Test completed	Yes

**Table 1.2.22.** – Test description

Test number	22
Test type	Electrical/Software/Thermal
Test facility	Manufacturer facility
Tested item	Heating the telescope (entire system)
Test level/procedure and duration	This test is performed by the manufacturer and the results provided to us
Test campaign duration	4 hours
Test campaign date	1 June 2017
Test completed	Yes

**Table 1.2.23. – Test description**

Test number	23
Test type	Integration
Test facility	University of Sheffield
Tested item	Full Assembly
Test level/procedure and duration	Test integration with telescope positioning system.
Test campaign duration	20-30 hours
Test campaign date	12 September 2017
Test completed	No

**Table 1.2.24. – Test description**

Test number	24
Test type	Electrical
Test facility	Northumbria University
Tested item	Actuator and all electronics
Test level/procedure and duration	Test actuator and electronics in vacuum chamber for 2 hours.
Test campaign duration	2 days
Test campaign date	21 August 2017
Test completed	Yes

**Table 1.2.25. – Test description**

Test number	25
Test type	Electrical
Test facility	University of Sheffield
Tested item	Magnetic compass sensor readings
Test level/procedure and duration	Test accuracy of magnetic compass sensor readings.
Test campaign duration	2 hours
Test campaign date	1 August 2017
Test completed	Yes

**Table 1.2.26. – Test description**

Test number	26
Test type	Electrical/Soft
Test facility	University of Sheffield
Tested item	Thermocouples
Test level/procedure and duration	Test the accuracy of the thermocouples for reading the temperature of the actuators in operation.
Test campaign duration	1 hour
Test campaign date	18 August 2017
Test completed	Yes

**Table 2.27.** – Test description

Test number	27
Test type	Electrical/Soft
Test facility	University of Sheffield
Tested item	Electronics
Test level/procedure and duration	Preparte electronics setting including motor under operation for vacuum testing at Northumbria University.
Test campaign duration	2 days
Test campaign date	20 August 2017
Test completed	Yes

**Table 1.2.28.** – Test description

Test number	28
Test type	Electrical/Soft
Test facility	University of Sheffield
Tested item	Electronics
Test level/procedure and duration	The datalogger shall able to receive signal and store it.
Test campaign duration	2 hours
Test campaign date	10 April
Test completed	No

**Table 1.2.29.** – Test description

Test number	27
Test type	Electrical/Soft
Test facility	University of Sheffield
Tested item	Electronics
Test level/procedure and duration	The main computer shall able to communicate with the ground station
Test campaign duration	2 hours
Test campaign date	20 May 2017
Test completed	No

**Table 1.2.30.** – Test description

Test number	27
Test type	Electrical/Soft
Test facility	University of Sheffield
Tested item	Electronics
Test level/procedure and duration	The focuser shall able to focus and keep the contrasts
Test campaign duration	2 hours
Test campaign date	20 April 2017
Test completed	Yes

## 1.2. Test results

**Table 1.3.1**

<b>Test</b>	<b>Outcome</b>	<b>Obtained Results</b>
F1	Success	The camera successfully tracked the Sun
F2	Pending	-
P1	Pending	Raspberry-Pi performs adequately
P2	Pending	-
P3	Pending	-
P4	Pending	-
P5	Success	A limit on the withdrawal of current beyond 3.5A achieved
P6	Pending	-
P7	Success	The sun sensor successfully detected intensities up to 100,000 lux
D1	Pending	-
D2	Pending	-
D3	Success	The actuator and electronics performed successfully in a vacuum chamber for 2 hours.
D9	Pending	-
D10	Partial Success	The camera successfully tracked the object indoors. More testing to be done outdoors
D11	Failed	Brackets to be manufactured to prevent twisting.
D12	Pending	-
D13	Pending	-
D14	Pending	-
D15	Pending	-
D16	Pending	-
O1	Pending	-
O2	Partial Success	Successful Tests: 15, 17, 26 Test 27: Most elements were fully functional except for the ethernet switch, pi camera (on but not under operation) and current sensors (on but now logging data)
O3	Pending	-
O4	Pending	-
O5	Partial Success	The magnetic compass is highly affected by PMs, solved by moving sensors into gimbal structure.

## 2. Additional Technical Information

### 2.1. Mechanical

#### 2.1.1. General assembly drawings

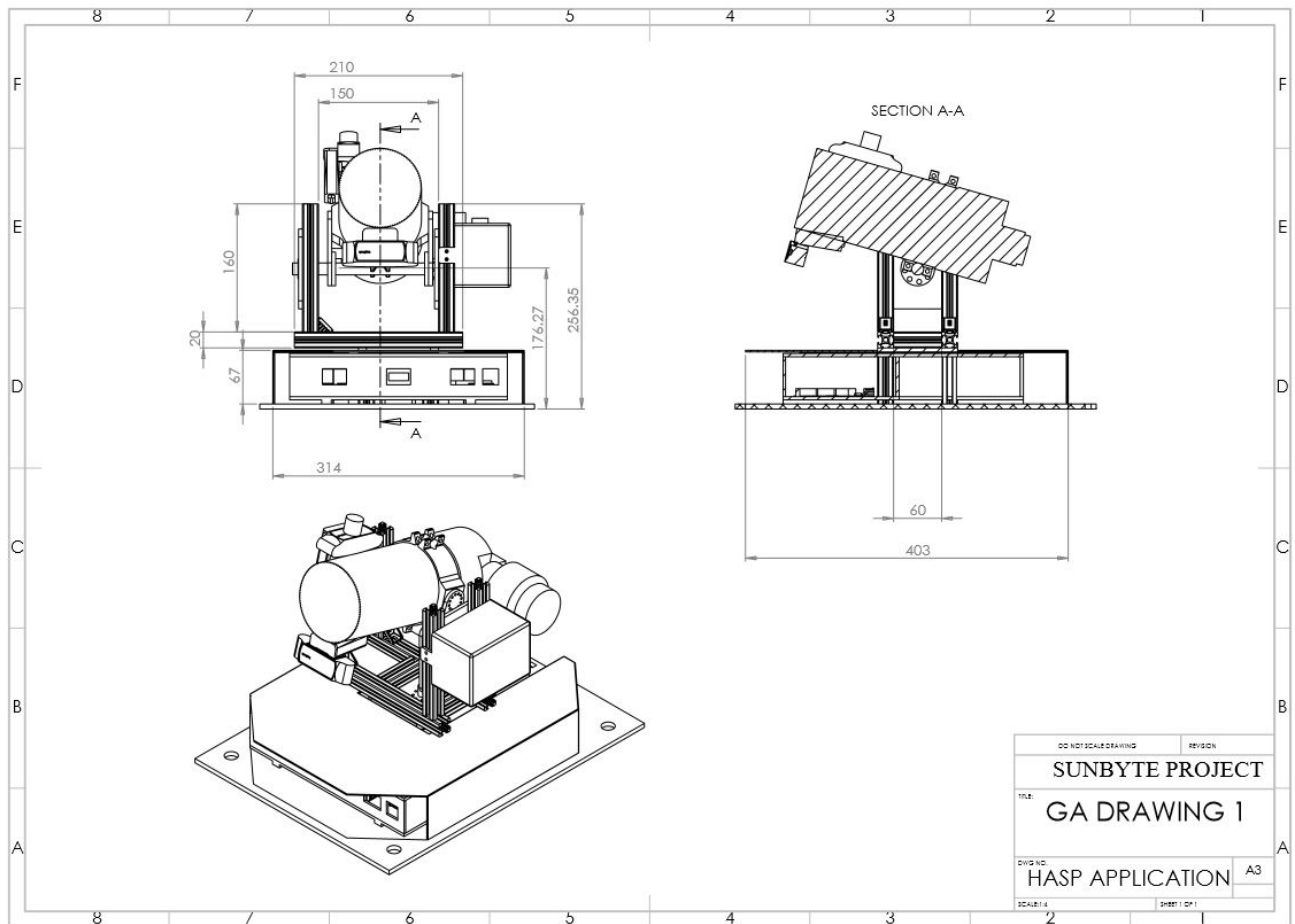


Figure 2.1.1.1. – General Assembly Drawing

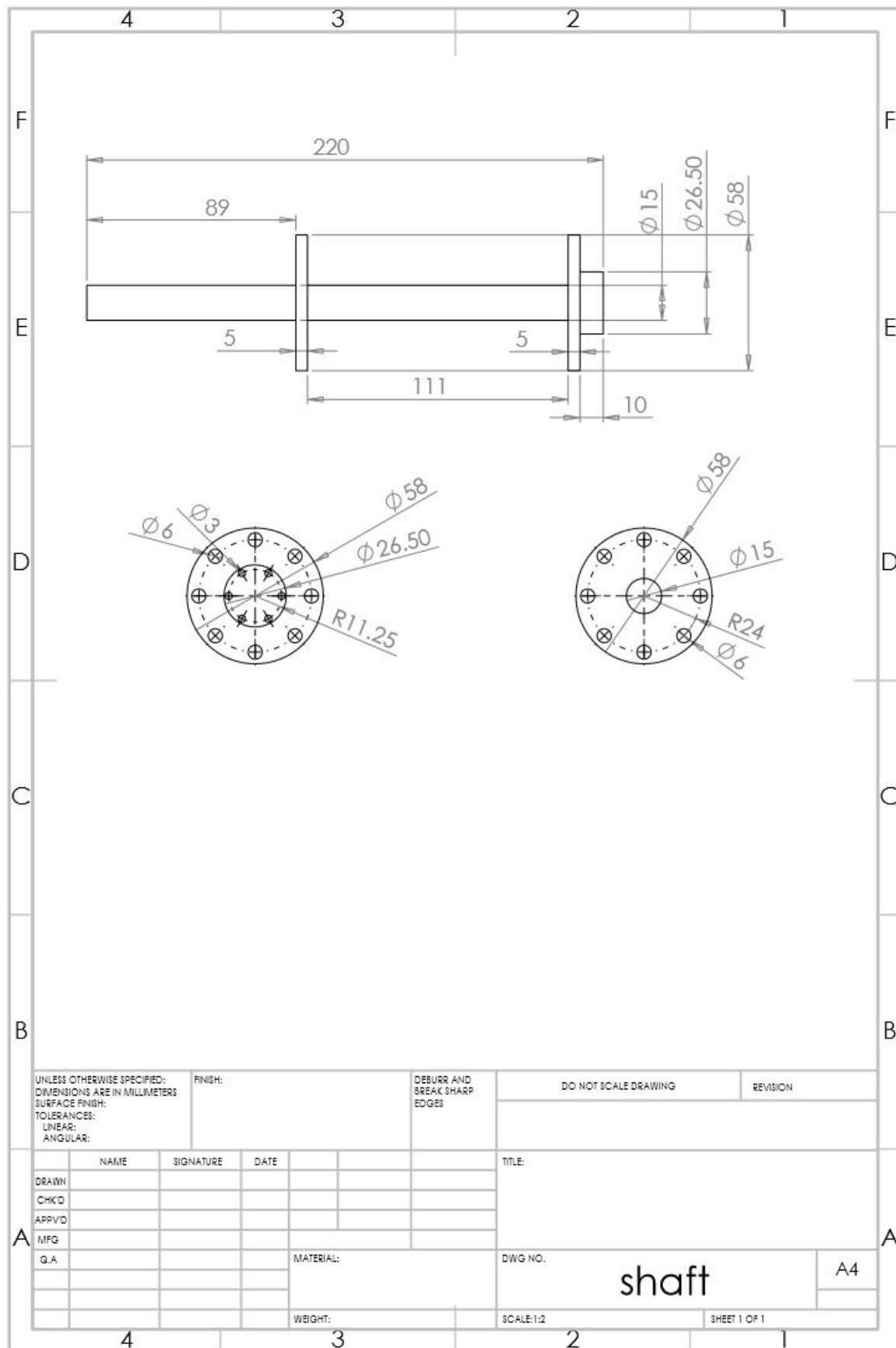


Figure 2.1.1.2. – Shaft dimension drawing.

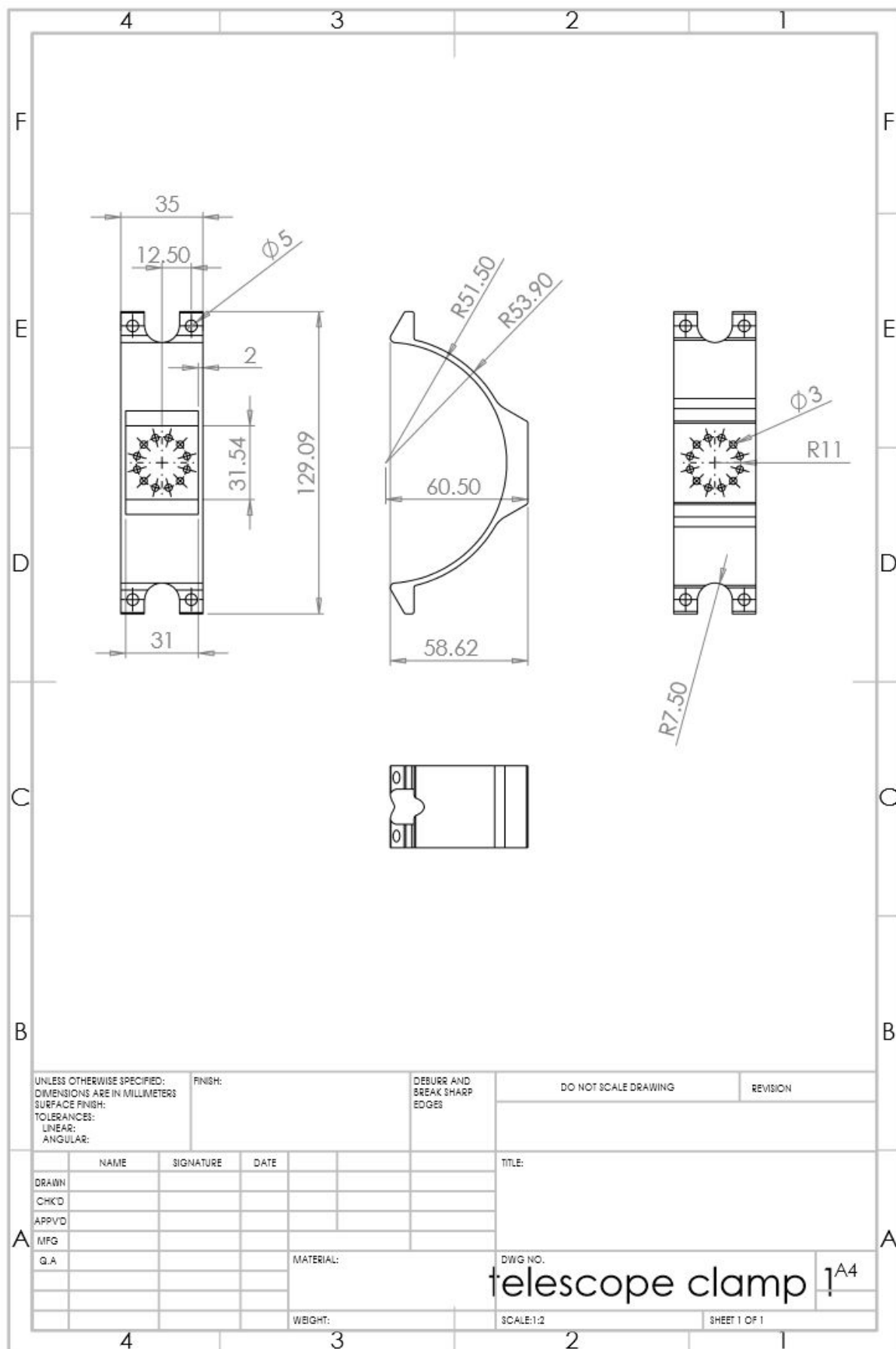


Figure 2.1.1.3. – Telescope clamp dimensions.



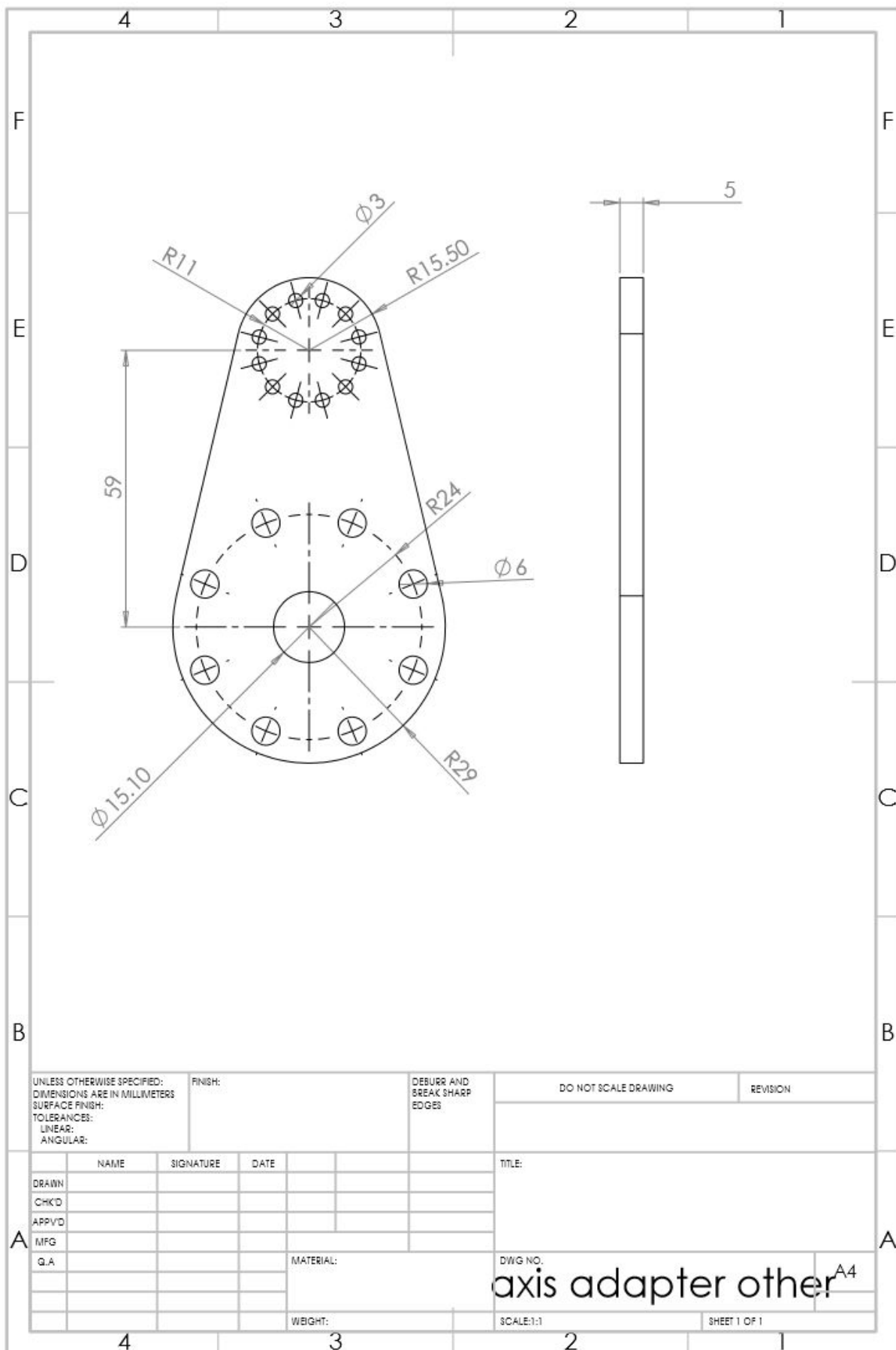


Figure 2.1.1.4. – Axis adapter technical drawing

### 2.1.2. Material Selection for the Gimbal and Support Structure

The possible materials that can be used for the gimbal are shown below in the table on the next page. The Yield strength of the materials has been taken over the expected temperature range to which the gimbal will be exposed to (approx -80 °C to 30 °C). The programme used to gather the data was CES Edupack 2016. Table 4.4 is a decision matrix used in order to choose the material we are most likely to use. Reliability was chosen to be the most important because at 25 km in the air, it would be impossible to change or fix any parts so they need to work as well in the air as they do on the ground. Only three of the materials have been shown as they are the most likely to be used for the gimbal. Using this matrix, Aluminium has the highest and most consistent scoring of the materials. Aluminium is also more readily available, easily extrudable and will still show some ductility at the approximate temperature ranges. It is difficult to 3D print the aluminium, so a different manufacturing process should also be considered. A key material property considered in the initial design selection process was the ability of the material to be 3D printed. However, after further testing a 3D printed model has been implemented. Further testing will be considered shortly and if the model survives the vacuum chamber test that is to be conducted, we might reconsider the possibility of using the aluminium model. At the moment, the possibility of using 3D printing as the main manufacturing route has to be confirmed by testing.

**3D printing metal for the current design is considered. If this method of manufacturing proves itself efficient and compatible with our mission we might consider using those components in the actual experiment assembly.**

Table 4.1.1 - Material selection

<u>Material</u>	<u>Strengths</u>	<u>Weaknesses</u>	<u>Yield Strength (MPa)</u>	<u>Density (kg/m<sup>3</sup>)</u>	<u>Cost (£/kg)</u>	<u>Cost (€/kg)</u>	<u>3D printable</u>	<u>Solutions to weakness</u>
<b>ABS</b> (40% carbon fibre)	Low density	Poor durability in UV radiation.	124-131	1220-1270	6.78-8.77	7.70-9.97	Yes	Use of some type of coating against UV
<b>Austenitic Steel 304</b>	-Excellent corrosion resistance against water	-Heavy -3D printing questionable	190-310	7900	3	3,41	Yes- not very common	Machining each of the parts
<b>Aluminium 6061</b>	-High strength - widely used in Aerospace applications -High corrosion resistance -Easily machined -Easily weldable	-Not as lightweight as other options -Not as strong as Kevlar	241-266	2700-2730	1.57-1.8	1.78-2.25	Yes	The size of the gimbal is not very big; so the weight will not affect the total structure too much
<b>Nylon 12</b> (with Aculon coating)	-Lightweight -Low water absorption -Good weather resistance	-Very low yield strength -Mechanical properties affected by moisture	34.8-43.4	1000-1020	7.16-8.7	8.14-9.89	Yes	Application of a coating to prevent moisture and UV
<b>Kevlar (with coating)</b>	-Tough, strong, impact resistant -Low coefficient of friction -Lightweight	-Affected by UV radiation -Mechanical properties affected by moisture	2500-3000	1460-1480	62.8-157	71.36-178.41	Yes	Application of a coating to prevent moisture and UV

**Table 4.1.2 - Material comparison**

	<b>Kevlar</b>	<b>Austenitic Steel 304</b>	<b>Aluminium 6061</b>
Weight (5)	3	1	2
Reliability (6)	1	3	2
Machinability (2)	1	2	3
Price Effectiveness (1)	1	2	3
3D Printability (1)	3	1	2
Corrosion Resistance (4)	1	2	3
<b>Total score</b>	<b>37</b>	<b>40</b>	<b>49</b>

Further material selection analysis has been conducted in order to decide upon the most suitable and compatible material to be used in the manufacturing processes. In conclusion, it has been decided that Aluminium 6082 would be the most suited material for both the gondola and the gimbal. The next step was getting in contact with potential suppliers and manufacturers. The final choice of the material was made between Austenitic Stainless Steel and Aluminium 6082. As the steel weighs approximately 3 times as much as the Aluminium. Therefore it was not a viable option as we need to put as little strain on the motors as possible to reduce that heat generation. AirCRAFTmaterials UK were contacted about having test samples made. One quote that we received for 10 samples to be used in various testing conditions was £420.

**Table 4.1.3 - Material properties**

	<b>Austenitic Steel 304LN</b>	<b>Aluminium 6082</b>
<b>Service Temperatures (deg C)</b>	-250 - 750	-273 - 150
<b>Thermal Conductivity (W/m*K)</b>	14.4 - 15.6	164 - 170
<b>Specific Heat Capacity (J/kg*K)</b>	500	882 - 918
<b>Thermal Expansions Coefficient (micro strain/K)</b>	16.5 - 17.5	22.5 - 23.7
<b>Durability</b>	Excellent	Excellent
<b>Density (kg/m<sup>3</sup>)</b>	7900	2670 - 2730
<b>Young's Modulus (GPa)</b>	195 - 205	70 - 74
<b>Yield Strength (MPa)</b>	270 - 290	162 - 179
<b>Tensile Strength (MPa)</b>	550 - 750	247 - 273
<b>Compressive Strength (MPa)</b>	270 - 290	162 - 179

### 2.1.3. Reinforcing connections between various systems

Most of the components used in the design are boards with a fixed type of ports and connectors which cannot be modified for reinforcing these against vibration and shock. Therefore, a reinforcement metal strip, secured using two screws and pinning down the connector is going to be used like in Figure 4.54 for example.

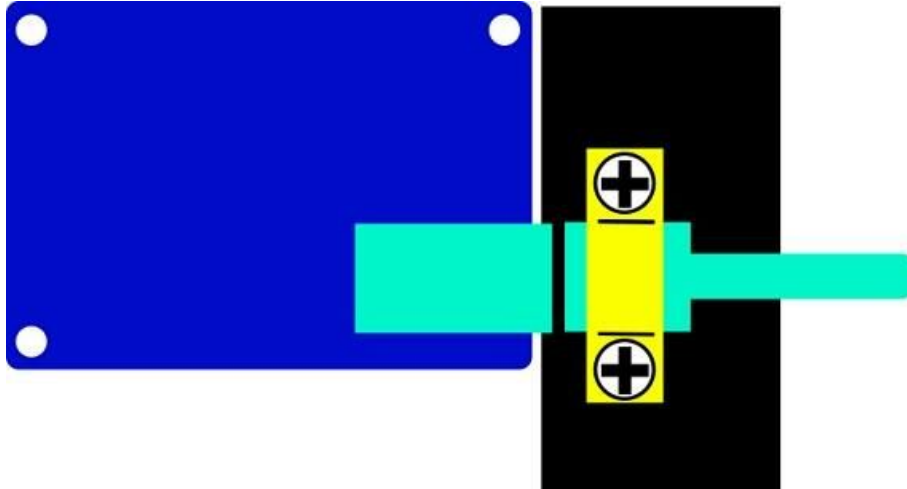


**Figure 4.52.** – Proposed reinforcement for connectors and ports.

A challenging issue is the ribbon like cable between camera and raspberry pi board. Not only is the cable not long enough, but it is not very reliable when it comes to twisting or protection against cold. Therefore two adapters are used from CSI to HDMI and HDMI to CSI - this means that the same port for the camera is used on the Raspberry Pi, but a much more robust HDMI extension cable is used between the camera and Raspberry Pi. The ends of the HDMI cable are secured in a similar fashion like in the Figure 4.54 ; while the ribbon cable is kept secure, can be located inside a protective case and will not be twisted anymore as the stress is moved to the HDMI cable extension.

Given concerns addressed with regards to wiring and connections during presentations at the training week at DLR-Oberpfaffenhofen, the internal wiring between all elements located inside the aluminium box will be following a single path per level (as shown previously the box is divided into several levels) which will make extensive use of cable ties and will additionally be screwed in several key areas, although there are not high vibrations expected since the described experiment will fly on HASP.

Finally, as pointed out in previous sections, most connections from the experiment to the aluminium box inside the gondola will be joined and passed through the Amphenol 62GB series connector ensuring a high degree of reliability.

### 2.1.4. Motors

Engineering drawings of the motors that are to be integrated in the current design can be accessed at: [https://www.oriental-motor.co.uk/media/images/640\\_ia\\_pkp5-42mm-highresol-dim.jpg](https://www.oriental-motor.co.uk/media/images/640_ia_pkp5-42mm-highresol-dim.jpg). The motor model is PKP546MN18A.



### 2.1.5. Optics

The chosen focuser is the TS-Optics short T2 Helical Focuser & Adapter which uses an M42 connector. It is capable of an adjustment distance of XX mm and precise focusing of up to XXX(1/20) mm accuracy. This was chosen as the inner tube does not rotate thus allowing the orientation of the camera to be retained. Two fixing screws hold the focus position.



**Figure 4.1.7.1.** – TS-Optics 2 Helical Extractor Screw Focuser

The focuser will be lubricated using Krytox GPL 203 grease, which is suited for cryogenic conditions of down to -60 °C. A gear wheel will be fabricated to fit over the knurled area. Adapters are required to set the correct distance from the telecentric to the etalon. The focusing design used for the camera not only acts as a way to automatically control the focus of the camera but to also support the mass of the camera. The design allows for the bigger gear fitted around the focuser to increase and decrease in length while still being attached to the smaller driving gear due to the length of the smaller gear. The design also adds support to improve the stability of the camera by fixing the smaller gear directly to the camera and fixing the smaller gear to a shaft which slides in and out of a hole fixed to the telecentric clamp. Doing this not only stops unwanted movement from the small gear but also the shaft and telecentric clamp configuration acts as a pivot to support some of the weight of the camera.

## 2.2. Electrical

### 2.2.1. Image detection

Getting into more details the image detection algorithm would raise the question of the amount of light and the exposure time required to achieve reliable performance in Sun's detection. This would ideally have to be correlated with the following steps (especially no. 3):

1. Obtaining the information (the 'R', 'G', 'B' value) of a range of pixels collected from the upper half of the image.
2. Using the data above to calculate the luminance.
3. Assign a luminance threshold, such that values above it would correspond to space atmosphere, and the values below would correspond to below stratosphere environment.

In order to deliver a proof of concept experiment, initial tests were conducted on the algorithm based on static stock images as input. Reasonably good results in both space and terrestrial environments were obtained. For example, the space environment results were obtained by processing stock images of the Sun captured in outer space. The success of the algorithm was appreciated by its ability to separate the Sun's shape in all available stock images. The results can be observed in Figure 4.2.1.1. and 4.2.1.2.

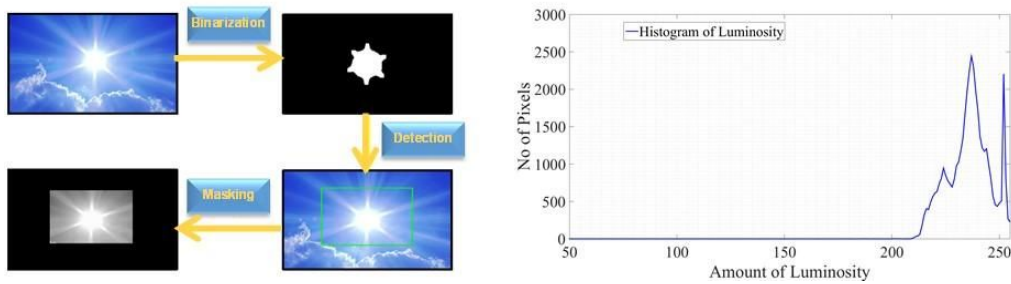


Figure 4.2.1.1. – Proposed algorithm running on daylight.

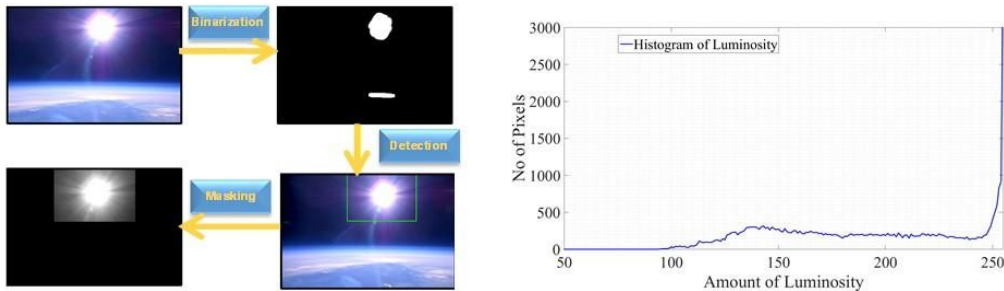


Figure 4.2.1.2. – Proposed algorithm running in upper atmosphere.

As for the method's limitations, these stems from lighting conditions available to the Sun tracking camera. We can see from the results above that if the light amount reaching the camera is **in a comfortable range** (i.e not too bright not too dark), the binary image of the Sun would appear as roughly a circle and hence would be manageable by the shape detection algorithm. Despite tests being performed in both Sunlight and stratosphere environments a clear distinction of Sun shape based on number of pixels being in the majority in the bright region of the histogram (i.e. the right-hand side) was always obtained. However there is a reason for concern shown in the first figure as an over-bright (overexposed) input can lead to production of a **'distorted shape'** (as illustrated in



the binary image). It is not possible to infer that there is a circular shape in the brightest region of Figure 4.2.1.1.

It can be concluded that there is a good chance that higher number of pixels in the bright region (i.e. large area to the left hand side of histogram to with luminosity < 200) can lead to shape distortion which would prevent shape detection algorithm to continue with obtaining the centroid of the Sun.

The initial results are encouraging however, more robust methods need to be tested. In order to improve the results, improvements have been made in the form of canny edge masking which allows trails of Sun to be detected once the computer vision algorithms are run.

## 2.2.2. Image focusing

As the environmental conditions change the focus of the telescope will vary due to strain on the structure and temperature related material contraction, this can be corrected by regularly refocusing the telescope which requires the imager to be mechanically moved forwards or backwards parallel to the telescope tube.

With the uplink bandwidth being limited, a live video stream is impractical and so manually focusing is impossible during flight.

An automatic software-based solution has been developed by the software team that is designed to operate completely independently of the operators.

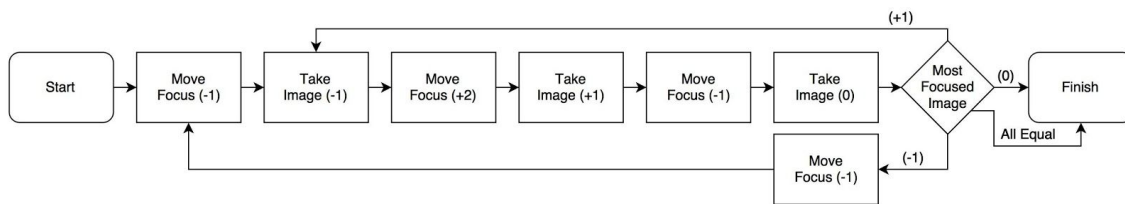


**Figure 4.2.2.1.** – A flowchart of the basic focusing implementation.

With this method, the system repetitively attempts to adjust the focus and check if the changed focus (moved one increment forwards or backwards) is better than the final resting position. The final resting position is expected to be close to the initial position, but the image is taken last to ensure there is no drift when trying to return to that position. The algorithm is not the fastest possible when the focus is too far off at the start of the process, as the system will need to repeatedly move backwards and forwards through the focal plane in small increments, however the telescope is expected to be focused on the ground and only need to maintain focus thereafter.

Focusing times. The focusing process is to be automatically undertaken at regular intervals, expected to be every 10 minutes but to be determined in testing.

During the focusing intervals the main telescope camera will be collecting data as normal and these images will be used to as the images to compare for focusing.

Additionally, a text log of the focusing times will be recorded to the main SSD to help in the removing of blurred images during post-processing.

Note: if the scientific camera is no longer acquiring images then improving focus will not be possible, instead the comparison will generally be of the latest image to itself and the process will terminate as it determines the current focus is as good as the other 3.

Testing focus. The focusing process requires a method of comparing the focus of 3 images and determining the sharpest (best focus) of these. The Sun, as a very strong light source, gives a very high signal-to-noise ratio making sharper focus lead to a higher dynamic range in the image, this can be used as a basic metric for focus.

The method involves taking the maximum intensity value ( $I_{\max}$ ) and subtracting the minimum intensity value ( $I_{\min}$ ) to get a quantity for the dynamic range. The highest value of dynamic range will generally correlate to the most focused image, see Figure 4.66

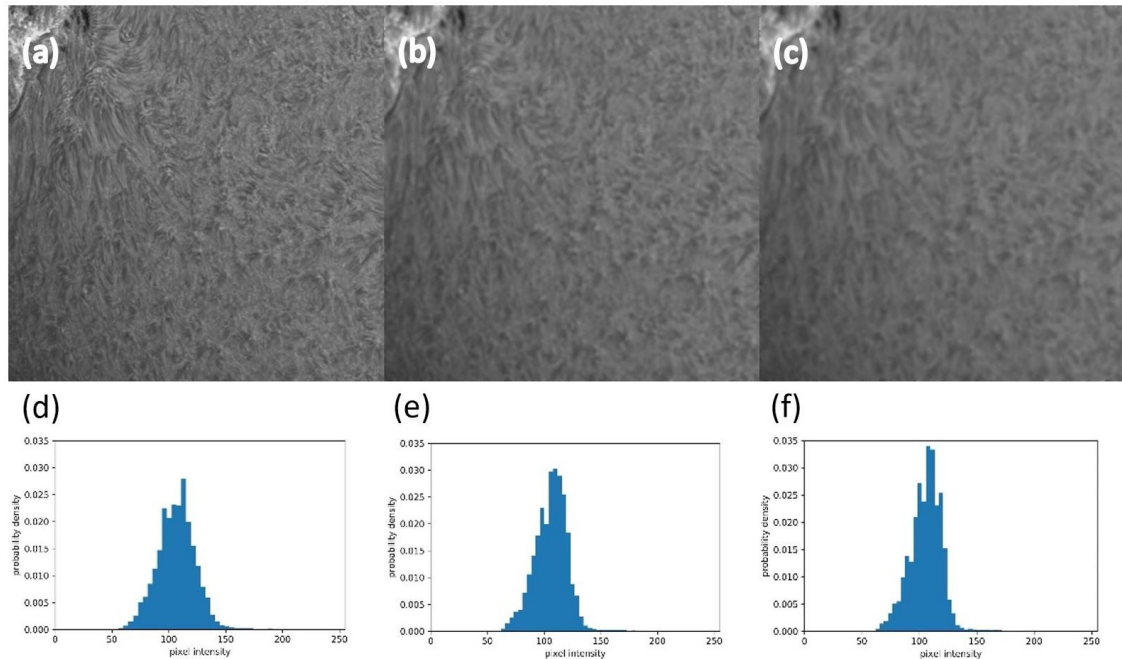


**Figure 4.2.2.2** – An initial H-alpha image (a) is filtered with a basic blue once in (b) and twice in (c), the resulting dynamic ranges are 211, 192 and 184, showing that (a) is recognised at the best focus. The histograms of (a), (b) and (c) are given in (d), (e) and (f), as can be seen, the increased blur tends to spread the range of intensity values towards high or lower values, leading to a higher dynamic range.

### 2.2.3. Motion blur

An additional source of blur other than incorrect focus can be if the telescope is in motion, this will cause a motion blur as the camera sweeps over an area during the exposure. Exposure times are expected to be at maximum 1/40 s (limited by the capture rate of the imager) and are likely to be substantially less due to the large aperture of the telescope providing a lot of light to measure. However, an additional control step will be added to the focus process to check if the projects accelerometer is detecting motion above a given threshold, if-so then a new image will be used for the focus reference at the given focus.

Full process. The resulting process adds a check for motion and waiting delays to allow the motion to settle down. This is simple to represent in a flowchart.

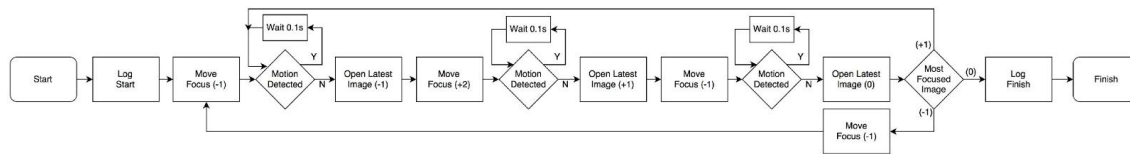


**Figure 4.2.3.1..** – A more comprehensive flowchart of the focusing process.

Consideration has been given to the possibility the telescope will under constant motion, in this case the telescope will be constantly waiting before it can adjust the focus. This won't interrupt the data acquisition and so is considered to be graceful degradation of functionality. Ground control over the motion threshold may be added to allow us to correct mid-flight if this is too sensitive.

Similarly, additional functionality can be added to change the focus adjustment distance increments if the system is too far out of focus to be able to return quickly enough, or in the event the small increments don't provide enough of a change to the dynamic range to allow focus.

## 2.2.4. Image processing

The purpose of this subsection is to roughly present an overview of the data acquisition software characteristics. This is based on the high-tech camera provided by Andor which will capture images directly from the telescope. It will run on top of a GNU/Linux based operating system due to its highly customisable characteristics. In terms of functionality it will provide the following:

- compress the raw images generated by the Andor camera to a suitable lossless format (for example zipped binary files) and write them to the available storage;
- run in batch mode to increase the speed and remove the unnecessary overhead. There will be no GUI for example;
- optimise the processes and make sure the ones required by task at hand gets maximum priority;
- configure the appropriate functionality (i.e. establish the connection with Andor camera, during the startup sequence) which should be used whenever the computer (re)starts; • provide a log of the current events (i.e. "image acquisition starting at ...") with basic diagnostics to test it pre-launch;
- only fire the Andor camera when the telescope is aligned with the Sun (i.e. no unnecessary data will be processed and stored - no blank images).
- generate external diagnostics signal (i.e. 'alive' signal) to communicate its current state to monitoring controller

The actual implementation relies on Andor SDK which is written in C++ and also available on Linux. The camera can take pictures with up to 40fps, however for the success of the experiment, this feature is not required. A list of steps defining a typical C++ program based on Andor SDK which acquires images is represented below:

1. Launch and initialize the Andor functionality - (AT InitialiseLibrary());

2. Open a connection with the camera (AT Open (int i cameraIndex, AT H Hndl) where the i cameraIndex is the index of the camera known a priori. The function returns a handle Hndl which allows accessing various camera states;
3. Set memory aside to accommodate the incoming images from the camera AT QueueBuffer(AT H Hndl, unsigned char\* pucAlignedBuffer, AT 64 ImageSizeBytes) - the ImageSizeBytes specifies the amount of memory to be allocated while pucAlignedBuffer is determined before and required for a byte offset alignment which increases the performance
4. Start frames acquisition, dump data to disk, end aquisition - AT Command(Hndl, L"AcquisitionStart") - the SDK does not provide functionality for writing or converting images into various formats - this will be provided separately. The aquisition ends with AT Command(Hndl, L"AcquisitionStop");
5. The program ends with AT FinaliseLibrary( ) call which releases any resources currently in use.

### 2.2.5. Testing

In the electrical part of the project there has been a constant progress with regards to testing. Since the final devices were not available, control of the motors has been tested by use of available components. Some of the employed are pictured below including L298N drivers and stepper motors with 1.8 degrees per step together with a simple connection example.

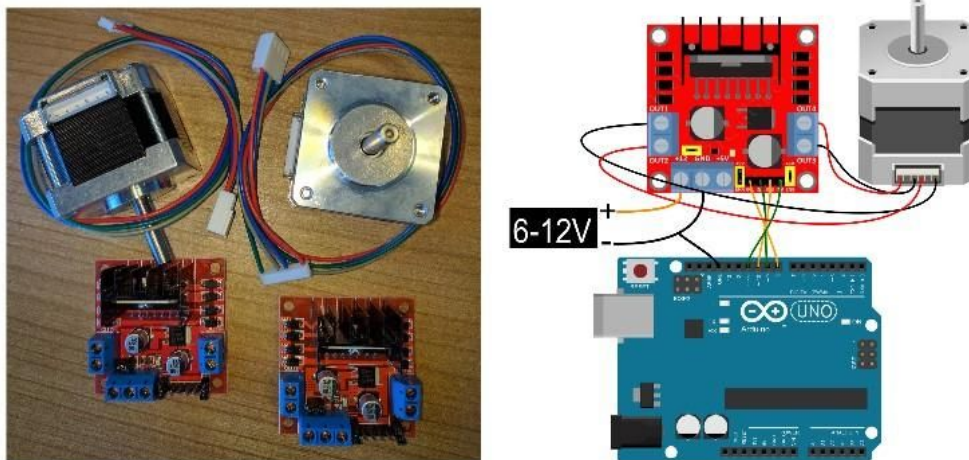


**Figure 4.2.5.1.** – Actuator motors and their drivers

Testing using these tools offer a lot of information about performance of control software built for Arduino, power consumption of the motors, relation between voltage available and maximum achieved speed and required torque and thus current drawn. The motors are controlled by the drivers which are themselves controlled by the Arduino.

As seen below, testing has been performed by use of a first gimbal prototype that allows two axis of rotation and already incorporates one of the cameras currently under consideration.



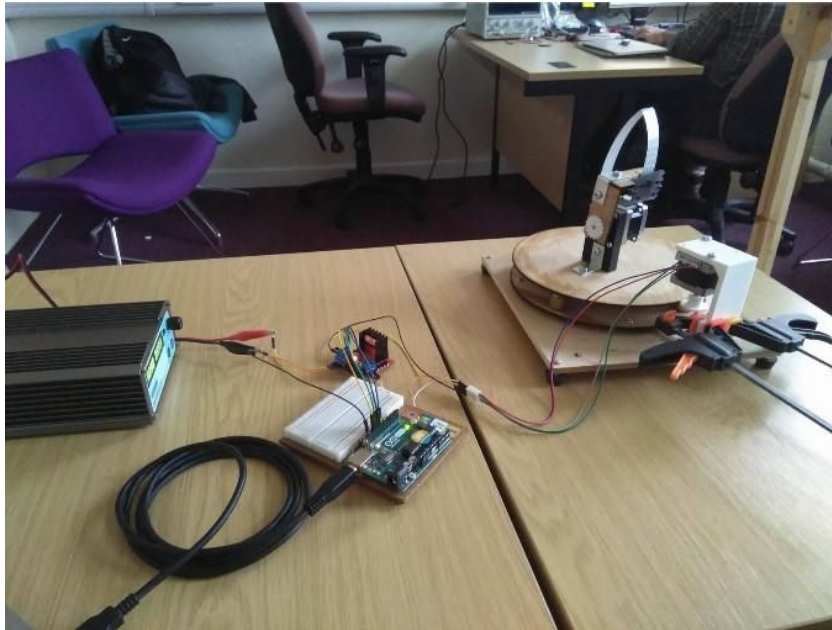


**Figure 4.2.5.2.** – Gimbal Prototype 1 interfaced with Arduino. Video is available here: <http://sunbyte.group.shef.ac.uk/galleryv2.html>)

Performing these tests allow us to get an insight into the behavior of our motors. The software located in the arduino is ultimately in charge of correcting the aim of the telescope for which a communication is needed between the Arduino and the Raspberry Pi where the sun tracking algorithm is running. For that purpose, the Arduino is constantly "listening" for commands that allow a two axis error compensation. Additionally, the possibility of controlling the motors directly from the Raspberry Pi seen in the following figure has also been studied with satisfactory results. Videos of these tests are available on the team website.

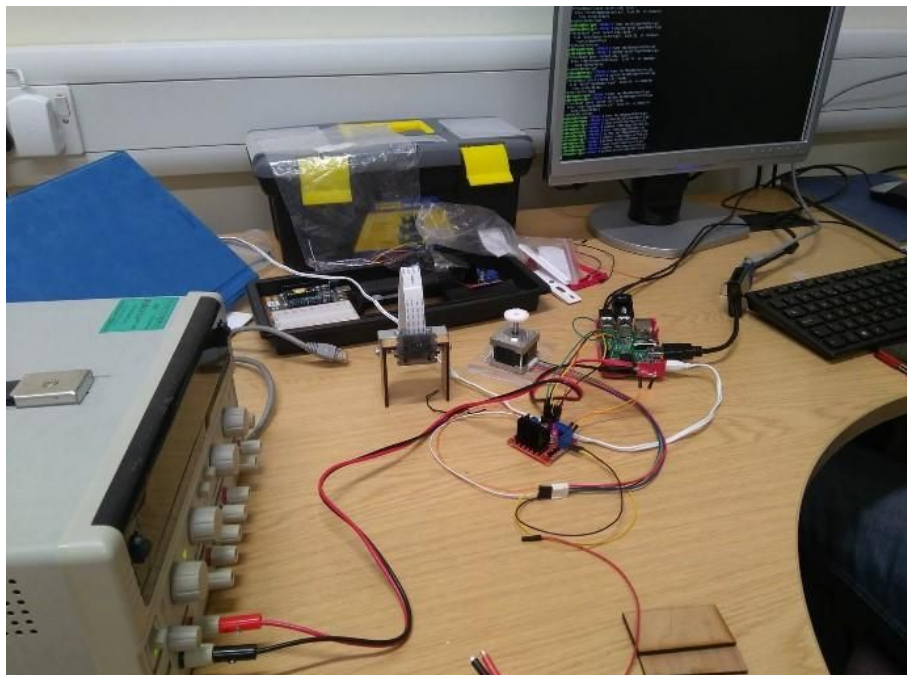


**Figure 4.2.5.3.** – Actuator motor controlled from Raspberry Pi. Video is available here: <http://sunbyte.group.shef.ac.uk/galleryv2.html>

Following testing on the first prototype, a second version of the gimbal was built, shown next, this time mounting a real telescope with the possibility of attaching our SCMOS camera.

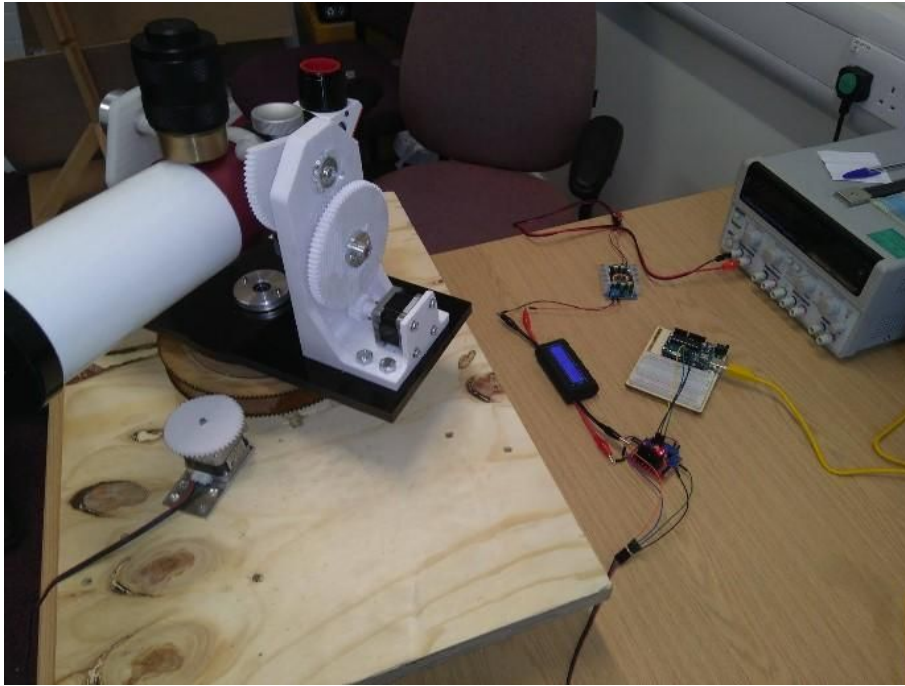


**Figure 4.2.5.4.** – Gimbal prototype two

A closer look at the right part of the figure allows seen that control of the motor during testing is being carried out with all elements associated including DC/DC converter, wattmeter for power consumption and driver. A zoom in of this section is presented next:

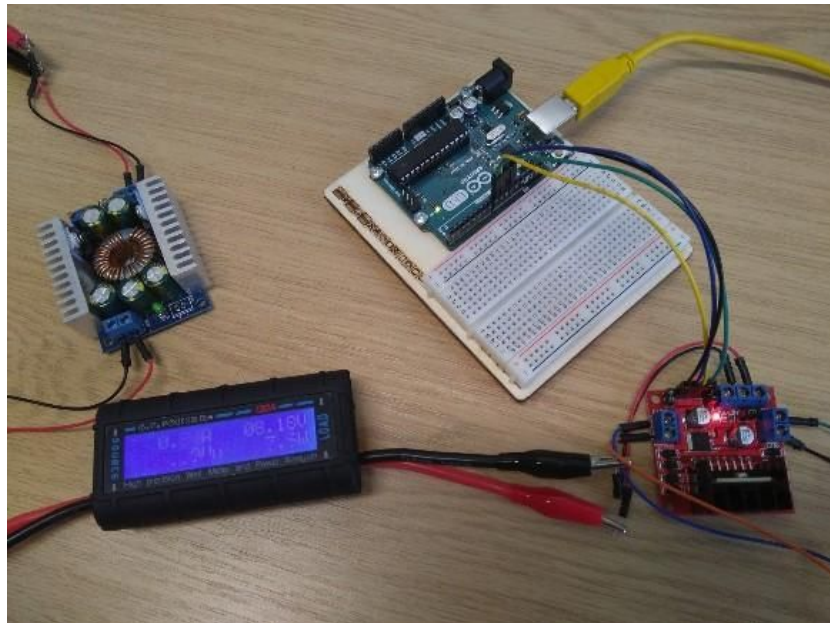


**Figure 4.2.5.5.** – Electronics associated with driver during test.

Finally, a last prototype has been built out of already available Lego with the aim of simplifying further testing, releasing the motors of a relatively high torque demand, lightening the testing platform and allowing the use of extra elements already available as well as lower power motors/drivers.



**Figure 4.2.5.6.** – Third gimbal prototype made out of Lego.

It is possible to see that for the third gimbal, seen on the figure above this lines, the pi-camera has been integrated, easy to spot due to the white ribbon connector. This last gimbal model presents no reduction apart from the internal gearing of the motors, given that the motor shaft is directly connected with the axis of rotation. The final aim, being a fully functioning two-axis actuation of the gimbal has been achieved, and more importantly, commands are given directly by the raspberry-pi as a result of execution of the sun-tracking algorithm. This Lego gimbal prototype has been presented at an outreach event for the UK Pint of Science 2017.



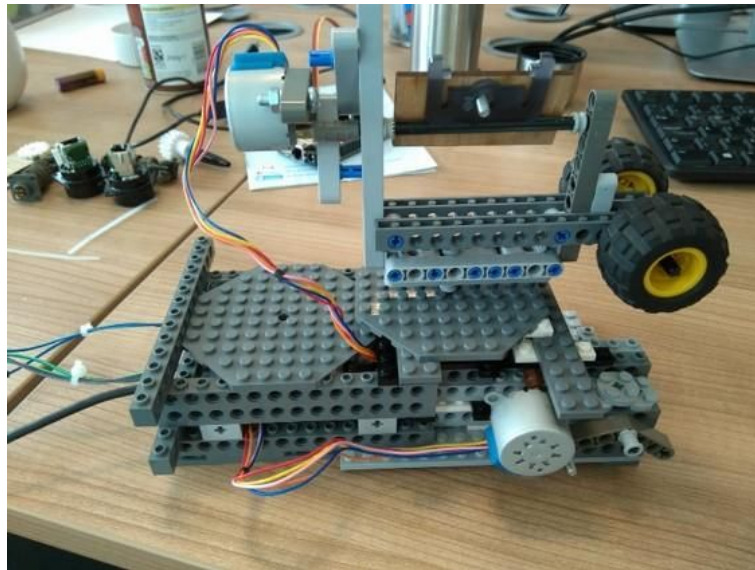


**Figure 4.2.5.7** – Fourth gimbal prototype and second made out of Lego

The final iteration of Lego gimbal prototype is presented in Figure 4.2.5.6. In this case a solid platform has been built and a gear reduction (40/8) has been included to improve the accuracy of even quick tests and to present a more experiment-wise prototype for outreach. This gimbal prototype has been presented at the "IET Present Around the World - Northern Area Final", at Preston, June 14th.

### Testing of the Stepper Motor and Driver

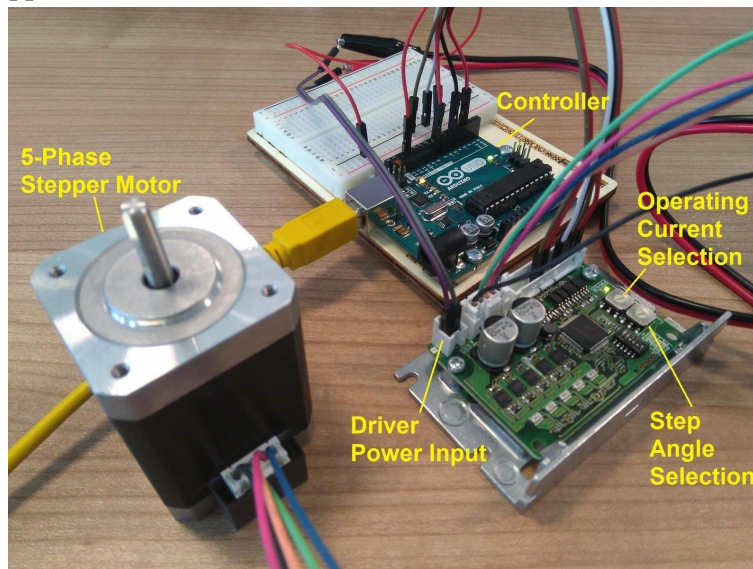
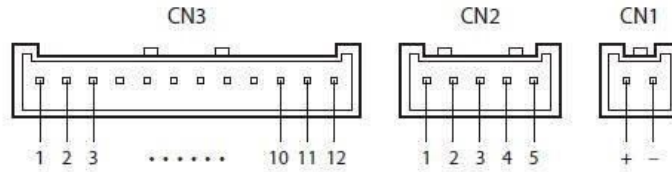


**Figure 4.2.5.8.** – Stepper motor and driver

Testing of the chosen stepper motor and driver are shown in Figure 4.2.5.8. The selected driver allows performing microstepping without the need of additional circuits or code. All that is needed is to select the step angle for the microstepping and set off port 7 (CS - Step angle switching input) of the Driver CN3 (I/O signals) as seen in Figure 4.2.5.9.



## ■ Connector pin assignment



### ● CN1 (power supply)

Pin No.	Direction	Signal name	Description
+	IN	POWER	+24 VDC
-			GND

### ● CN2 (motor)

Pin No.	Direction	Signal name	Description
1	OUT	MOTOR	Blue motor lead wire
2			Red motor lead wire
3			Orange motor lead wire *
4			Green motor lead wire
5			Black motor lead wire

\* This orange lead wire is for 5-phase stepping motor. For 2-phase stepping motor, do not connect anything to the pin No.3 since there is no orange lead wire.

### ● CN3 (I/O signals)

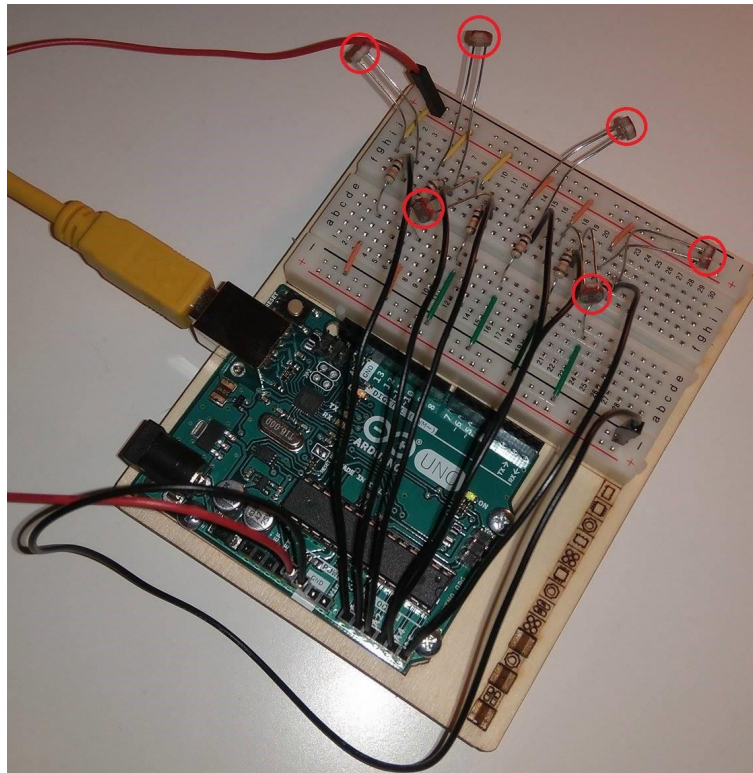
Pin No.	Direction	Signal name	Description
1	IN	PLS (CW)	+
2			-
3		DIR (CCW)	+
4			-
5		AWO	+
6			-
7		CS	+
8			-
9	OUT	ALM	+
10			-
11		TIM	+
12			-

Figure 4.2.5.9. - I/O pins

Given that the microstepping position needs to be fixed at a certain value of step angle for the entire duration of the flight, there will only be two modes of operation available, the default step angle of 0.36 degrees per step and another one, between the minimum needed of 0.036 and 0.00288 degrees per step. This selection is based on a tradeoff between the accuracy needed to meet our requirements and the speed needed to compensate for the rotation of the gondola. Maximum speed achieved so far is 130rpm, considered enough to meet our requirements.

### 2.2.6. Sun position estimation by means of photoresistors:

As explained before, an array of photoresistors was being considered as a possible back up solution in case all Sun tracking and position systems fail. On its most basic forms it was to be formed of 6 elements connected to 6 analog ports of the Arduino and placed in a frame shaped like a hexagon.



**Figure 4.2.6.1.** – Photoresistor array test.

The way it was carried out was by computing the analog magnitude of the resistance read from each photoresistor and comparing it to the rest. In this way, if one read was far superior from the rest it was possible to assume that the Sun position was in the vicinity of that element ( $60^\circ$ ), if it was almost the same in two elements will be located in between them ( $30^\circ$ ), and if it was higher in one, closely followed by another it was possible to assume it was in the closest  $15^\circ$  starting from the first and towards the second. To compute a higher degree of accuracy with just 6 photoresistors seemed out of reach. The possibility of using far more than 6 elements was also available given the choice of Arduino MEGA as microcontroller platform (16 analog inputs) but the need to shield them from the outside environment, a large amount of extra wiring and the extra computational load resulted in not pursuing this method.

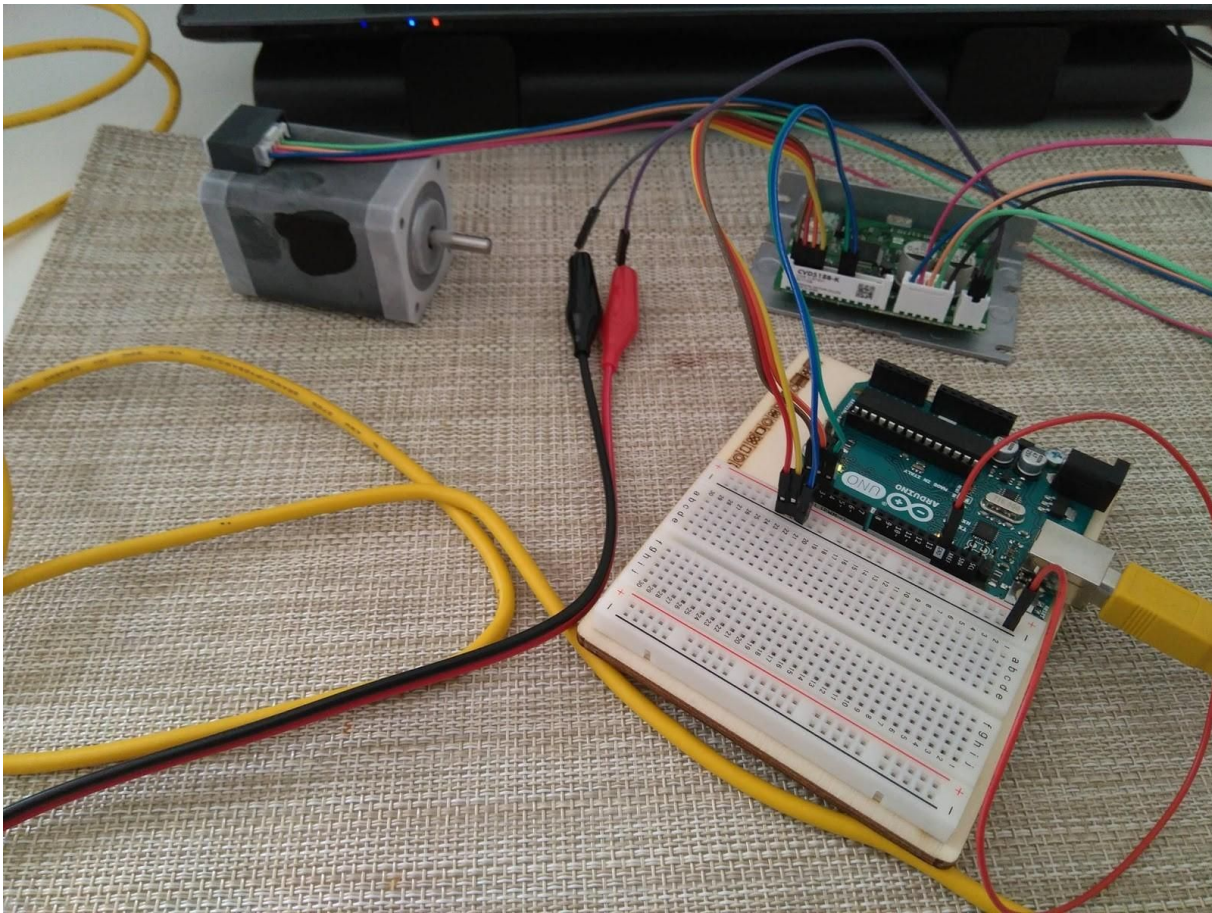


**Figure 4.2.6.2. – Cold Test**

The motor and driver were placed in a freezer and allowed to cool for 2 hours until a temperature of 18 degrees Celsius was reached. They were tested immediately after and were still functional.

## 2.3. Software

### 2.3.1. Sun Positioning System

First stage Sun tracking using astronomical calculations have been prototyped using LabVIEW. The output of the algorithm was first tested by comparing results to NOAA Solar Position Calculator [10] and the results matched.

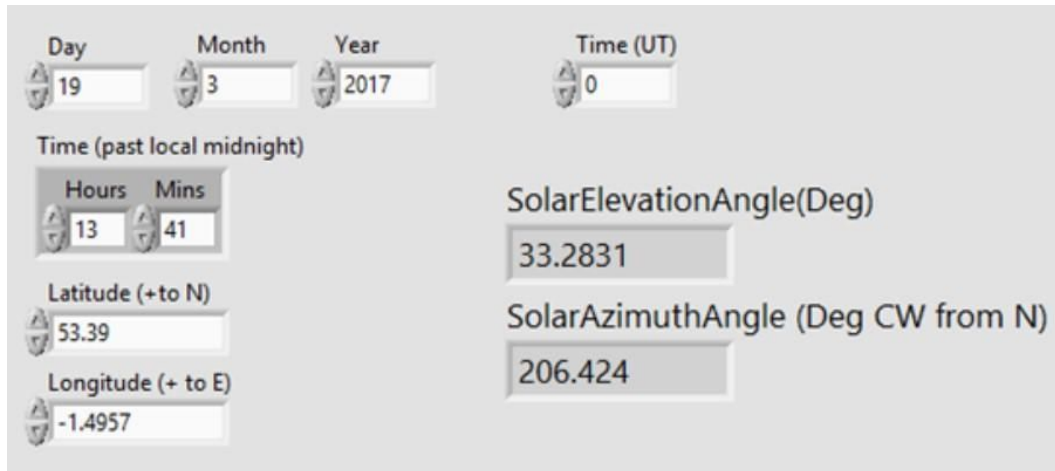


**Figure 4.3.1.1.** – Sun Locating based on Astronomical calculations, LabVIEW program front panel.

Furthermore a simple hardware prototype was built using two servo motors attached perpendicular to each other to represent the Azimuth and Elevation angle as shown in figure below. The prototype was tested on a sunny day and give very satisfying results and could track the Sun with a relatively small error of +/- 2 degrees.



**Figure 4.3.1.2** – Sun locating simple hardware prototype using servo motors.

Video is available here: <http://sunbyte.group.shef.ac.uk/galleryv2.html>.

Thus the concept was proven to work and this method is the primary choice to be used in the first stage tracking. Other methods are investigated as well. Currently, this algorithm was ported to Python and awaits integration with the stage two algorithm.



### 2.3.2. Sun Visual Tracking System

#### Experimentation with Tennis Ball

Due to the lack of data set at the time being, the experiment for the visual tracking system was performed on a tennis ball. The main idea was to ensure whether the algorithm was capable of running smoothly and be able to track a circular object with ease. The following result was obtained. The red trails indicate the location of previously stored results i.e. the past visiting instances of the ball. However point to be noted is that this info is rather superfluous for actual test where storing past instances would be unnecessary and rather consume more of precious memory. But that is unless the velocity would be required to be calculated but that again would be unnecessary because the on-board IMU sensors are more than enough and much more accurate than vision based speed inferences. This leads us to the discussion of the difference between projectile deviation vectors (PDVs) and centroid deviation vectors (CDVs). The CDVs, by virtue of the name, tells us the horizontal and the vertical distance (cX, cY respectively) of the centroid of the ball to the centroid of the tennis ball. On the other hand, the PDVs tell us the displacement from the last known position to the current position and can be used to calculate the velocity.

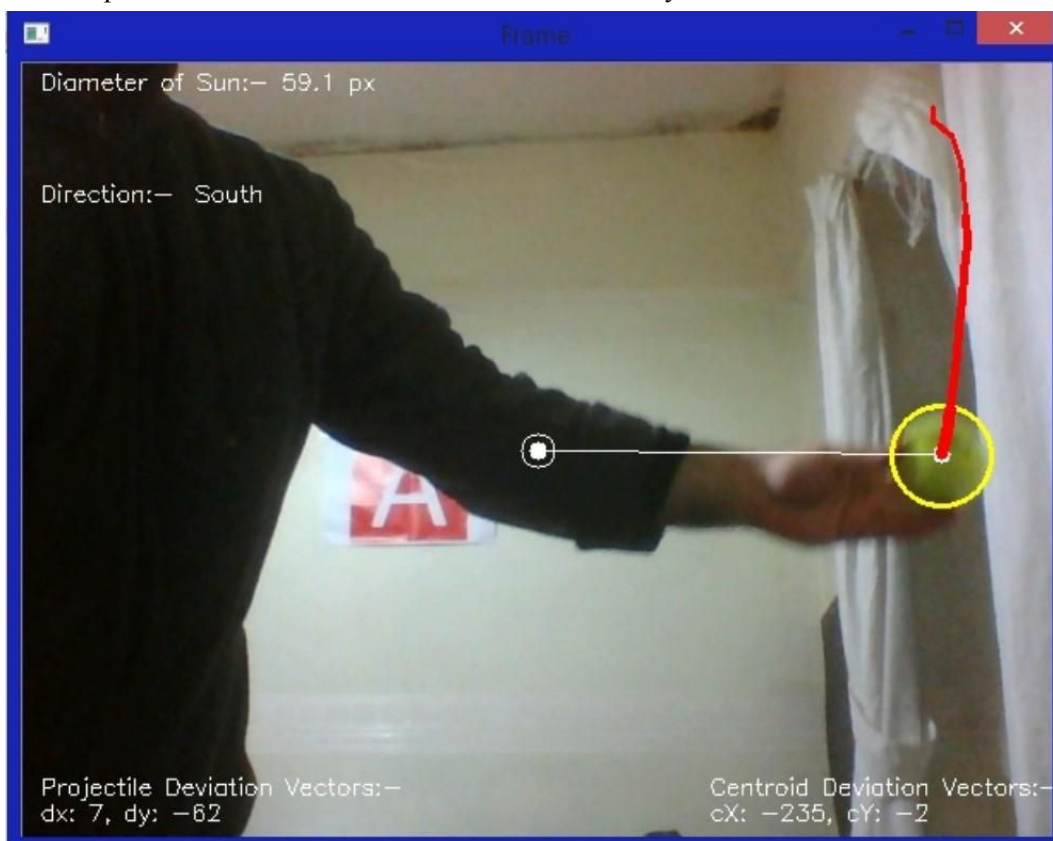


**Figure 4.3.2.1.** – Visual tracking algorithm tested on a tennis ball prototype.

#### Experimentation with Capture Dataset

With dataset captured from one of the software team member, the algorithm tested on the tennis ball as shown above was made to test on the data captured and the following result was obtained. The dark background was achieved using neutral particle density filter.

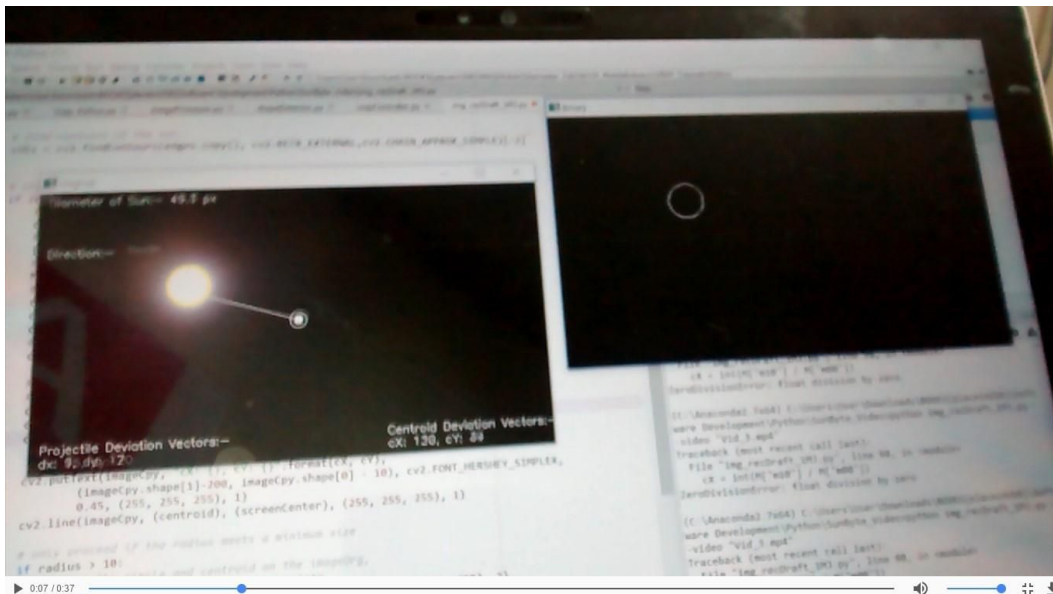


**Figure 4.3.2.2.** – Visual tracking algorithm tested on dataset Please see the entire. video on our website :<http://sunbyte.group.shef.ac.uk/galleryv2.html>

Testing the 360 degrees camera with Raspberry Pi and OpenCV

The raspberry pi was associated with a 360 degrees cameras (RICOH Theta), obtaining a two fisheye live stream at a satisfactory frame-rate. This was not pursued further (i.e. the image processing algorithm was not adapted) as we already have an acceptable solution for first stage tracking.



**Figure 4.3.2.3.** – Sample output from the 360°camera

### 3. Data analysis and Results

#### 3.1. Data Analysis Plan

One simple way to assess the quality of the images is to estimate the Fried parameter (otherwise known as  $r_0$ ) which is a measure of "seeing" in astronomical circles. Most ground-based observatories use this to monitor the level of atmospheric turbulence in real time. The Fried parameter has units of length and is typically expressed in centimetres. It is defined as the diameter of the circular pupil for which the diffraction limited image and the seeing limited image have the same angular resolution. So telescope images with apertures smaller than this parameter are less affected by seeing effects than diffraction due to the small aperture. Telescopes with larger apertures than the parameter are more limited by the turbulence in the atmosphere (seeing). In short, if the desired accuracy in determining the fried parameter is 10% then for a telescope with diameter less than 1m then approx.:

$$r_0(cm) = 1.5 * (\text{RMS of the image intensity contrast}) \quad (\text{Eq. 7.1})$$

The best telescope sites on Earth have  $r_0$  greater than 200 mm. This calculation could possibly be run in real time in our experiment i.e. to calculate the intensity contrast one could take the mean of the intensities over the image and divide by the image standard deviation over time. The determine the RMS periodically to estimate  $r_0$  as above and monitor that value as a way of comparing between periods of good and back seeing i.e. in real time. The Strehl intensity ratio is another measure of seeing and it is the ratio between the heights of the PSF peak of the actual image and the ideal diffraction limited image. Possibly, this could be attempted in real time on computer on the instrument using a predetermined model of the telescope PSF in controlled conditions.

## 4. Risk Analysis

### 4.1. Safety Risks

Risk	Key Characteristics	Mitigation
Sharp edges, machined Aluminium	Sheet and tubing, some sharp edges exist after machining.	Deburr edges where possible. Contain sharp edges in tough material. During transportation, use protective gloves when handling if sharp edges are still present.
Massive bulky structure	The mass of the assembly poses risk of trapped and damaged digits or feet being crushed.	Order of assembly should be well thought out and practiced. A safe number of people are present during assembly and that there is a dedicated space for assembly.
Motor speed > 10rev/s	During testing motors will be running at over 500 rpm.	Care should be taken to avoid hair getting caught around motor shaft. Long hair tied back.
Batteries exposed to low ambient temperature and pressure	Lithium type based on SAFT LSH20 cells grouped together. Number of : 2	Environmental testing will be conducted. Batteries are approved and provided by ESA.
Parts dropping from gondola	Parts are heavy enough to cause harm if they fall onto people	All parts sufficiently fastened. Testing conducted to ensure fastening is able to hold all parts in place in case of turbulence.

**Table 6.1.1.** – Experiment safety risks

### 4.2. Risk Register

#### Risk ID

TC - technical/implementation

MS - mission (operational performance)

SF - safety

VE - vehicle

PE - personnel

EN - environmental

#### Probability (P)

A. Minimum - Almost impossible to occur

B. Low - Small chance to occur

C. Medium - Reasonable chance to occur

D. High - Quite likely to occur



E. Maximum - Certain to occur, maybe more than once

**Severity (S)**

1. Negligible - Minimal or no impact
2. Significant - Leads to reduced experiment performance
3. Major - Leads to failure of subsystem or loss of flight data
4. Critical - Leads to experiment failure or creates minor health hazards
5. Catastrophic - Leads to termination of the HASP programme, damage to the vehicle or injury to personnel

**Table 3.2. - Risk register**

<b>Risk</b>	<b>Risk and Consequences</b>	<b>Probability</b>	<b>Severity</b>	<b>PxS</b>	<b>Action</b>
TC10	Sun not Found	A	4	Very low	Calibrate the telescope to find the Sun
TC20	Breakage of telescope	C	3	Low	Simulations done on the material to prevent it from breaking
MS10	Sun found but accurate pointing not achieved	B	2	Very low	The telescope calibrated under a light source so that it recognizes the intensity of the Sun
MS20	Telescope not focused	C	3	Low	Change the resolution and refocus
MS30	Motors overloaded	A	2	Very low	Multiple tests run before the launch to check the motor isn't overloaded
MS40	Control boards fail	B	4	Low	Multiple tests run before the launch to check the control boards work
MS50	Hard drives full	B	3	Low	Complete measures taken to ensure the hard drives are empty
MS60	Telemetry fails during focus	C	4	Medium	Recalibrate to refocus
MS70	Outgassing of the 3D printed parts	B	2	Very low	Specific care to be taken during the selection of appropriate materials

**Table 3.3.**

<b>Risk</b>	<b>Risk and Consequences</b>	<b>Probability</b>	<b>Severity</b>	<b>PxS</b>	<b>Action</b>
MS80	Gears get jammed	C	2	Low	The gears must properly oiled before launch
MS90	Heavy winds might make it disbalanced	D	2	Low	A gyroscope will be used to get alerts for proper orientation
SF10	Parts of gondola fall off	A	5	Low	It is ensured that the all the parts are properly bolted in
EN10	Rays focused on someone due to damage to telescope camera	B	4	Low	Calibration of telescope set properly so that rays do not get misguided
EN20	Short circuiting of the system	B	3	Low	Implementation of a fuse or Mini circuit breaker to stop the system from burning down.
VE10	Side strut breaks	C	3	Low	Analysis of side struss done under excessive weight to make it strong
VE20	Collision of support structure with launching mechanism	B	4	Low	The angle of launching mechanism calculated to prevent collision
PE10	Delay in achieving deadlines due to shortage of engineers	C	3	Medium	Recruitment of able engineers expediently by the management team.
PE20	Unprecedented cancellation of meetings	C	2	Medium	The management team must ensure the timings are appropriate and everyone abides by them

Table 3.4.

<b>Risk</b>	<b>Risk and Consequences</b>	<b>Probability</b>	<b>Severity</b>	<b>PxS</b>	<b>Action</b>
PE30	Lack of skills for use of modelling and analysis softwares	B	2	Medium	Hiring across multiple disciplines using working groups rather than sole experts
PE40	Sudden resignation of members	C	1	Medium	Management team ensure morale remains high through a variety of techniques
PE50	Miscommunication of Information	D	2	Medium	The management team should be responsible for ensuring proper information is conveyed to all team members